COPY 1

Report No. FAA-RD-74-170, IV

FAA WJH Technical Center
00090692

MICROWAVE LANDING SYSTEM (MLS) DEVELOPMENT PLAN AS PROPOSED BY TEXAS INSTRUMENTS, INC. DURING THE TECHNIQUE ANALYSIS AND CONTRACT DEFINITION PHASE OF THE NATIONAL MLS DEVELOPMENT PROGRAM

Volume IV -

Appendix D, Supplementary Military Systems Analysis

TRAFEC
LIBRARY
RECEIVED

September 1972

Document is available to the public through the
National Technical Information Service,
Springfield, Virginia 22151

Prepared for

U.S. DEPARTMENT OF TRANSPORTATION
FEDERAL AVIATION ADMINISTRATION
Systems Research & Development Service
Washington, D.C. 20590

NOTICE

THE CONTENTS OF THIS REPORT REFLECT THE VIEWS OF TEXAS INSTRUMENTS, INC., WHICH IS RESPONSIBLE FOR THE FACTS AND ACCURACY OF THE HEREIN PRESENTED DATA. THE UNITED STATES GOVERNMENT ASSUMES NO LIABILITY FOR ITS CONTENT OR USE THEREOF.

Texas Instruments, Inc.
Microwave Landing System (MLS) Development Plan as Proposed by Texas Instruments, Inc. During the Technique Analysis and Contract Definition Phase of the National MLS Development Program. Dallas, Texas., September 27, 1972.

162 p. (RD-74-170)
Contract No FA72WA-2803

Technical Report Documentation Page

1. Report No. FAA-RD-74-170, IV	2. Government Accession No.	3. Recipient's Catalog No.
4. Title and Subtitle Microwave Landing System (MLS) Development Plan as Proposed by Texas Instruments, Inc. during the Technique Analysis and Contract Definition Phase of the National MLS Development Program		5. Report Date September 27, 1972
		6. Performing Organization Code
7. Author(s)		8. Performing Organization Report No.
9. Performing Organization Name and Address Texas Instruments, Inc. P. O. Box 6015 Dallas, Texas 75222		10. Work Unit No. (TRAIS) 075-325-013 25173
		11. Contract or Grant No. DOT-FA72WA-2803
12. Sponsoring Agency Name and Address DEPARTMENT OF TRANSPORTATION FEDERAL AVIATION ADMINISTRATION SRDS, MLS DIVISION 2100 - 2ND STREET, S.W., WASH DC 20590		13. Type of Report and Period Covered
		14. Sponsoring Agency Code
15. Supplementary Notes		

16. Abstract

This report details technical aspects of Texas Instruments, Inc. proposed MLS hardware development.

Volume I - includes an index and system development highlights.
Volume II - covers performance validation, system trades and system compatibility.
Volume III - contains a portion of system performance summary and signal format summary.
Volume IV - contains Appendix D, Supplementary Military Systems Analysis
Volume V - contains Appendixes E1 and E 2
Volume VI - contains Appendixes E3 through E 11
Volume VII - contains Appendixes E12 through E 20
Volume VIII - contains Appendix F 1
Volume IX - contains Appendixes F2 and F 3

17. Key Words Microwave Landing System, MLS, C-Band, Ku-Band, Conventional Scanning Beam, Flare Guidance, Multipath	18. Distribution Statement DOCUMENT IS AVAILABLE TO THE PUBLIC THROUGH THE NATIONAL TECHNICAL INFORMATION SERVICE, SPRINGFIELD, VIRGINIA 22151

19. Security Classif. (of this report)	20. Security Classif. (of this page)	21. No. of Pages	22. Price
UNCLASSIFIED	UNCLASSIFIED	162	

Form DOT F 1700.7 (8-72) Reproduction of completed page authorized

TEXAS INSTRUMENTS INCORPORATED
12501 Research Blvd
P. O. Box 2909
Austin, Texas 78767

27 September 1972

MICROWAVE LANDING SYSTEM

TACD Final Report

U1-140502-1

APPENDIX D

SUPPLEMENTARY MILITARY SYSTEMS ANALYSES

I. INTRODUCTION

This appendix presents the detailed supporting analyses for accuracy, range, stabilization, etc. of the proposed military configurations of Section 1.1.4.4.3.3. The summarized results of these analyses were presented as part of the general system description. The subsections of this appendix are:

II. Navy Shipboard System Range Performance

III. US Army/US Marine Man-Transportable Systems Range Performance

IV. Navy Shipboard Accuracy Analysis

V. Army/USMC Man-Transportable Systems Accuracy Analysis

VI. Navy Shipboard Siting and Stabilization Analysis

VII. Power Programming for the Navy Shipboard System

VIII. A7E Carrier Landing Simulation Results (LSI Report)

IX. ECM/ECCM Analysis

X. Carrier Based MLS (ACLS Report).

Appendices VIII and X are final reports from Texas Instruments subcontractors, Lear Siegler, Inc. and Automatic Carrier Landing System Corp., relating to military systems.

II. NAVY SHIPBOARD SYSTEM RANGE PERFORMANCE

a. General

The performance of the Navy Microwave Landing System is highly dependent upon the environment in which it must operate. At the Navy system operating frequency of 15.5 GHz, the effects of adverse weather (i.e., rainfall) impose a severe limitation on the performance of the system. In this section, the effects of weather on the system range are investigated.

b. Signal-to-Noise Analysis

The signal power received by the airborne receiver can be calculated as the sum of the transmitted power, plus the antenna gains, minus all losses in the propagation path. This received power in dB minus the receiver noise in dB is the carrier-to-noise ratio, which is the parameter of interest.

The received signal power may thus be written as

$$C = P_T - L_T + G_T - L_a - L_S - L_g - L_W - L_R + G_R$$

where

C = received signal power

P_T = transmitted power

L_T = sum of all losses at the transmitter site

G_T = gain of transmitting antenna

L_a = off-axis reduction of antenna gain (pattern factor)

L_S = space loss

L_g = loss due to absorption by gasses in the atmosphere

L_W = attenuation due to rain

L_R = losses in the receiving system

G_R = gain of the receiving antenna

The total receiver noise power may be written as

$$N = KTB + NF$$

where

K = Boltzmann's constant (1.38×10^{-23} W/Hz-deg K)

T = system noise temperature (taken as 290° K)

B = system bandwidth in Hz

NF = receiver noise figure.

The carrier-to-noise ratio as a function of range may be plotted after evaluation of the above relationship. The following values apply to the proposed Navy system:

Transmitter power - This is a design variable and two different values are used:

0.25 watts = -6.0 dBW, and 3.0 watts = +4.77 dBW

Transmitter losses = -3.5 dB

Transmitting antenna gain = +34 dB for the azimuth antenna

Off-axis reduction of gain - 0 dB assuming the receiver is at the peak of the beam

Space loss - this factor accounts for the dispersion of the signal and is given by

$$L_S = 10 \log \frac{(4\pi R)^2}{\lambda} = 10 \log \frac{(4\pi)^2}{\lambda} + 20 \log R$$

Thus, the space loss consists of a fixed or constant term and a term which is dependent on the range. Evaluating the fixed term, using:

$\lambda = 1.93$ cm, gives $L_S = -(121.6 \text{ dB} + 20 \log R)$

where

R = range in nautical miles

Atmospheric absorption - This loss is mainly due to absorption of the RF energy by oxygen and by water vapor in the atmosphere. Blake[1] shows the two-way attenuation at short range (<20 nautical miles) to be 0.0833 dB/nmi. Thus the one-way loss would be 0.0416 dB/nmi. However, since the maximum range of interest in the Navy system is 10 nmi, this term is only 0.4 dB at 10 nmi. We will therefore neglect the contribution of this loss.

[1] Blake, L. V., "A Guide to Basic Pulse-Radar Maximum-Range Calculation: Part I - Equations, Definitions, and Aids to Calculation", Naval Research Laboratory Report 5868, Dec. 28, 1962.

Rain attenuation - This term has the most pronounced effect on the system operation and yet it is the one term for which there is no universally accepted value. This loss is a function of rainfall rates and the distribution of drop sizes. Much experimental work has been done, but results have not correlated closely with present theory. Because of the highly variable nature of rainfall both in time and extent and the inability to measure a sufficiently great number of sample points, the actual meteorological data is not sufficiently accurate to make accurate predictions of attenuation by rainfall. Nathanson[2] reviews much of the work done in this field. In particular, measured values of attenuation in dB/nmi/MM/HR of rainfall are plotted as a function of frequency. The values shown for a frequency of 15.5-GHz range from a minimum of 0.07 dB/nmi/mm/hr to 0.27 dB/nmi/mm/hr for a one-way attenuation. For a rainfall rate of 25.4 mm/hr, these values are 1.78 dB/nm to 6.8 dB/nmi with a modified mean value of 3.6 dB/nmi. The Thomson-CSF MLS study (Appendix E2) summarizes most available data which indicates a nominal value of 3.3 dB/nmi for 25.4 mm/hr rainfall at 15 GHz. This later value will be assumed.

Receiving system losses - These losses include the radome loss and waveguide or cable loss to the input of the receiver. In our calculations these losses are included with the value for the antenna gain, therefore, a separate value is not included for L_R.

Receiving antenna gain - Design data indicates that a value of +4 dB, which includes cable loss, is appropriate for this term.

Using these values, the total received carrier signal power (dBW) then is

$$C = P_T - 3.5 + 34 - 121.6 - 20 \log R - 3.3\,(R) + 4$$

The total receiver noise, N, is evaluated using a receiver noise figure = 11 dB and a receiver bandwidth of 400 kHz, which converts to +56.0 dB Hz.

$$KT = 1.38 \times 10^{-22} \times 290 = -204 \text{ dBW/Hz}$$

Thus, $KTB = -204 + 56 = -148$ dBW

And $N = KTB + NF$

$$N = -148 + 11 = -137 \text{ dB}$$

The desired carrier-to-noise ratio is, thus

$$(C/N)_{dB} = P_T - 87.1 - 20 \log R - 3.3\,(R) - (-137)$$

[2]Nathanson, Fred E., "Radar Design Principles", McGraw-Hill Book Co., New York 1969.

The preceding equation gives the carrier-to-noise ratio at range R for adverse weather over the entire range. Although Navy "adverse weather" conditions are not defined in the MLS RFP, the AN/SPN-41 system uses a 1-inch/hr raincell 5 miles in diameter. This condition is also specified in the USMC MRAALS specification. If we assume that the specified rainfall rate of 1 inch per hour extends over a range of 5 nautical miles, then when R is greater than 5 nautical miles, the rainfall attenuation term 3.3 (R) is set to a maximum value of 16.5 dB. For the case of clear weather, this term is set to zero.

When plotting the carrier-to-noise ratio for the adverse weather case, the location of the 5-mile raincell must be known if the absolute carrier-to-noise ratio at a particular range is desired. However, the ratio at 10 nautical miles will always be the same regardless of where the 5-mile raincell is located within the 10-mile range. Location of the cell in the touchdown area is a worst case assumption.

The carrier-to-noise (C/N) ratio versus range is plotted in Figure D-1 for transmitter output powers of 0.25 watt and 3.0 watts for both the clear-weather case and for a 5-mile raincell with rainfall rate of 1 inch per hour. In clear weather, a 24-dB C/N ratio is obtained at 10 nautical miles with a transmitter power of 0.25 watt. However, with 5-nautical miles of intervening rain with a rainfall rate of 1 inch per hour a C/N ratio of 7.5 dB results (which is inadequate). A power output of 3.0 watts provides a C/N ratio of 18 dB at 10 nautical miles and is more than adequate for proper MLS operation.

These calculations and curves consider only the attenuation associated with the intervening rainfall. The limiting effect of added noise generated by the non-coherent forward scattering is discussed in the following paragraphs.

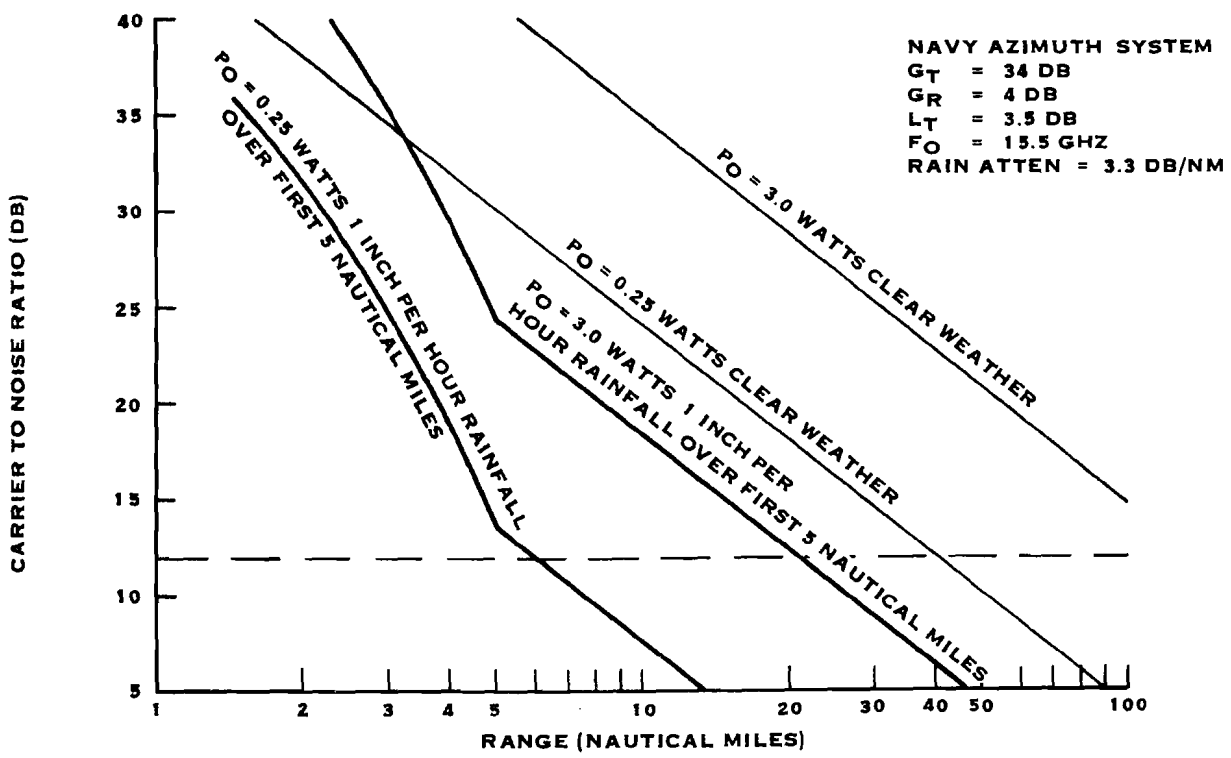

Figure D-1. Navy I_2 MLS Carrier-to-Noise Ratio Versus Range

c. Limiting Effect of Added Noise

The increase in received noise due to forward scattering is discussed in greater depth in Appendix E-2 of this report. In summary, Appendix E2 shows that the received carrier-to-noise ratio reaches a limit due to non-coherent forward scattering which effectively increases the receiver noise as a function of the intervening rain randomly scattering the transmitted energy. The result is shown to be related to the total path attenuation.

Using the antenna gains for the Navy I_2 configuration of 34 dB for the shipboard azimuth antenna and 4 dB for the airborne antenna, the resulting limits for received C/N levels of 10, 12, and 14 dB are plotted in Figure D-2.

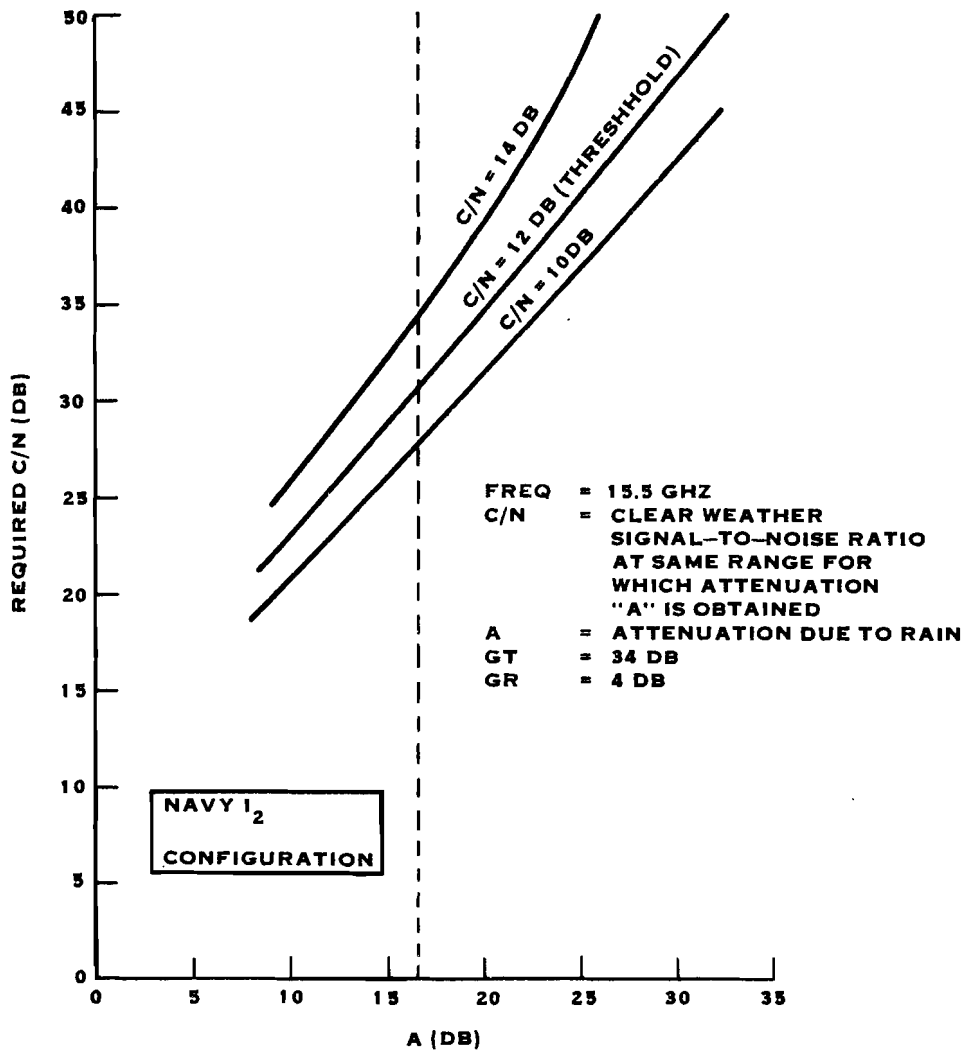

Figure D-2. Limits for Received C/N Levels

From these curves, we may determine the clear weather carrier-to-noise ratio required to provide a given carrier-to-noise ratio for any condition where the total signal attenuation due to rain is known. Thus, for a rainfall rate of 1 inch per hour over a 5-mile range, with an attenuation of 3.3 dB/nmi, the total rainfall attenuation is 16.5 dB. Assuming that a minimum C/N level of 12 dB is required the curves of Figure D-2 show that A = 16.5 intersects C/N - 12 dB line at a C_O/N_O of 30.5 dB. Thus, to maintain a receiver C/N of 12 dB in rainfall giving 16.5-dB attenuation, the transmitter power output must be increased to a value which would result in a C/N of 30.5 dB in clear weather at the range of interest. From Figure D-1 it is seen that, at 10 nautical miles with a transmitter power of 3.0 watts, a clear weather carrier-to-noise ratio of 35 dB is obtained. Thus, satisfactory performance will be obtained under these rainfall conditions.

d. Summary of Angle System Performance

Paragraph D.2.3 has shown that if sufficient rainfall attenuation is present along a given path that a limiting point will be reached at which further increases in transmitted power will not improve the received carrier-to-noise ratios. At that point only increased antenna gain (i.e., smaller beamwidth) could improve the C/N ratio.

The preceding calculations show that the proposed transmitter power levels of 250 nmi for clear air and 3 watts for adverse weather conditions will result in adequate carrier-to-noise values at the ranges of interest. These curves and equations can be used to extrapolate the effects of other weather conditions and/or system parameters as desired.

e. DME Performance

The Navy I_2 DME is essentially identical to that of the civil I/K system. The Navy installation will have slightly more antenna gain at the lower elevation angles and the cable losses will be less due to siting advantages. Table D-1 presents the Navy DME range performance calculations and Figure D-3 presents the system losses in graphical form. It is seen that adequate power margin for a 30-nmi range is obtained for both air-to-ground and ground-to-air links.

Table D-1. I_2 DME Power Budget

Air-to-Ground Link

A/B system	Transmitter power 2 kW	+63 dBm
	Cable loss	-3.5 dB
	Circulator	-0.5 dB
	Minimum antenna gain	0 dB
	30-nmi path loss	-142 dB

Table D-1. I_2 DME Power Budget (Continued)

G/B system	Antenna gain for 1 degree elevation over 40 degrees azimuth		+9.5 dB
	Loss between antenna and receiver		-3.25 dB
	Input signal to receiver		-77 dBm
	Receiver sensitivity	-85 dBm	
	IF bandwidth	8 MHz	
	S/N minimum	+12 dB	
	NF	8 dBm	
	Power margin	8 dBm	

Ground-to-Air Link

G/B system	Transmitter power 2 kW		+63 dBm
	Loss between transmitter and antenna		-3.8 dB
	Antenna gain for 1 degree elevation over 40 degrees azimuth		+9.5 dB
	Path loss for 30 nmi		-142 dB
A/B system	Antenna gain		0 dB
	Circulator		-0.5 dB
	Input signal to the receiver		-74 dBm
	Receiver sensitivity	-82.5 dBm	
	IF bandwidth	8 MHz	
	S/N minimum	+12 dB	
	NF	10.5 dB	
	Power margin	8.5 dB	

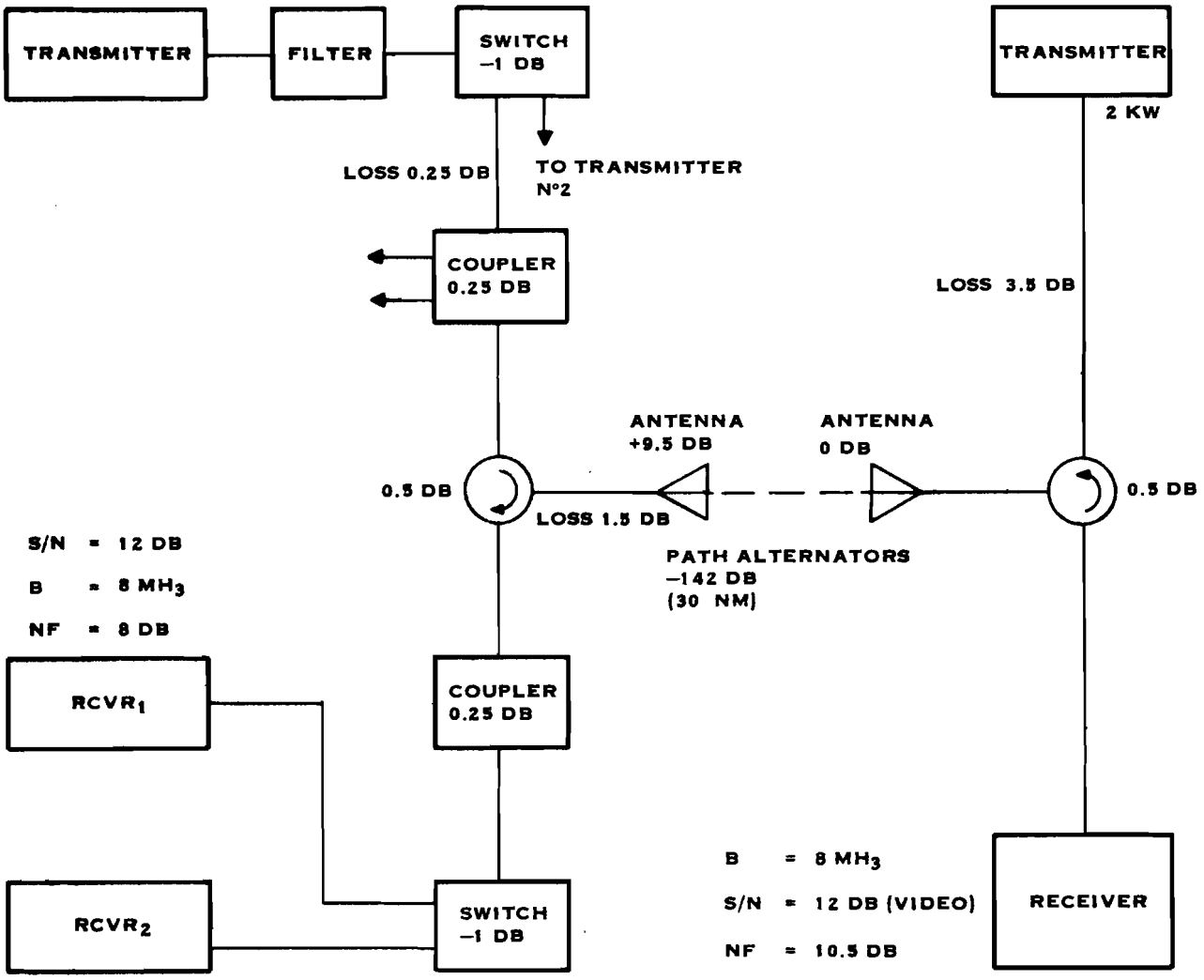

Figure D-3. I_2 DME Block Diagram

III. ARMY/USMC MAN-TRANSPORTABLE SYSTEMS RANGE PERFORMANCE

a. General

The effects of range and weather on the performance of a Ku-band microwave landing system have been discussed in Section II (Navy Shipboard System Range Performance). The Army/USMC man-transportable MLS also operates at this same frequency and the same system analysis applies when appropriate values for system parameters are used.

b. Signal-to-Noise Analysis

The signal-to-noise ratio at the receiver input terminals is the parameter of interest and may be calculated as the difference between the carrier power received at the

airborne receiver and the noise power present at the receiver when both values are expressed in dB.

The received signal power is the sum of the transmitted power, plus the antenna gains, minus all losses in the propagation path. The received power may then be written as

$$C = P_T - L_T - G_T - L_a - L_S - L_g - L_W - L_R + G_R$$

where

C = received signal power in dBW

P_T = transmitted power in dBW, which is a design variable

G_T = gain of transmitting antenna = 31 dB

L_T = sum of all losses at the transmitter site = 2 dB

L_a = off-axis reduction of antenna gain (pattern factor) = 0 dB for on-axis calculations.

L_S = space loss = 121.6 dB + 20 log R (R in nautical miles)

L_g = losses due to absorption by gasses in the atmosphere = 0 dB (These losses are small and will be neglected)

L_W = attenuation due to rain = 1.95 DB/NM for rainfall rate of 15mm/hr (Reference Appendix E2)
= 0 for the clear weather case.

L_R = losses in the receiving system. These losses will be included in the term of receiving antenna gain and, therefore, a separate value for this term is not included.

G_R = gain of the receiving antenna = 4 dB which includes losses associated with the receiving system

The received signal power is then

$$C = P_T + 31 - 2 - 121.6 - 20 \log R - 1.95R + 4 = P_T - 88.6 - 20 \log R - 1.95R.$$

The total receiver noise power may be written as

$$N = KTB + NF$$

where

K = Boltzmann's constant $= 1.38 \times 10^{-23}$ W/Hz - deg K

T = system noise temperature = 290°K

B = system bandwidth in Hz = 400 kHz

NF = receiver noise figure = 11 dB.

Expressing these values in dB, the noise power is

$$N = -204 \text{ dB} = 56 \text{ dB} + 11 \text{ dB} = -137 \text{ dB}$$

The carrier-to-noise ratio is then

$$C/N = P_T - 20 \log R - 1.95 R - 88.6 - (-137)$$

$$= P_T - 20 \log R - 1.95 R + 48.4.$$

The above equation gives the received C/N ratio at range R for adverse weather over the entire range. For the clear weather case, the rain attenuation term, 1.95 R, is of course set to zero.

The carrier-to-noise ratios versus range are plotted in Figure D-4 for transmitter output powers of 0.25 watt and for 3.0 watts for both the clear weather case and for the adverse weather case. The adverse weather is defined by the MLS RFP as 15mm/hr over a 10-nmi range for the Army system. For the USMC MRAALS specification defines USMC adverse weather as 1 inch/hr over a 5-nmi cell. This results in a total attenuation of 16.5 dB versus 19.5 dB for the Army system. Thus, the Army requirement is more severe and will be used in this example. In clear weather, a carrier-to-noise ratio of 22.5 dB is obtained at a range of 10 nautical miles with a power output of 0.25 watt. However, in adverse weather with a rainfall rate of 15mm/hr, a power output of 3.0 watts provides a carrier-to-noise ratio of 13.7 dB at a range of 10 nautical miles during adverse weather.

c. Noise Due to Forward Scattering by Rainfall

The above range calculations and curves consider only the attenuation associated with the intervening rainfall. They do not consider the added noise generated by the non-coherent scattering of the transmitted signal which can be a significant factor.

The increase in received noise due to the forward scattering is discussed in greater depth in Appendix E2 of this report. In summary, Appendix E2 shows that the received carrier-to-noise ratio reaches a limit due to non-coherent forward scattering which

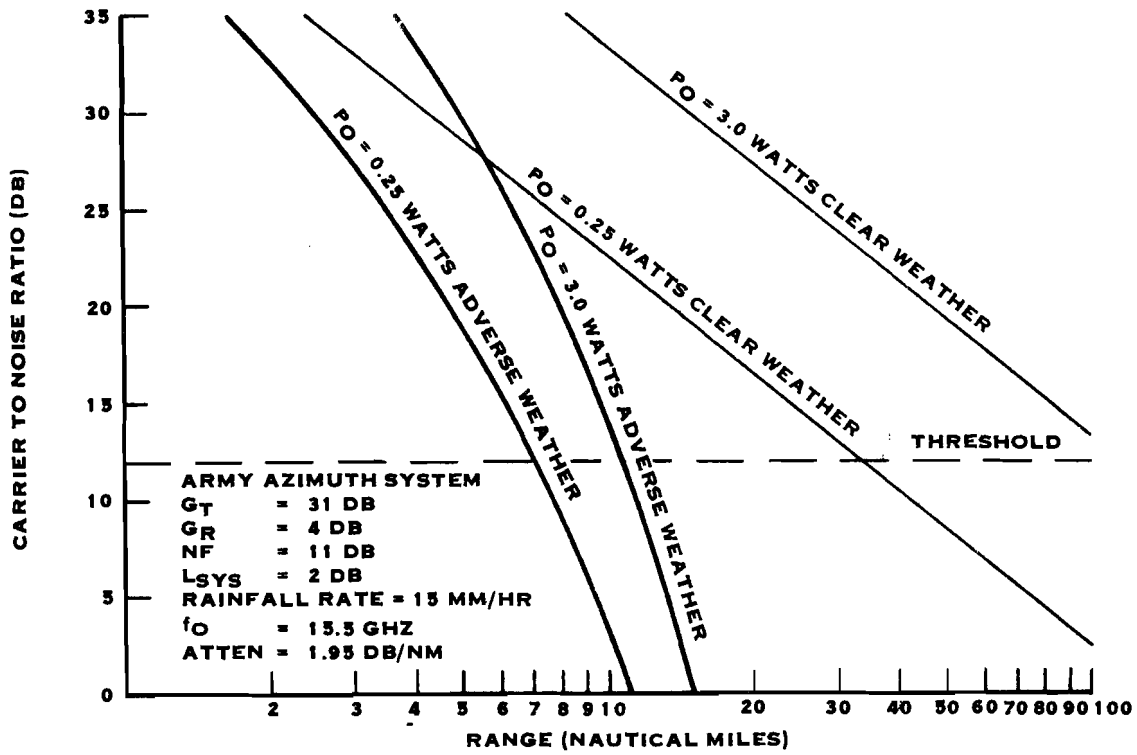

Figure D-4. Carrier-to-Noise Versus Range

effectively increases the receiver noise as a function of the intervening rain randomly scattering the transmitted energy. Thus, at this limit, increasing transmitter power increases the received noise as much as the received signal and, thus, no improvement in C/N ratio is achieved. The resultant is shown to be related to the total path attenuation.

Using the antenna gain of 31 dB for the ground azimuth antenna and 4 dB for the airborne antenna, the resulting C/N limits for 10, 12, 14, and 24 dB are plotted in Figure D-5.

From these curves, one may determine the clear weather carrier-to-noise ratio required to provide a given carrier-to-noise ratio for any condition where the total signal attenuation due to rain is known. For a rainfall rate of 15mm/hr over a 10-mile range, with an attenuation of 1.95 dB/nmi, the total rainfall attenuation is 19.5 dB. From Figure D-5 it is seen that, for A = 19.5, a clear weather carrier-to-noise ratio (C_o/N_o) of 35.5 dB is required to provide a receiver carrier-to-noise ratio of 12 dB which is the minimum threshold for reliable operation. However, from Figure D-4 it is seen that, at 10 nautical miles and 3.0 watts transmitter power output, the Army system provides only a 33.2-dB clear weather carrier-to-noise ratio; thus, the system would be noise limited for the given C/N ratio at 10 NM under the stated conditions.

The system clear weather carrier-to-noise ratio may also be plotted on Figure D-5 as a function of the rain attenuation (the range which results in the attenuation A). This curve makes clear the tradeoff between operating carrier-to-noise ratio and range. Thus, for

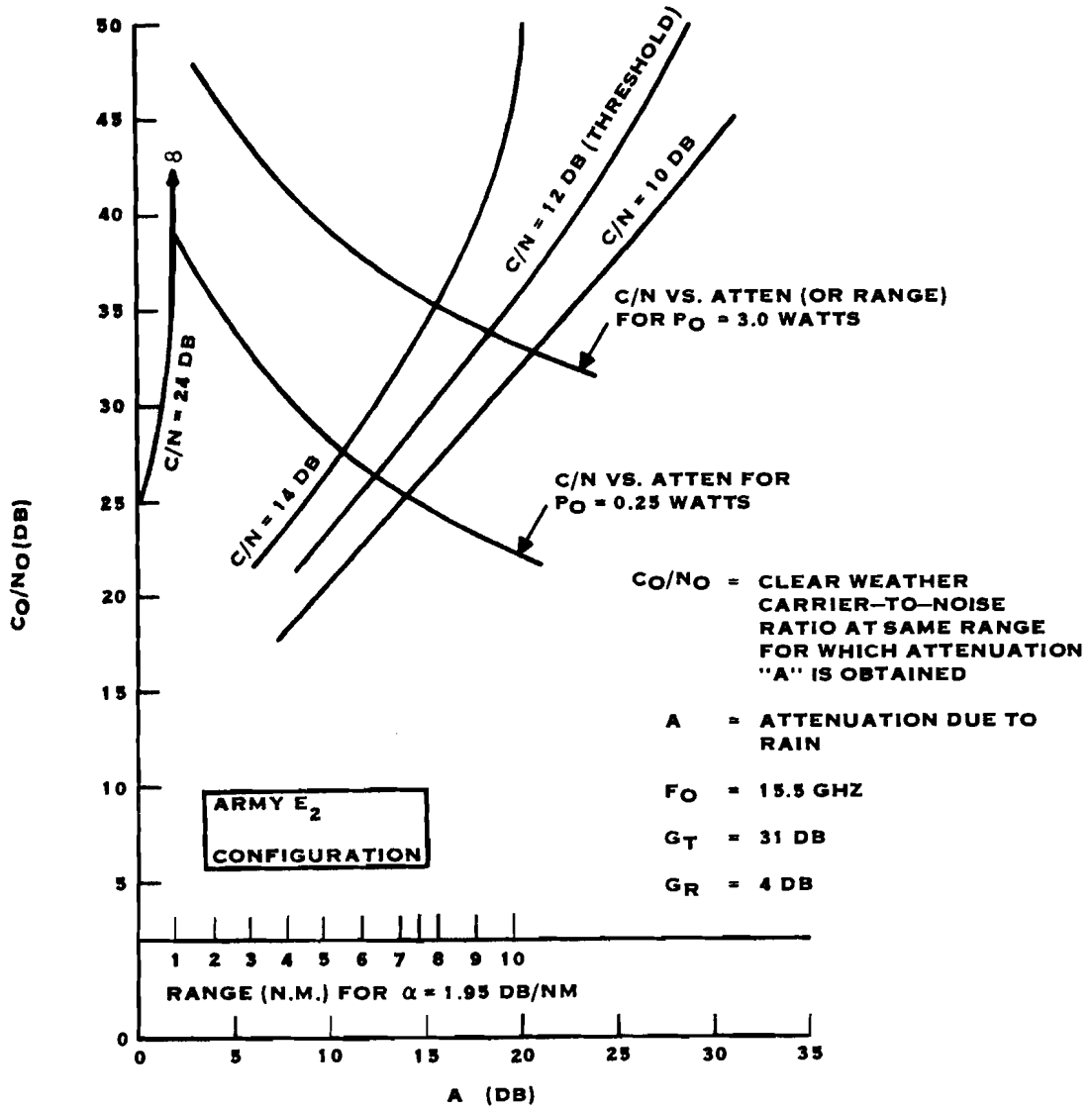

Figure D-5. C/N Limits

the Army system with a transmitter power output of 3.0 watts and 15mm/hr rain, a carrier-to-noise ratio of 12 dB (minimum allowable) is obtained at 9.5 nautical miles. The carrier-to-noise ratio drops at 10 dB at 11 nautical miles. Receiver operation at this C/N level (10 dB) is marginal due to FM "clicks".

The clear weather carrier-to-noise ratio for a power output of 0.25 watt is also shown. This curve shows that for a power of only 0.25 watt an operating carrier-to-noise ratio of 10 dB (which is below minimum threshold) is obtained at a range of just over 7 nautical miles in adverse weather. At 6.5 nautical miles the carrier-to-noise ratio is approximately 12 dB (minimum allowable).

d. Summary of Angle System Performance

The C/N increases rapidly with decreasing range so that at about 1 mile, the carrier-to-noise ratio for 0.25 watt is 24 dB. But from the curve, it is evident that increased power at this range will not significantly improve the carrier-to-noise ratio. The C/N ratio could only be improved by the use of higher gain (i.e., narrower beamwidth) antennas, since this would reduce the volume of rainfall from which forward scattered energy would be received. Narrower beamwidths would, of course, result in larger antennas and increased drive power and weight. As an example, adequate C/N is available for operation with 3 watts, resulting in 12 dB C/N at 9.5 nmi in weather. If the power is increased 3 dB to 6 watts, the range would be increased to 10 nmi for a 12 dB C/N ratio. Thus, doubling the power resulted in only a 5 percent increase in range. Error analysis shows that with a carrier-to-noise ratio in the range of 24 dB the angular errors due to noise are less than 1/2 milliradian. Thus, at short ranges, where highest accuracy is required, the required carrier-to-noise ratios are obtained with lowest power, even in adverse weather.

e. DME Performance

The DME range calculations are given in Table D-2. Figure D-6 graphically gives the system losses. It is seen that adequate performance from both the ground-to-air and air-to-ground line is obtained at 15 nmi.

Table D-2. Power Budget for E_2 DME Equipment

Air-to-Ground Link

A/B system	Transmitter power 2 kW		63 dBm
	RG 211 cable loss		-2.75 dB
	RF head circulator		-0.5 dB
	Minimum antenna gain		+1 dB
	15-nmi path loss		-135.5 dB
	Atmospheric attenuation		-1 dB
G/B system	Antenna gain for 3-degree elevation		+2 dB
	Loss between antenna and receiver front end		-1 dB
	Receiver input signal		-74.75 dBm
	Receiver sensitivity	-82 dBm	
	IF bandwidth	8 MHz	
	minimal S/N	12 dB	
	NF	11 dB	

Table D-2. Power Budget for E_2 DME Equipment (continued)

Ground-to-Air Link

G/B system	Transmitter power, 0.5 kW		-57 dBm
	Loss between transmitter and antenna		-1 dB
	Antenna gain for 3-degree elevation angle		+2 dB
	Atmospheric attenuation		-1 dB
	15-nmi path loss		-135.5 dB
A/B system	Antenna gain		+1 dB
	Circulator between antenna and receiver front end		-0.5
	Receiver input signal		-78.0 dBm
	Receiver sensitivity	-79.5 dBm	
	IF bandwidth	8 MHz	
	S/N ratio	12 dB	
	NF	10.5 dB	

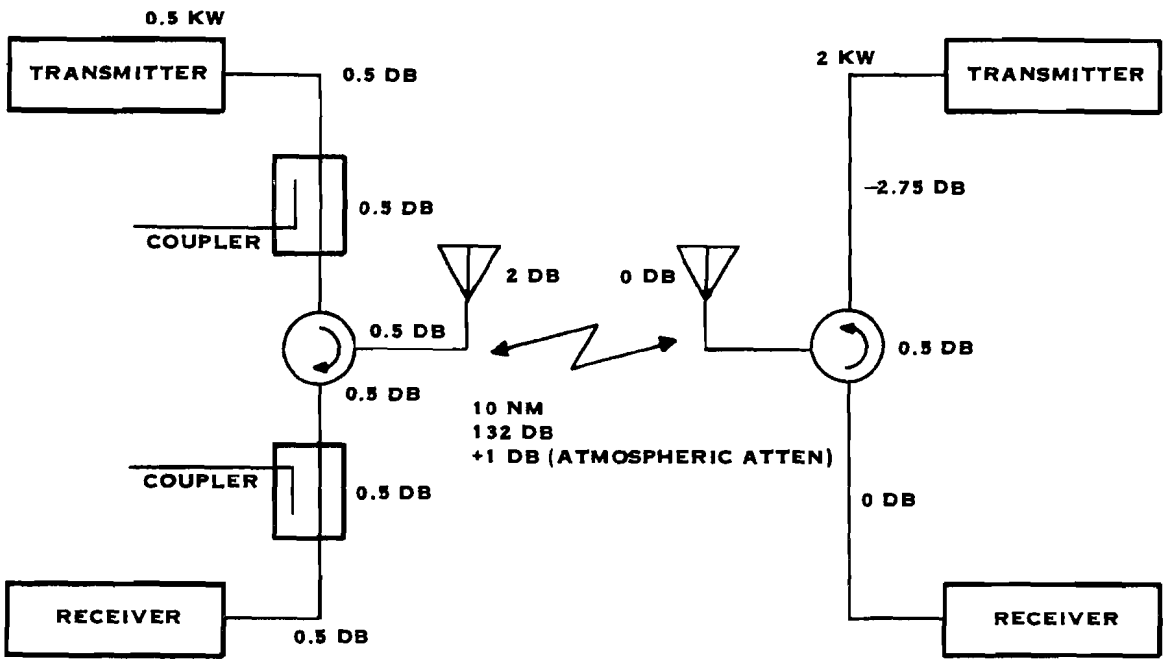

Figure D-6. $E_2/E_3/G_2$ DME Block Diagram

FAA WJH Technical Center
00090692

IV. NAVY SHIPBOARD SYSTEM ACCURACY ANALYSIS

a. Introduction

This analysis presents the predicted I_2 system signal-in-space-accuracy using the proposed Navy configuration and parameters. Noise errors are shown to be minimum for the ranges of interest for carrier approaches. Because of signal-in-space stabilization in roll, pitch, and yaw, and heave due to motion of the ship, there are a greater number of potential error sources which can induce bias errors relative to a ground-based system. The bias errors are particularly important in adequately defining the stabilization accuracies required.

This analysis does not include the control computation accuracies or the aircraft flight dynamics in a closed-loop control system. A cursory analysis of these items was conducted by Lear Siegler on an A-7E during this phase. Section VIII of this Appendix indicates that the I_2 configuration appears to satisfy all navy performance requirements. A full configuration simulation with statistical outputs for dispersion, sink rate, etc. will be conducted during Phase II. The DME accuracy analysis is identical to that for the Type I DME (Section 1.1.1.1.4.2).

b. Noise Errors

The major sources of noise error in the angular system have been identified and relationships defining the magnitude of these errors have been derived.[3] Airborne decoding is the major source of noise errors, but they are influenced by the shipboard system parameters which affect the received S/N ratio. These errors are:

Dwell-gate jitter

Measurement time jitter

Baseband quantizing error

Reference clock quantizing error.

1. Dwell Gate Jitter

In the airborne angle decoder, the receiver senses the time during which the received signal exceeds a given level (3 dB below the peak signal). During this time the average tone frequency is measured to provide the angle information. Any noise on the signal will cause the time at which the signal-plus-noise crosses the threshold to vary, and, thus,

[3] "Proposal to Develop a Microwave Landing System", Texas Instruments, Equipment Group Proposal No. EG71-237, 21 September 1971

the time of measurement of the angle tone will vary. This error in measurement time or dwell-time jitter is given as

$$\sigma_1 = \frac{(0.67)\theta_3}{\sqrt{\rho_1}}$$

where

σ_1 = dwell-gate jitter in seconds

θ_3 = 3-dB beamwidth of the transmitter scanning antenna

ρ_1 = signal-to-noise ratio at the output of the IF amplifier

Thus, the dwell-time jitter is a function of the antenna beamwidth and the received signal-to-noise ratio. The received signal-to-noise ratio is, in turn, determined by the transmitter power output, range and weather effects, and the receiver bandwidth.

2. Measurement Time Jitter

Measurement time is defined as the time between the first and last zero crossings of the signal which lie within the dwell-gate time. Jitter is introduced into the measurement time because of additive noise on the signal. The measurement time jitter is given as

$$\sigma_2 = \frac{0.225}{At_m\sqrt{\rho_2}}$$

where

A = scale factor in Hz/degree

t_m = measurement time in seconds

ρ_2 = S/N at output of angle data filter

The scale factor A in the proposal system design is 500 Hz per degree. The measurement time is determined by the length of the dwell gate which is the antenna beamwidth at the threshold level divided by the scan rate. Thus, the measurement time may be written as $t_m = \theta_3/W_s$ for the design dwell-gate threshold of 3 dB where W_s = antenna scan rate in degrees per second.

Therefore, the measurement time jitter may be written as

$$\sigma_2 = \frac{0.45 \times 10^{-3}}{\sqrt{\rho_2}} \cdot \frac{W_s}{\theta_3}$$

3. Baseband Quantizing Error

A measurement error is also introduced because of the quantizing effect of the baseband signal. The measurement time is determined by the signal zero crossings within the dwell gate and the number of zero crossings within the dwell gate may vary by one count as the phasing between the signal and the dwell gate varies. The measurement time jitter is given as

$$\sigma_3 = \frac{1.02\ W_s}{\overline{F}}$$

where $\overline{F}$ is the average angle tone frequency within the dwell gate.

4. Reference Clock Error

The final decoder error is due to the quantizing effect of the reference clock. The reference clock is used to measure the duration of the dwell gate. This is accomplished by counting the number of reference clock pulses occurring within the dwell gate and the reference clock. This count may vary by one count, giving rise to the quantizing error and the quantizing error is given by

$$\sigma_4 = \frac{0.4\ 08\ \overline{F}}{A\ t_m\ f_r}$$

where

A = scale factor in Hz/degree

t_m = measurement time in seconds

f_r = reference clock frequency

$\overline{F}$ = average angle tone frequency within the dwell gate.

Again, we may use 500 Hz/deg for the scale factor A, $t_m = \theta_3/W_s$, and the design reference clock frequency = 48 MHz. The average angle tone frequency may be taken as 110 kHz which is the tone of the azimuth signal on centerline of the canted deck.

Using these constants, the reference clock quantizing error is

$$\sigma_4 = 0.187 \times 10^{-5} \cdot \frac{W_s}{\theta_3}$$

5. Composite Noise Error

An examination of these relationships shows that the antenna scan rate, W_s, occurs in the numerator of three of them. Thus, to minimize these errors, the

antenna scan rate should be made as low as possible. The minimum antenna scan rate is determined by the required data update rate. Using back-to-back continuously rotating antennas for the Navy azimuth system, a minimum scan rate of 900 degrees/second is required to provide an update rate of 10 degrees per second.

Other variable in the equations are the antenna 3-dB beamwidth, θ_3, and the signal-to-noise ratios ρ_1 and ρ_2.

Using an antenna scan rate of 900 degrees/second and the other system constants defined above, the errors versus antenna beamwidth are plotted in Figure D-7 for input signal-to-noise ratios of 15 dB, 25 dB, and 45 dB. The baseband quantizing error, σ_3 is

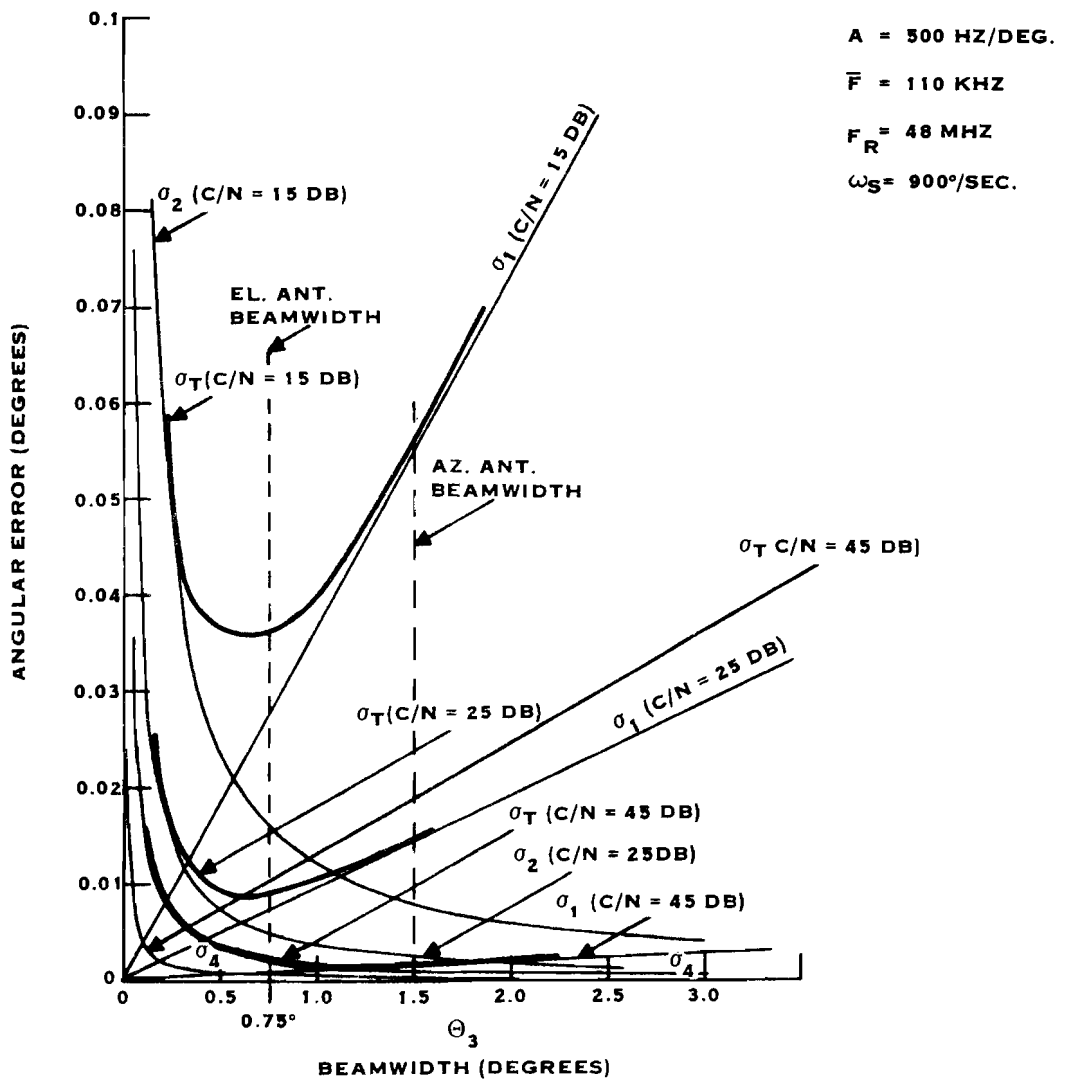

Figure D-7. System Noise Errors

not dependent on either the signal-to-noise ratio or the scan rate, and for the constants chosen reduces to $\sigma_3 = 0.00835$ degree.

The total noise error due to these errors is $\sigma_T = \sqrt{\sigma_1^2+\sigma_2^2+\sigma_3^2+\sigma_4^2}$. This value has been calculated for the three different carrier-to-noise ratios and plotted in Figure D-7.

From these curves it is evident that for antenna beamwidths greater than 1/2 degree, the dominant error is σ_1 and the total noise error is only very slightly greater than σ_1. Also, the total error decreases very rapidly with increasing signal-to-noise ratios. Signal-to-noise ratios greater than 25 dB will be obtained at short ranges (2 nautical miles or less) even in adverse weather. At these signal-to-noise ratios, the errors become quite small and are very insensitive to antenna beamwidths for beamwidths greater than 0.5 degree.

The Navy shipboard system uses an elevation antenna with a beamwidth of 0.75 degree in the elevation plane. From the curves, it is seen that this beamwidth results in essentially minimum noise errors for any signal-to-noise ratio. The azimuth beamwidth of 1.5 degree is near enough to the optimum to provide excellent performance. This is especially true for the higher signal-to-noise ratios which will be obtained at the shorter operating ranges. At these signal-to-noise ratios, the noise errors are quite insensitive to antenna beamwidth and no significant improvement in performance would be realized by the use of a narrower beamwidth (therefore, larger) antenna.

The noise error analysis is based on a "single hit" basis. The use of recursive filtering in the airborne signal processing (as proposed) will essentially reduce the noise errors by a factor of 5 to 10 dependent on filter parameters. The resultant noise error for various ranges of interest are tabulated below for the elevation signal and are seen to be very small.

Range (nmi)	S/N (Clear WX) (dB)	σ_n (Single Hit) (Degrees)	σ_n' (Effective) (Degrees)
10	18	0.03	0.006
5	24	0.01	0.002
1/2	44	0.002	0.0004

c. Bias Errors

The preceding analysis has considered the noise errors in the angle system. There are other errors which are constant or vary only slowly. These are the system bias errors.

There are two possible sources of bias errors in the angle encoder. The first is because of the staircase step function approximation of the desired linear frequency by the digital encoder. The magnitude of this error is a function of the number of pulses from the shaft angle encoder. For the Navy shipboard system using a 2^{12} angle encoder, the maximum error from this source is 0.001 degree. The second source of error is the possible frequency variation of the oscillator clock used in the tone generator. The error

is directly related to the accuracy of this clock and the bias error associated with an oscillator accuracy of 10^{-5} is about 0.002 degree. Thus, both of these errors are very small.

Since the ship is a moving platform and has roll, pitch, yaw, and heave motions, the stabilization of the antennas is a possible error source. These errors are discussed in Section VI of this appendix. The elevation and azimuth beams will be mechanically roll stabilized to within ±0.3 degree. The analysis in Section VI shows that this error results in vertical and lateral displacements of less than 3 feet at a range of 3000 feet. At the data freeze point of 300 feet, the errors due to roll are much less than 1 foot.

Pitch and yaw stabilization is electronic. The limit on the accuracy of these corrections is set by the accuracy of the stable platform and this may be maintained to within ±0.05 degree. This would result in a maximum error from this cause to approximately ±0.25 feet at the data freeze point.

Another source of bias error is the alignment error which results from the misalignment between the incremental shaft encoder used for frequency encoding and the antenna true-beam position. This alignment will be constantly monitored by means of the near-field monitors located on the fantail of the ship. The location of the monitor with respect to the antenna will be determined by surveying the site at the time of equipment installation. The monitor location can thus be determined to an accuracy of approximately ±1 mrad. Once the monitor location is known, the shaft angle encoder may be mechanically and electrically aligned so that the correct angle tone frequency is received by the monitor. The alignment errors may thus be calibrated to within about ±1 mrad which would result in vertical and lateral displacement errors at the data freeze point of approximately ±0.3 foot.

Other minor bias errors are discussed in Section 1.1.1.1.4.1.2.3. Assuming that the bias errors may add linearly in the worst case they would result in a maximum error of 1.25 feet at the data freeze point, which is acceptable. Thus, the MLS contributed errors will probably account for only 1/4 of the allowable touchdown dispersion. The major errors will be those of the aircraft performance in the closed-loop automatic landing. A major simulation effort is planned for Phase II which would include the motion of the aircraft and the ship in addition to the MLS error budget.

V. ARMY/USMC MAN-TRANSPORTABLE SYSTEM ACCURACY ANALYSIS

a. Introduction

The Navy system analysis of the preceding section is also applicable to the Army/USMC man-transportable systems by appropriately modifying the system parameters. The DME error analysis is identical to that of the Type II DME (Section 1.1.1.1.4.2).

b. Noise Errors

The noise error analysis of the Navy system, as plotted in Figure D-7, is modified only by the difference in antenna rotation speed (W_s) which is 450 degrees/second for the Army system (1/2 that of the Navy). This parameter change will double the noise errors σ_2, σ_3, and σ_4 expanding the curves to the left. Alternately, the curves may be used directly

by doubling the abcissa values (θ_3) as a close approximation. Thus, the σ_T minima will occur at approximately 1.2 degrees for a C/N ratio of 15 dB and 1.3 degrees for a C/N ration of 25 dB. This indicates that the 1.5-degree elevation antenna beamwidth is near optimum considering the other Army system parameters. Again, the data is plotted for a "single hit", and filtering and integration in the airborne receiver will reduce the total noise error by a factor of 5 to 10. The resultant noise errors for various selected ranges are tabulated below for the elevation signal and are seen to be very small.

Range (nmi)	S/N (Clear WX) (dB)	σ_n (Single Hit) (Degrees)	σ_n' (Effective) (Degrees)
10	16.5	0.03	≃0.006
5	23.5	0.01	≃0.002
1/2	42.5	0.002	≃0.0004

c. Bias Errors

The bias errors for the Army system are similar to those encountered for the Navy system without stabilization. In general, the errors will all be small compared to the alignment error of the ground station which is ±0.05 degree. If we assume that the other system errors might jointly contribute an additional ±0.05 degree, then the resulting maximum error on a linear basis will be ±0.1 degree or ±0.01 degree for an RMS combination. In any case, the resulting error will not be sufficient to limit the use of the system for CAT II operations.

d. Conclusions

The analysis indicates that the E_2, E_3, G_2 system configuration will meet the USMC CAT II requirement and exceed the Army CAT I requirements for accuracy. The major error in IFR operations will, thus, be related to the ability of the pilot to manually maintain the aircraft on glidepath.

VI. NAVY SHIPBOARD SITING AND STABILIZATION ANALYSIS

a. Introduction

The selection of a suitable location for the MLS antennas aboard the Navy aircraft carrier presents some conflicting requirements between coverage and available sites. The selection of a suitable site is also influenced by the motion of the ship and its effect upon the stabilization of the signal in space. The variations of angles and offsets affect the complexity and accuracy of the computation of aircraft flight commands. These considerations are discussed in the following sections. A discussion of the antenna stabilization requirements and error compensations associated with the ships motion is also presented.

b. Siting

The site chosen for the shipboard MLS antennas must satisfy several requirements; namely a clear scan volume, minimum angular rate change, and meeting available site constraints. First, the antenna must have an unobstructed view of all the volume in space in which an aircraft could be positioned when making an approach and landing. The desired angular coverage (centered on touchdown point) is ±40 degrees in azimuth and 0 degrees to +20 degrees in elevation. It is not possible, however, to position the antennas at the touchdown point. To ensure coverage when the antennas are offset from touchdown, the angular limits of the antenna scan must be increased.

The antennas must be positioned such that there are no obstructions, such as parked aircraft, towers, other equipment, etc. between the antenna and the landing aircraft. Also, the offset distances must be chosen to minimize, as much as possible, angle and rate errors associated with the offsets. The requirement to minimize errors and the requirement to avoid obstructions may not be compatible for all carriers.

In addition to the technical requirements which influence the location of the MLS antennas, the physical construction of the carrier limits the locations available for antenna placement. Since the configuration of each carrier varies because of construction and equipment complement, the individual installation on each carrier will be different. These variations have been considered in the design of the Navy MLS. Several possible sites, with variations in antenna offset distances have been considered. It is shown that for several possible locations and different offset distances, satisfactory operation may be obtained. The elevation and azimuth systems may, in fact, be installed at different locations on the carrier. Thus, the installation of the system aboard the carrier is quite flexible.

Several hypothetical sites have been postulated and the effect of various offset distances investigated. The geometry of the problem involved in a typical installation is shown in Figure D-8. The MLS antenna will be offset from the touchdown point in three dimensions. It will be offset to the side of the canted deck centerline by y feet, forward of the touchdown point by x feet, and z feet above the flight deck. Table D-3 gives some of the site dimensions evaluated (based on actual carriers).

Table D-3. Evaluated Site Dimensions

Site	x (feet)	y (feet)	z (feet)	Notes
A	142	92	57	Island
B	239	92	26	Island
C	-200	0	-10	Ramp edge
D	70	103	24	Between ramp and touchdown

Because the antennas are not located at the touchdown point, the angles measured to the antenna by the aircraft will change as the aircraft flies toward touchdown. As the aircraft nears touchdown, the azimuth and elevation angles measured may become large, and

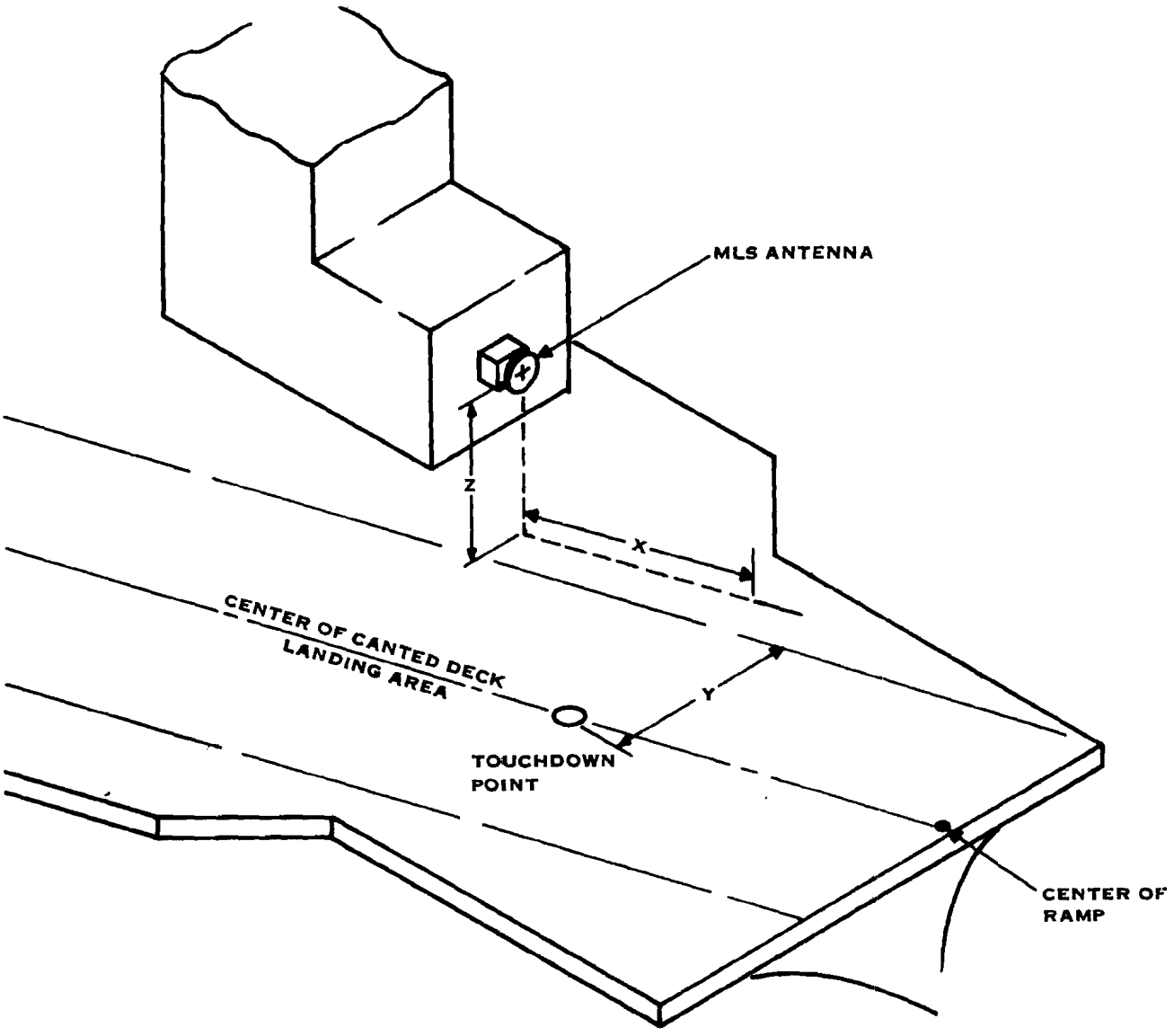

Figure D-8. Siting Coordinate Geometry

the rate of change of these angles may become large. These large values of rates of change can adversely affect the accuracy of computed flight commands to the aircraft. These rates of change are greatest at, and near touchdown. Highest accuracy is required just before touchdown at the data freeze point, which is 1.5 seconds before touchdown. These changes, and rates of change have been calculated by computer for several combinations of offset distances. Plots of angular error for two of these sites are shown in Figures D-9 and D-10. In all cases, an effective glideslope of 3.2 degrees is assumed. These curves indicate the magnitude of the corrections which must be computed by the shipboard computer (or the airborne processor) to provide accurate flight commands to the aircraft.

Of more importance, however, is the rate of change of these parameters because of the limited data rates of the NTDS data link and aircraft dynamic response. The rate of change of these angular measurements is shown in Figures D-11 and D-12. Site C is for the antenna mounted on the stern of the ship below the ramp. This location is undesirable for the

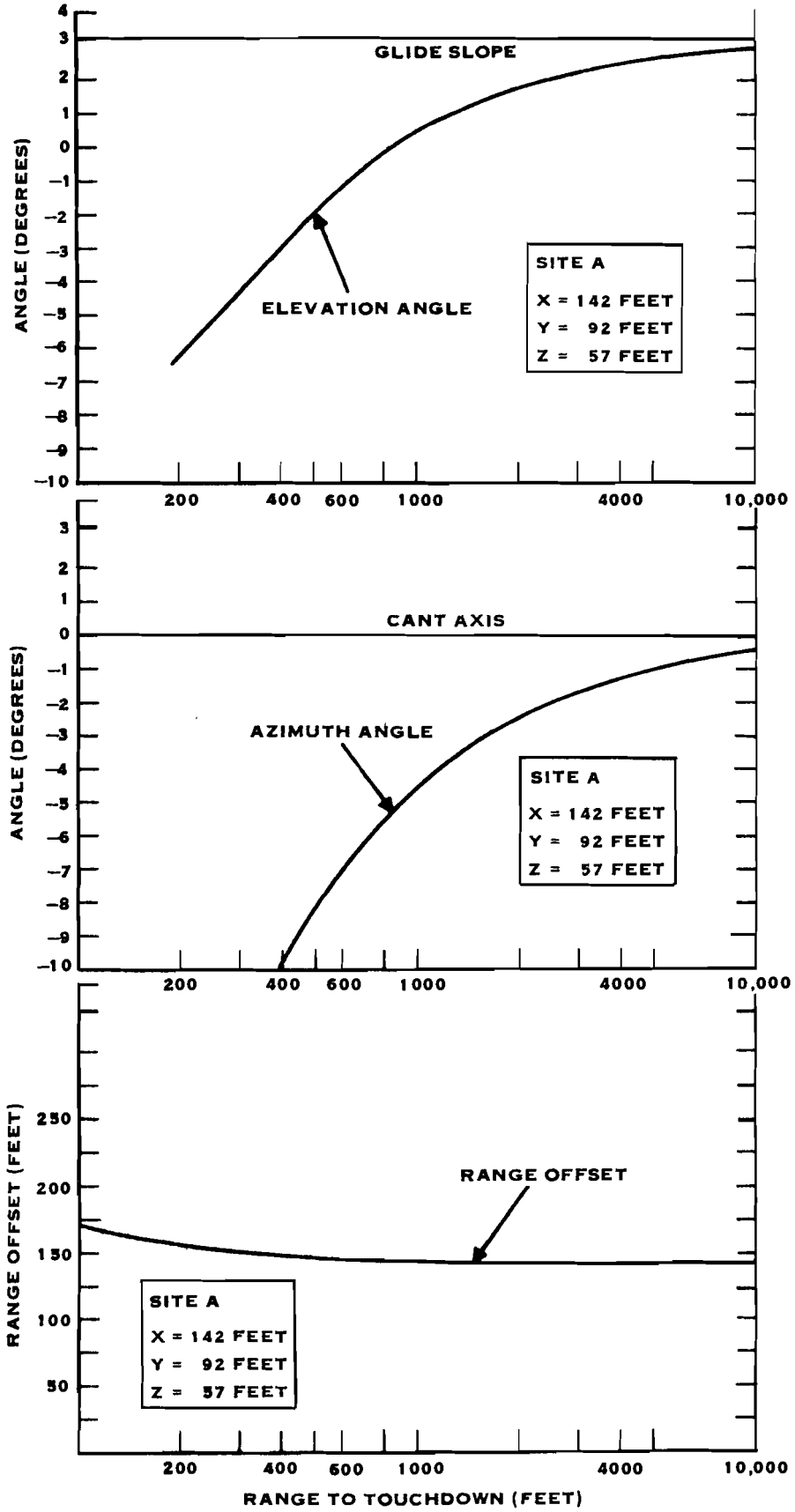

Figure D-9. Angular Error Plots

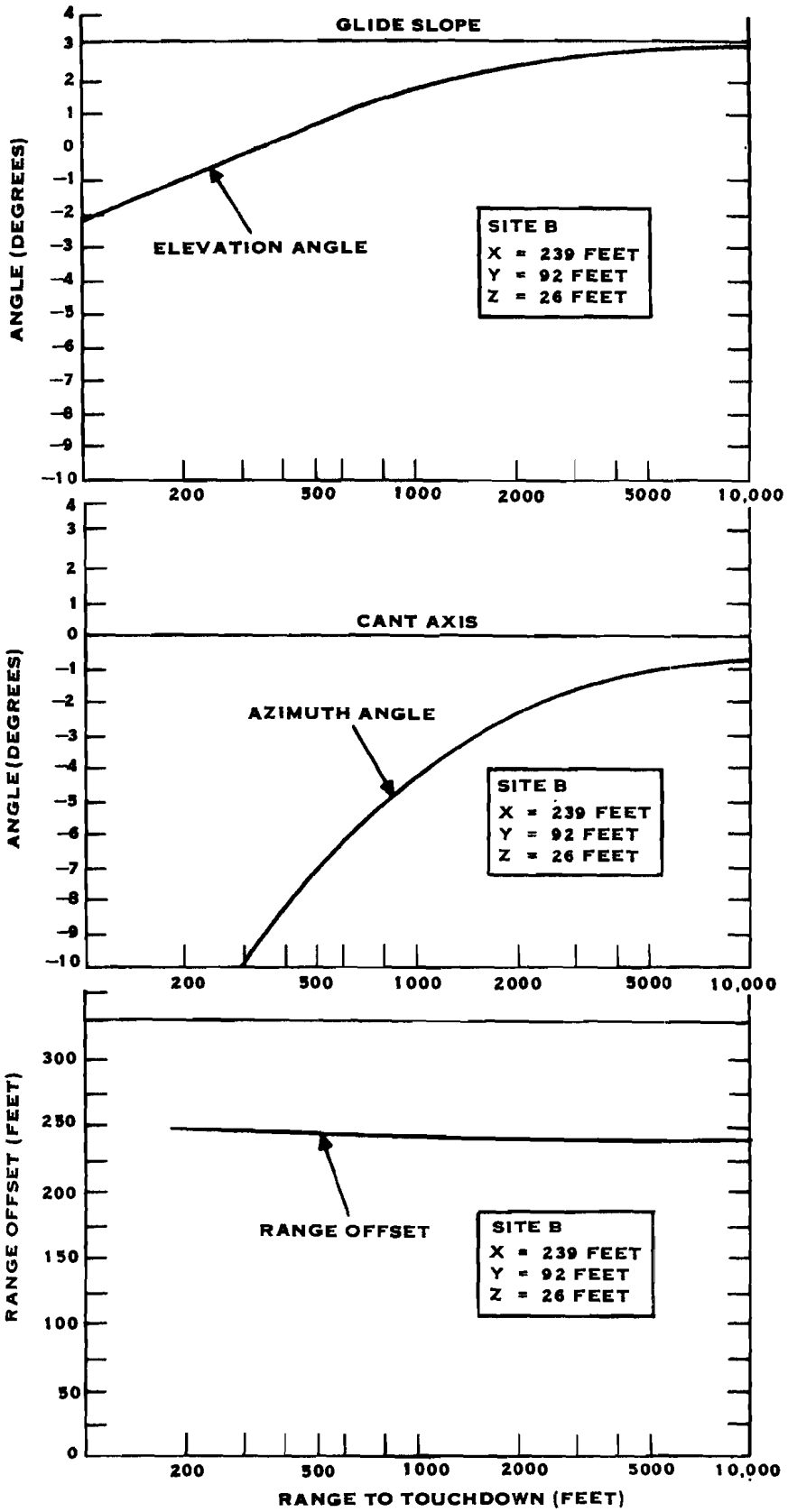

Figure D-10. Angular Error Plots

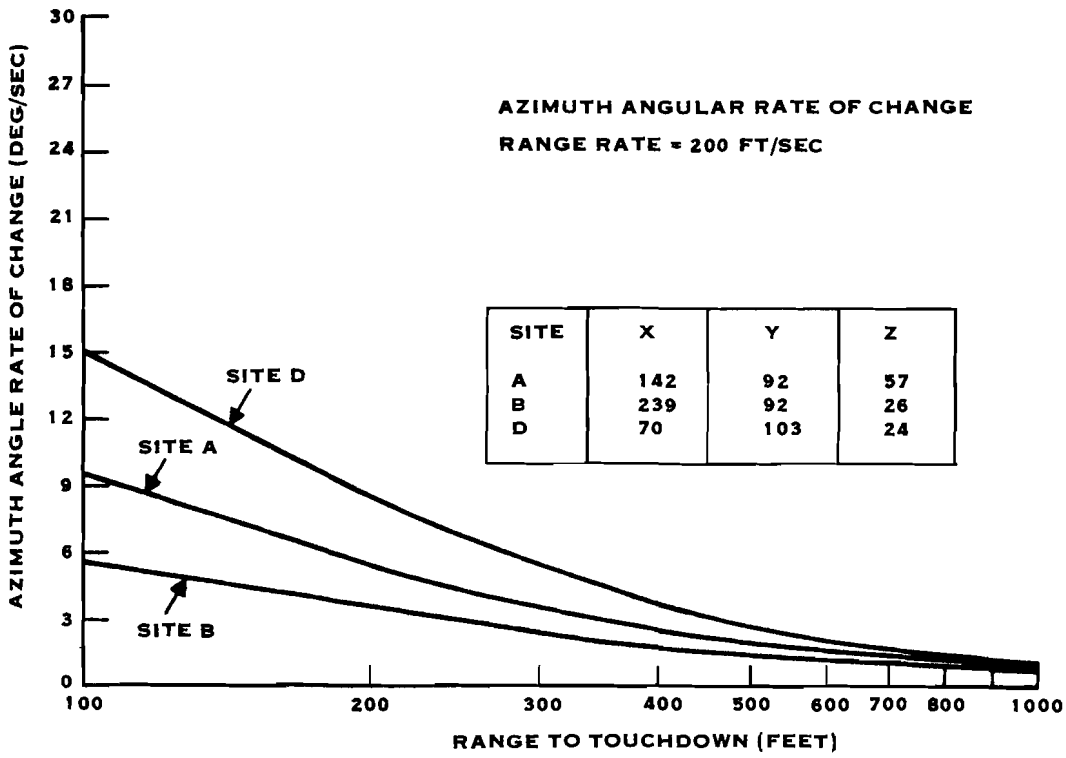

SITE	X	Y	Z
A	142	92	57
B	239	92	26
D	70	103	24

Figure D-11. Azimuth Angular Rate of Change

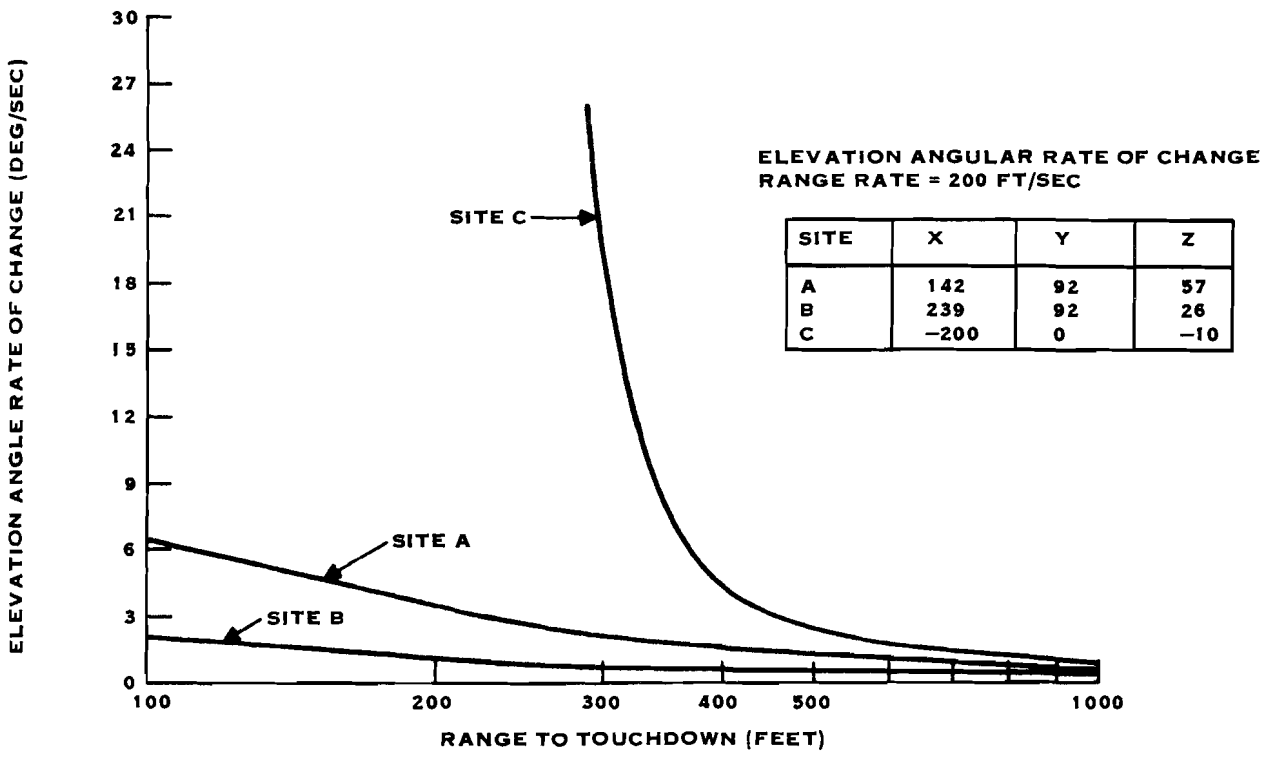

SITE	X	Y	Z
A	142	92	57
B	239	92	26
C	−200	0	−10

Figure D-12. Elevation Angular Rate of Change

elevation antenna because the elevation scan would have to extend up to +90 degrees to provide coverage down to the data freeze point. In addition, it is seen that the elevation angular rate of change becomes excessive. Site D is for a location to the side and forward of the touchdown point with the offset distance forward relatively small. This causes the azimuth angle to the touchdown point to be large and consequently the azimuth angular rate is high. Therefore, this is not a good location for the azimuth antenna.

From a consideration of these requirements, and possible sites, it appears that a location on the island of the carrier, or on a tower aft of the island, is the best choice for placement of the MLS antennas. This location offers adequate unobstructed view of the glideslope path and rates of change of angular data are generally within acceptable limits. In addition, this location is a good choice in terms of reducing problems due to reflections as discussed in Section VII of this appendix.

c. Stabilization

Because the aircraft carrier is in constant motion, the touchdown presents a moving target to the landing aircraft. These motions are roll, pitch, yaw, and heave, as well as the forward motion of the carrier. The acceptable landing area on the carrier is about 130 feet long and 30 feet wide. The acceptable touchdown dispersion for the MLS is ±40 feet longitudinal and ±14 feet lateral (1 σ values) under conditions of motions of a ship listed below:

Roll	5 degrees rms
Pitch	1.25 degrees rms
Yaw	0.25 degrees/second
Heave	4 feet rms
Speed	30 knots

As the aircraft nears the carrier, it must follow the motion of the carrier deck to make a successful landing. Thus, at about 1/2 mile from touchdown, the aircraft begins to follow the deck motions. At longer ranges, the aircraft must fly toward a virtual touchdown point, which is the stable position, with deck motions removed.

In the Mode I (fully automatic) approach and landing, flight commands are sent to the aircraft via the data link. These flight commands have been computed by the shipboard computer, which has all the deck motions as inputs. These deck motions can be eliminated from the flight commands when the aircraft is at a range greater than 1/2 mile. Then, when the aircraft is 12.5 seconds from touchdown, the computer begins to allow the deck motions to be included in the flight command, so that, from that point on to touchdown, the aircraft is increasingly following the motions of the deck. Thus, because flight commands are generated aboard ship and deck motion inputs are available, it would not be necessary to stabilize the MLS antennas.

However, in Mode II, which is a manual landing mode, the pilot flys the aircraft by reference to the crossed needles in the cockpit display. These crossed needles are driven by angular error signals generated by the airborne signal processor. Obviously, no deck motion information is available in the aircraft, and, therefore, the MLS signal in space must

be stabilized. At the weather minimums of 200 feet ceiling and 1/2-mile visibility (15 seconds out), the optical landing aid (FLOS) on the carrier must be in sight, whereupon the pilot continues his landing manually. Thus, even though antenna stabilization is not required for automatic operation, it is a requirement for the manual backup, landing where flight commands are air-derived.

Since stabilization must be included for the manual mode, it must meet the accuracy requirements for Mode I operation. The point of greatest accuracy requirement for the MLS is at the point of data freeze. This is at 1.5 seconds from touchdown or at a range of 300 feet from touchdown, assuming a closing rate of 200 feet per second. The specified touchdown dispersion of ±40 feet longitudinally and ±14 feet laterally with deck motions requires that the elevation error be no greater than +0.376 degree or -0.492 degree and that the azimuth error relative to the canted deck be no greater than ±2.67 degrees. These errors include those contributed from all sources, including aircraft dynamics.

1. Roll Effects

Roll of the aircraft carrier affects the MLS antennas in two ways. First, the beam coverage is changed and secondly, and more importantly, the beam is canted or tilted. The normally vertical fan beam of the azimuth antenna would be tilted to one side or the other by the roll. Thus, a target aircraft would derive azimuth angular data which is in error, the magnitude of which depends upon the amount of roll and the aircraft altitude.

In the case of the elevation antenna, roll causes the normally horizontal fan beam to be tilted. The magnitude and sense of the elevation error caused by roll is dependent on the amount and direction of roll, and the aircraft position in azimuth.

The magnitude of the errors induced by roll is shown in Figure D-13 and Figure D-14. Two values of inclination are shown. First, when the roll stabilization is in operation, the antennas will be stabilized to within ±0.3 degree of true vertical. In the unlikely event of a roll stabilization failure, the platform will be locked in the center position and, thus, the roll of the antennas will be the same as that of the ship (0 to 5 degrees rms). Using these values of inclination for the azimuth and elevation beams, the vertical and lateral errors in feet are plotted as functions of range to touchdown as the aircraft flies down the indicated glideslope path. A glideslope of 3.2 degrees is assumed. The aircraft, when on the glideslope path, is displaced more in azimuth than in elevation from the roll axis (canted deck makes a 10-degree angle with the roll axis, and glideslope is only 3.2 degrees). Because the magnitude of the elevation error is dependent on the aircraft azimuth relative to the roll axis, the elevation errors are larger than the lateral errors. This is shown in the figures which also show that, even for the 5-degree inclination, the errors are well within the allowable errors for a Mode II landing at 3000 feet or 15 seconds from touchdown.

2. Pitch Effects

As the carrier pitches, the azimuth antenna beam is shifted up and down on the keel centerline and is inclined slightly as the antenna is scanned from side to side. The pitch limit for normal operation of the MLS is 1.5 degrees rms or 1.77 degrees peak. This peak limit of pitch results in a beam inclination of 0.58 degree when the antenna is scanned

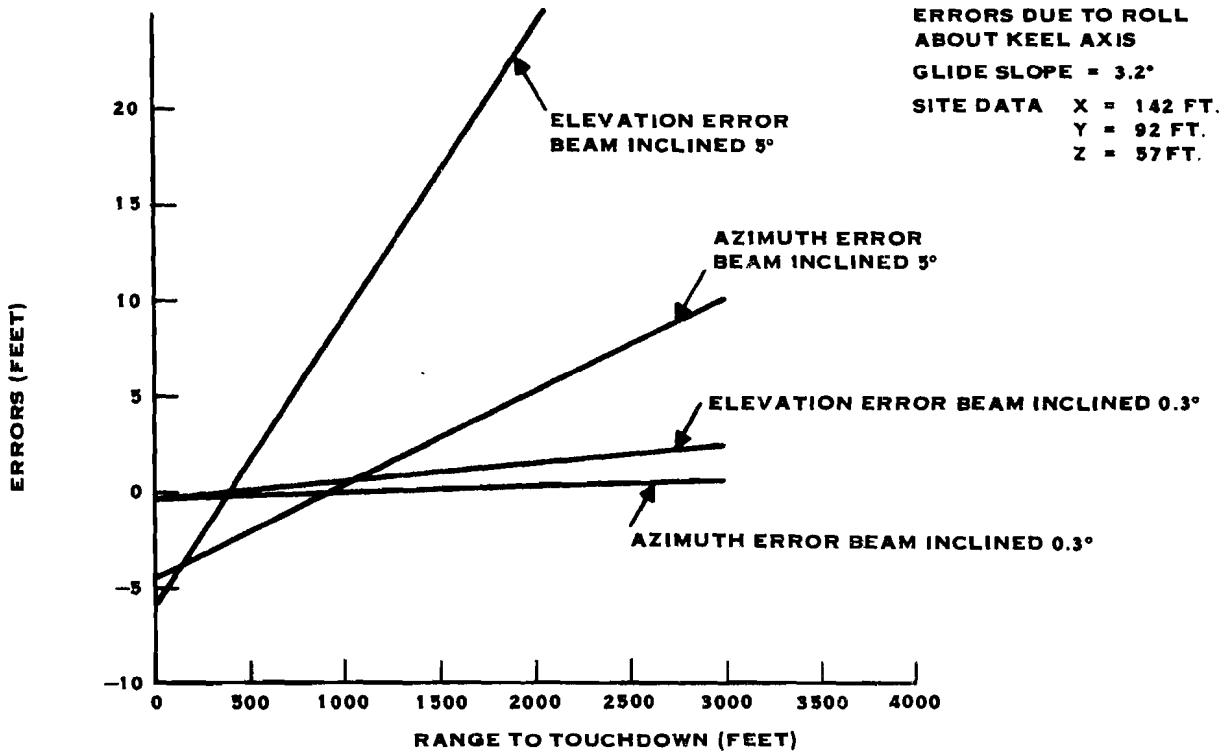

Figure D-13. Errors Due to Roll about Keel Axis

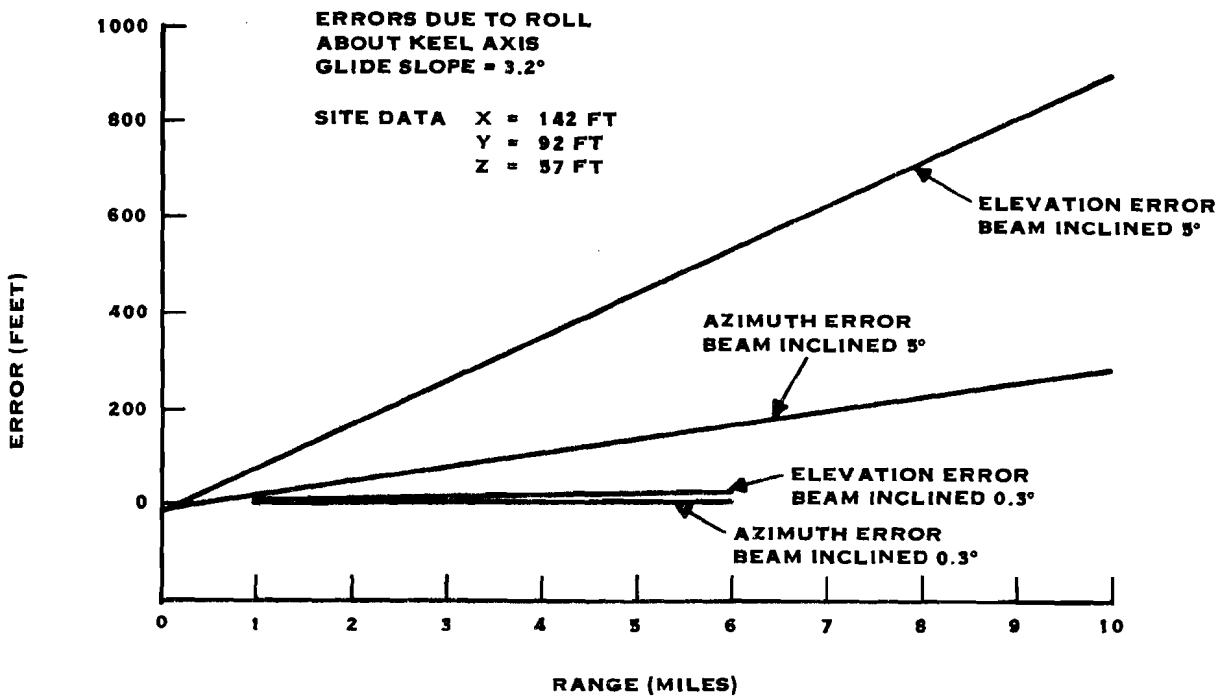

Figure D-14. Errors Due to Roll about Keel Axis

to ±20 degrees. At the cant angle of 10 degrees, there is less than 0.3-degree inclination of the azimuth beam. Therefore, no pitch stabilization of the azimuth antenna of the MLS is recommended.

The elevation antenna will have the same pitch motion as the ship; thus, the elevation beam in space will be shifted up and down with the pitch of the ship. As stated previously, it is undesirable for the aircraft to try to follow the motion of the ship when at far ranges. For example, for an uncorrected elevation beam with a pitch of 1.77 degrees, the elevation change for a 3.2-degree glideslope would be approximately 1900 feet at 10 miles. It is obviously unnecessary and impractical for the aircraft to try to follow these elevation changes. Thus, the elevation antenna beam must be stabilized in space. This is done in the MLS shipboard system by electronically stabilizing the beam in space by correcting the frequency of the angle tone by the amount of the mechanical pitch. Thus, the elevation beam angle tones are stabilized in space and provides a stable glideslope path regardless of the pitch of the ship.

In Mode II the pilot will fly the selected glideslope by reference to the cockpit display until he is 1/2 mile from touchdown. At this point, he will use the optical landing aid on the carrier to complete his landing.

In Mode I, the flight commands computed computed by the shipboard computer will be transmitted to the aircraft via the data link. These commands will be for the stabilized flight path until the aircraft reaches the point where it must begin following the deck motion. At this point, the computer re-inserts the pitch motion into the generated flight commands. The aircraft then follows the deck motion to touchdown.

The stabilization by electronic means is limited by the accuracy of the pitch sensors. Stabilization over a ±3-degree range to an accuracy of ±0.1-degree is feasible and is recommended for the Navy MLS.

3. Yaw Effects

The basic yaw period is 40 seconds for yaw produced by the helmsman's rudder control, and a faster 12- to 14-second period produced by wave effects on the bow of the ship. It is undesirable for the aircraft to follow short period yawing of the ship at long ranges, but it is essential for the aircraft to follow the yaw at short ranges and long-period yaw at long ranges.

The MLS elevation antenna beamwidth is wide and requires no yaw stabilization. The yaw stabilization is applied only to the azimuth scan such that the heading of the aircraft is essentially constant despite short-term navigations in the ship's course. Long-term changes in ship's course must result in the MLS designated boresight maintaining alignment with the ship's course. To solve both the short- and long-term changes in heading, the MLS azimuth alignment must tend toward boresight at a small constant slew rate (a rate of approximately 0.1 degree per second) whenever an angular displacement has resulted from yaw. When rapid changes in yaw cause a large displacement, the slewing must cease and the MLS centerline follows the yaw of the ship with a lag of about 3 degrees until the yaw rate becomes less than the slew rate. This solves both the long- and short-term stabilization problems for Mode II. For Mode I, the offset centerline designation because of yaw is known and the factor can be removed by computation and the aircraft will follow ship's yaw at short

ranges. The stabilization of MLS is electronic and the accuracy of the stabilization is limited primarily by the yaw sensor (ship's Mark 19 gyro).

4. Heave Effects

The limit of ship's heave during MLS landing operations is given as 4 feet rms. This translation of the ship's position will not adversely affect the angles presented to the aircraft at long ranges. At short ranges, however, this position translation does result in a change of the elevation angle. At 3000 feet, heave results in an angular change of about ±0.1 degree which is acceptable for Mode II landings. This elevation angular change increases as the aircraft flies toward touchdown, until at the data freeze point of 300 feet, the angular change increases to ±1.0 degree. These errors due to ship's heave are simply elevation errors and are processed as such during a Mode I landing. Thus, the aircraft will follow the deck motion because of heave as it does any other deck motions.

d. Conclusions

It has also been shown that for the Mode I, fully automatic landing, stabilization of the MLS antennas is not required, because the shipboard computer can make the proper corrections. However, it is desirable to roll stabilize both antennas to prevent large changes in antenna coverage.

During Mode II operations the beams must be stabilized so that the aircraft does not attempt to follow the deck motion at long ranges. The accuracy requirement is only that they be within acceptable limits to continue the landing with the aid of the shipboard optical landing aid when the aircraft breaks out at weather minimums of 200 feet and 1/2 mile. Stabilization accuracies of ±0.3 degree for the roll stabilization (which is mechanical) and ±0.1 degree for the electronic stabilization of pitch and yaw are acceptable.

The study of possible locations for the MLS antennas onboard the Navy aircraft carrier indicates that the location is not overly critical with the shipboard computation configuration chosen by Texas Instruments/TH-CSF. Within certain requirements of coverage and rate of change of data, the installation may be quite flexible. However, the logical choice of a mounting location is on the carrier island or on a tower on the starboard side of the ship just aft of the island. The antenna at this location is high enough above the flight deck so that the beam is not obstructed by parked aircraft or other objects.

VII. POWER PROGRAMMING FOR NAVY SHIPBOARD SYSTEMS

In a typical MLS installation aboard a Navy aircraft carrier, the MLS antennas will most likely be mounted higher than the touchdown point. Using a nominal antenna location of 40 feet above the flight deck and a zero-degree elevation scan angle (flat), an aircraft would still be at an altitude of 40 feet above the touchdown point and some 764 feet from the touchdown when on a 3-degree glideslope. Since guidance information must be provided to the aircraft within 300 feet of touchdown (the "freeze" point), the elevation antenna must scan to negative angles. This downscan of the elevation antenna can give rise to problems because of reflections off the flight deck of the carrier and the surface of the sea.

a. Deck Reflections

Reflections off the flight deck are considered first. A typical installation is shown in Figure D-15A. An aircraft approaching the touchdown point will be lined up with the flight deck which is canted at a 10-degree angle relative to the carrier. Any energy reflected off the deck will be essentially directed to the rear and to the port side of the carrier; thus, it will not cause any problem for an aircraft on the proper approach. Figure D-15B also shows that any specular reflection from the elevation antenna will be well above the glideslope. It is unlikely that any reflection at the MLS operating frequency (Ku-band) will be purely specular. It will be further complicated by parked aircraft, deck vehicles, and other obstructions. Any non-specular reflections received by the aircraft will be less than the receiver threshold level and, thus, will not result in false angular data being generated.

b. Sea Reflections

The reflections from the surface of the sea could pose a much more severe problem. Nathanson[2] gives the forward scattering coefficient for power reflected from the surface of the sea as

[2]Nathanson, Fred E., "Radar Design Principles" McGraw-Hill Book Co., New York 1969

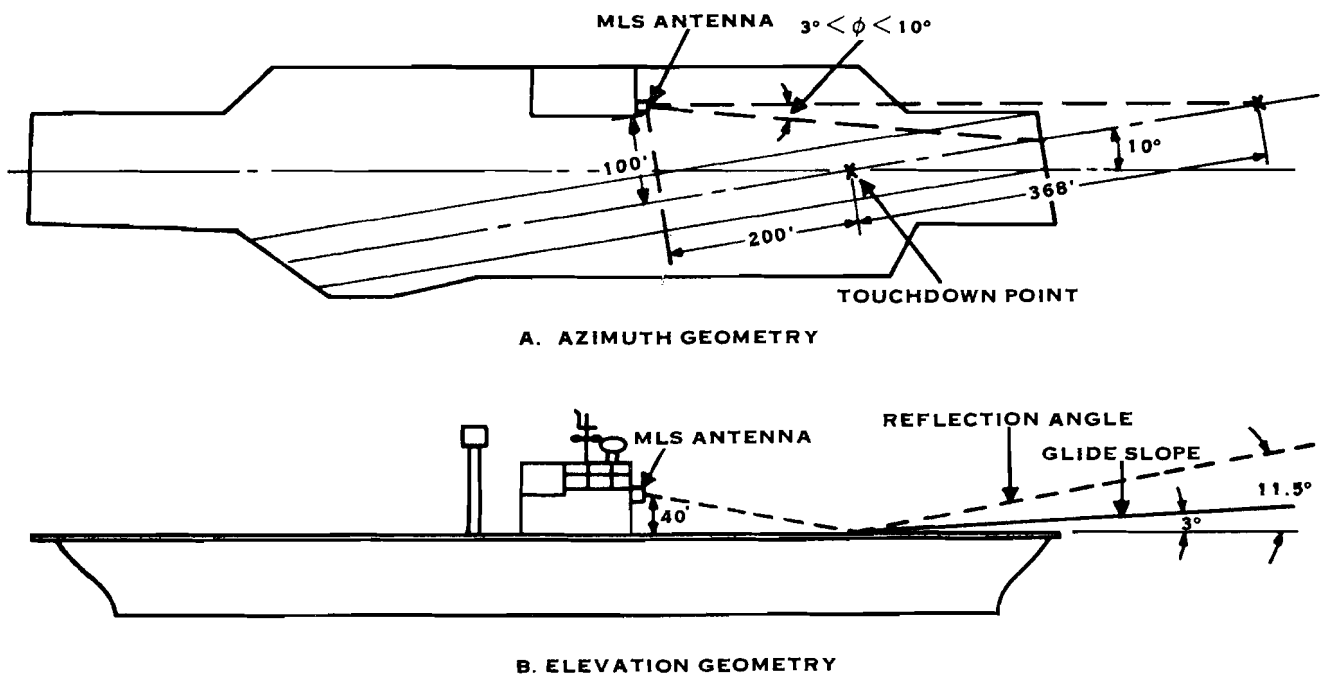

Figure D-15. Typical Carrier Deck Reflection Geometry

$$= e^{-\left(\frac{8\pi^2\sigma_h^2}{\lambda 2} \sin^2\psi\right)}$$

where

$\bar{\rho}$ = average value of forward scattering coefficient

σ_h = variance of the surface height about the mean height

λ = signal wavelength

ψ = grazing angle

Figure D-16 is a plot of the forward scattering coefficient for sea state 1 and sea state 3 as a function of the grazing angle at 15.5 GHz. For sea state 1 the forward scattering coefficient is 0.7 at a 1.0-degree grazing angle. Thus, for a sea state 1, the energy received by the reflected path would be down only 1.5 dB from the direct path for a grazing angle of 1.0 degree. At 2.0 degrees the difference is 6.6 dB. Also, it is seen from the plot that, at very small grazing angles, the scattering coefficient is large for all sea states. The curve shows it to be unity, but this neglects the shadowing caused by the surface roughness, the

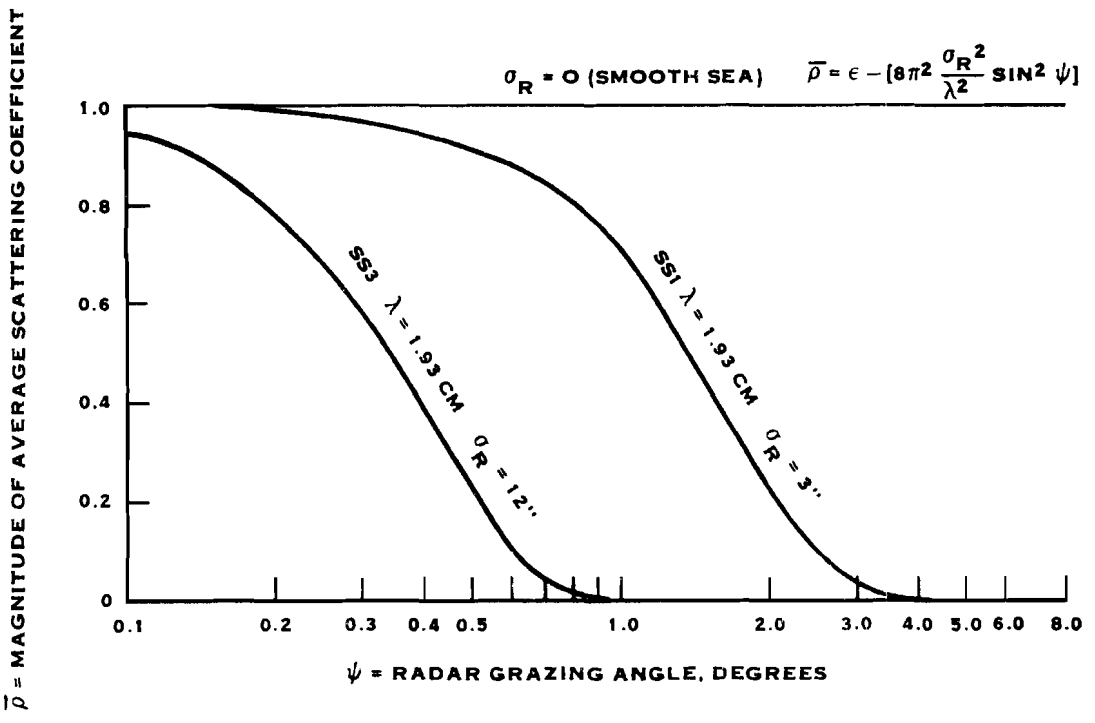

Figure D-16. Forward Scattering Coefficient from Surface of Sea

divergence due to a non-flat reflecting surface, and the absorption by spray and water droplets near the surface.

If we assume that the landing aircraft will remain above some minimum glideslope, a lower limit on the reflection angle may be established. Figure D-17 shows the geometry of the situation. For an aircraft at a 10-mile range and on a 2.0-degree glideslope (lower wave-off limit), the elevation antenna pointing angle is +1.96 degree. For the reflected energy to be received by the aircraft, the antenna scan angle must be -2.08 degrees (4.04 degrees below the aircraft). The reflection coefficient is 0.2, and, thus, the reflected energy received by the aircraft is only 7 dB below the energy received by the direct path.

The airborne receiver detects the peak of the received signal and uses this level as a reference for setting a threshold level on the next scan of the shipboard antenna. Whenever the received signal exceeds the threshold level, a conditional dwell gate is generated. This conditional dwell gate is used to inhibit the DME interrogator, to enable the sample gate to detect a new value of peak received signal, and to process angle data in the event the normal dwell gate does not provide good data. The threshold for the conditional dwell gate is set 8 dB below the peak signal. Thus, a reflected power level only 7 dB below the peak can generate a false dwell gate unless steps are taken to prevent this from happening.

Thus, in the case assumed above, i.e., an aircraft on a 2-degree glideslope, as the transmitter antenna scans downward, a conditional dwell gate will be generated by the direct path as the antenna scans through +2 degrees. Another conditional dwell gate (delayed in time) will be generated by the reflected energy as the antenna scans through -2 degrees even though the reflected power is 7 dB lower than the direct signal.

One method of avoiding this problem is to reduce the power transmitted by the elevation transmitter when the elevation antenna is scanned to angles below 0 degree. Since the ranges to the aircraft will be shorter in this area there is no accuracy penalty from reduced S/N ratios. A linear reduction of transmitter power of 2 dB per degree for scan angles below 0 degree will give a power reduction of 4 dB for the case cited above. Since the conditional dwell-gate threshold is set at -8 dB, the reflected power is down 7 dB due to the reflection coefficient, an additional 4 dB from transmitter power programming will provide a 3-dB margin, and, thus, prevent the generation of false dwell gates. For aircraft on steeper

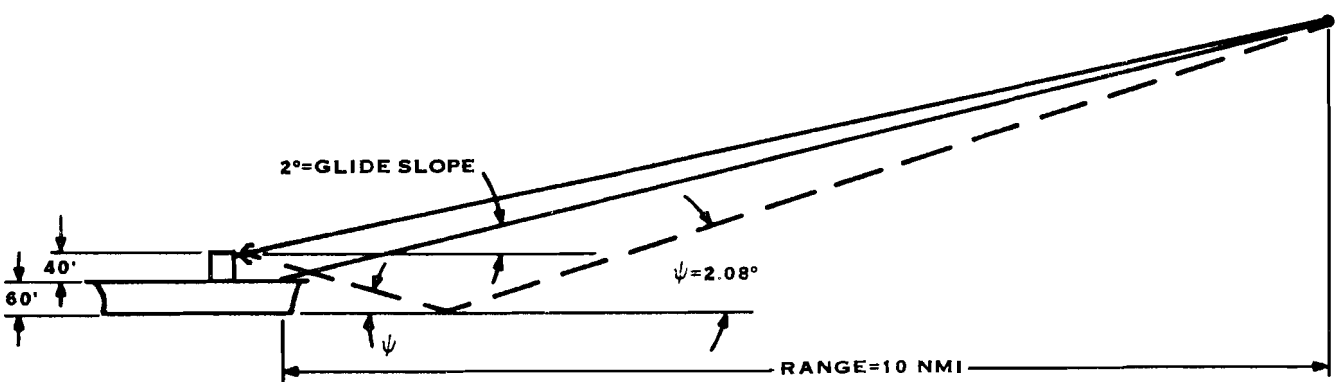

Figure D-17. Angle of Reflection from Sea

glideslopes, the scan angle required for the reception of reflected energy is greater. This improves the situation in two ways. First, the scattering coefficient is less, so that less reflected/scattered power is received at the aircraft. Second, the actual transmitted power at negative angles is reduced, resulting in less reflected energy being received at the aircraft.

The previous example was for a sea state 1. For rougher sea conditions the forward scattering coefficient decreases rapidly. For example, for sea state 3 and a grazing angle of 0.6 degree, the scattering coefficient is only 0.1, or the reflected power is down by 10 dB (not including power programming). However, if aircraft must be recovered when the sea state is smoother than sea state 1, the opposite situation exists. For a perfectly smooth sea, the forward scattering coefficient becomes approximately unity for all angles. In this case, much greater power programming rates would have to be employed to prevent generation of false dwell gates by the reflected energy. This could possibly generate other errors which might be serious. However, the probability of the occurrence of a sea state 0 is very small. In the unlikely event that aircraft are being recovered under these conditions, the wake and turbulence in the sea generated by the carrier itself will probably be sufficient to prevent operational problems because of reflections.

c. Power Programming Error Analysis

Two possible errors resulting from reducing transmitter power as a function of scan angle are (1) an apparent distortion of the antenna pattern which results in an angular error, and (2) a reduction of power received by the aircraft from one sample time to the next, which results in the actual threshold for the dwell gate being something less than 3 dB.

The apparent received signal distortion as a result of transmitter power programming is illustrated in Figure D-18. The true antenna pattern is shown as the solid line, with the desired dwell gate occurring between the -3 dB points. When the transmitted power is varied as the beam scans by the receiver, a distorted pattern is received. Since the peak of the beam is used by the receiver as a reference to set the threshold levels for generating the dwell gates, this point is taken as the reference. At elevation angles below the peak, the received power will be less than the undistorted pattern. Thus, the distorted pattern as shown by the dashed line results. The actual received power crosses the threshold level at an angle point above the undistorted pattern threshold for both the start and end of the dwell gate causing an offset of the dwell gate and causing the average angle tone frequency to be higher than the correct value. This error indicates that the aircraft is too high, and will, thus, cause the aircraft to fly too low if not corrected.

The magnitude of this error is a function of the antenna beamwidth (and pattern shape) and the rate of transmitter power reduction. Using the power reduction of 2 dB per degree, and a 0.75 degree beamwidth, an elevation angular error of 0.068 degree is introduced. This corresponds to an angle tone frequency error of 34 Hz. This error is constant for a linear power reduction (dB/degree).

Among the several possible means of correcting this fixed offset error caused by the programmed reduction of transmitter power are the following:

Program the airborne processor to correct for the fixed error whenever the measured elevation angle is less than zero degree

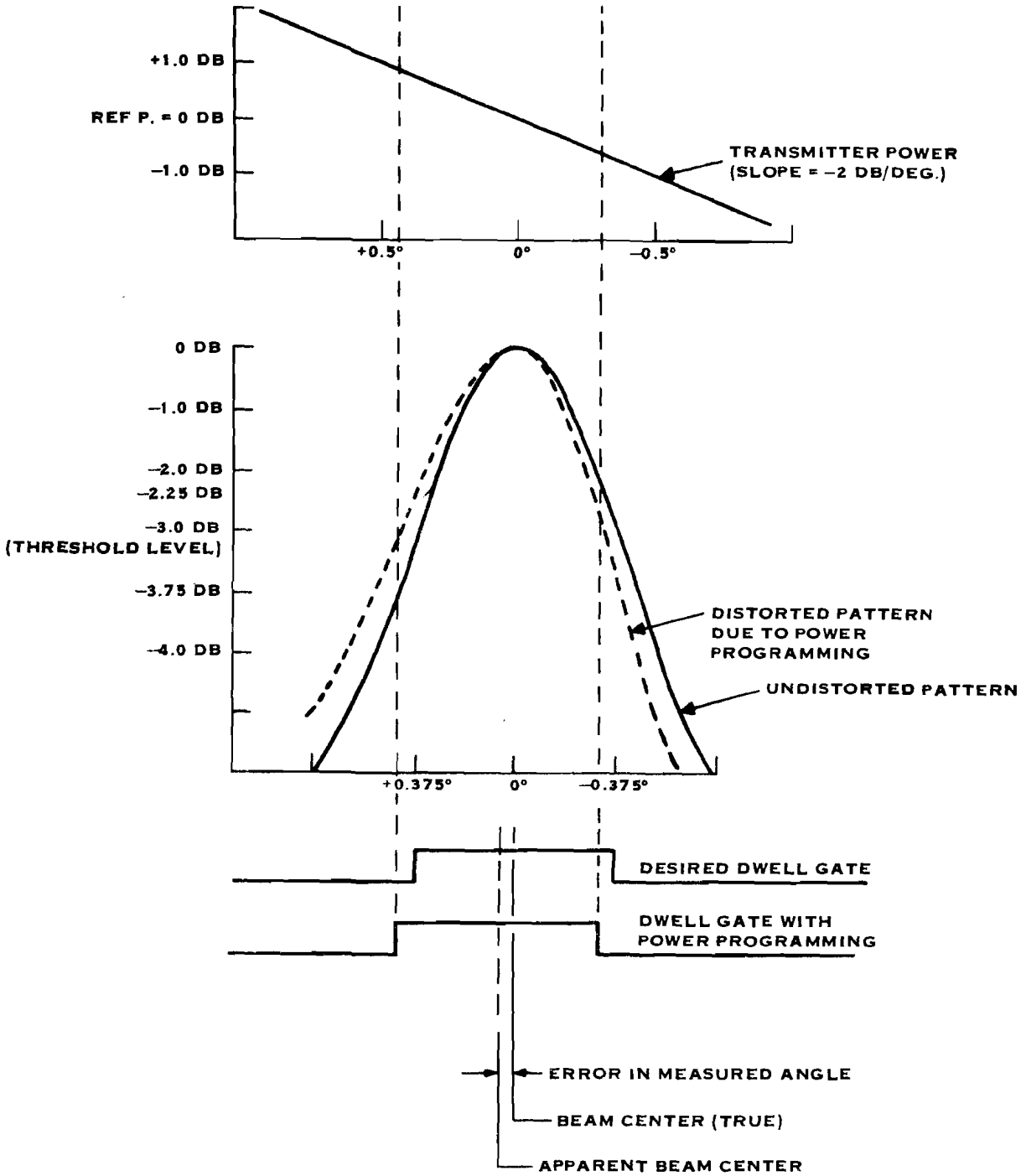

Figure D-18. Antenna Pattern Distortion Due to Transmitter Power Programming

Program the shipboard computer software to correct for the error when generating aircraft flight commands

Introduce a frequency offset in the tone generator for angles less than zero degrees.

It appears that the second solution offers the most flexible solution with the least impact on hardware and commonality of MLS systems. There would be no change in any of the MLS system hardware. Also, this method offers the flexibility of changing the rate of power programming to provide optimum performance for various sea state conditions if required.

One other aspect of programming transmitter power which must be investigated is that of the change of power received by the aircraft receiver on successive update times. Referring again to Figure D-17, it is seen that the aircraft enters a region of changing transmitter power only when it is at an altitude below the elevation antenna. On a given glideslope, the aircraft will be at very short ranges from the antenna whenever it enters this region. For a typical installation and the normal 3-degree to 4-degree glideslope zone, the aircraft will be 572 to 764 feet from touchdown when it enters the region of power reduction. The power received by the airborne receiver is plotted in Figure D-19. The received power is plotted versus range to the antenna for two different transmitter output powers for a 3-degree and a 4-degree glideslope.

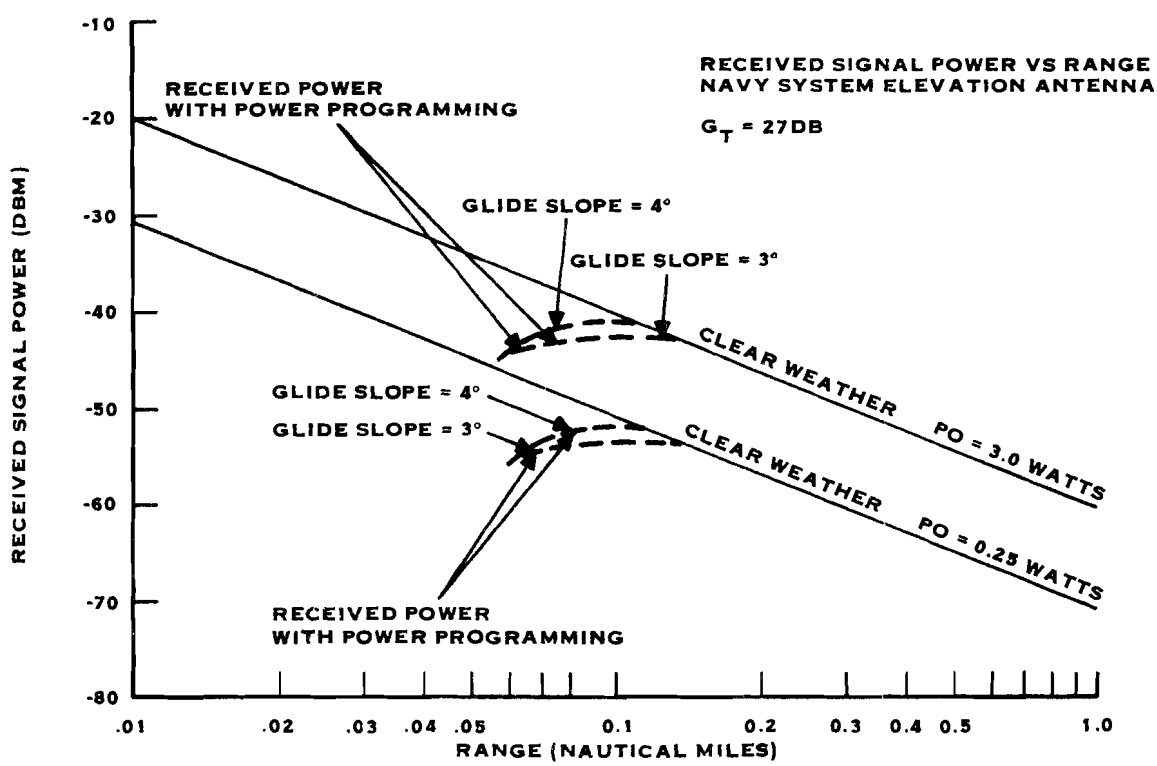

Figure D-19. Received Signal Power Versus Range, Navy System Elevation Antenna

The point of interest in plotting these curves is to determine the magnitude of the change of peak signal from one antenna scan to the next. The threshold level used by the receiver angle data system is determined by the peak of envelope of the last previously received signal. Thus, if the amplitude change is excessive from one antenna scan to the next, the actual threshold level departs markedly from the -3-dB level.

Figure D-19 shows the received power as a function of aircraft range to the antenna. What is needed is a plot of received power as a function of time. This is shown in Figure D-20, assuming an aircraft closing speed of 1200 feet per second. It is seen that at times greater than 1.5 seconds (the data freeze point), the maximum power change in any 0.1-second period (the data update time) is only 0.1 dB or less. The sampled data threshold will depart from the -3.0-dB level by only 0.1 dB and no problems will result from this small change. For aircraft approach speeds less than 200 feet per second, even smaller changes would occur.

d. Conclusion

In conclusion it can be said that power programming will be a viable technique for reducing the effects of reflections on the Navy MLS.

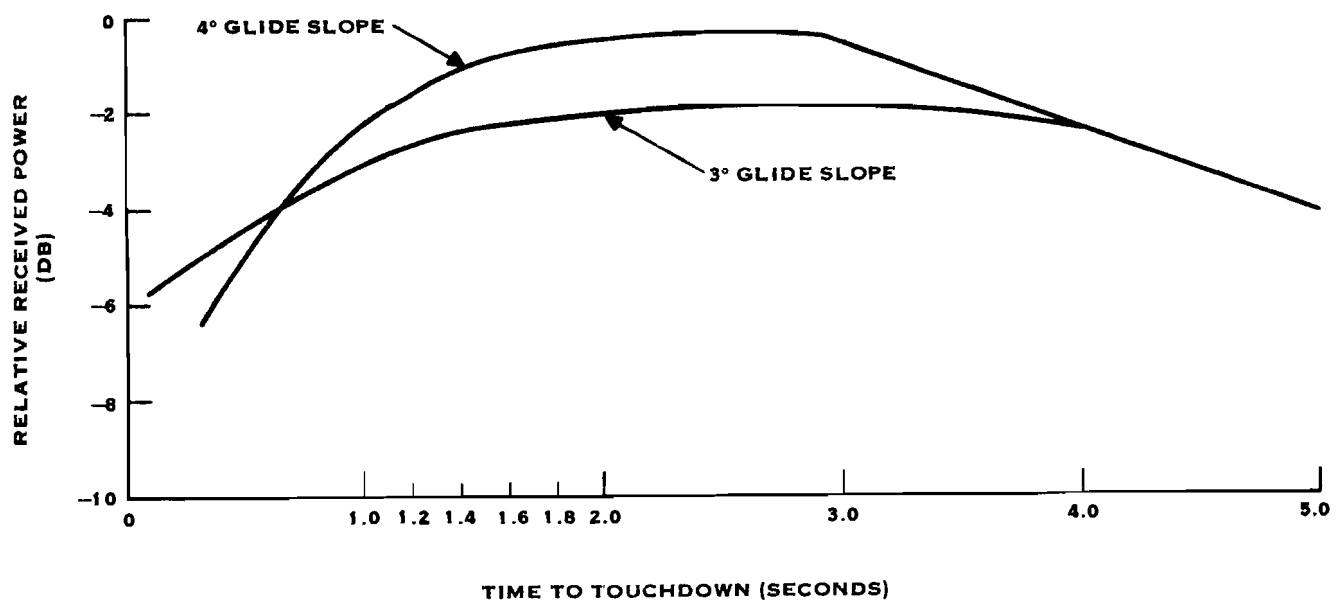

Figure D-20. Received Power as a Function of Time

VIII. A-7E CARRIER LANDING SIMULATION RESULTS (LEAR SIEGLER INC., ASTRONICS DIVISION)

This section presents the final report of a carrier landing simulation effort conducted by the Astronics Division of Lear Siegler, Inc. The flight dynamics of the A-7E aircraft and the MLS error models used during the civil L-1011 simulations previously accomplished were used to investigate the suitability of the MLS concept for carrier landing application. To simplify the study only ship heave, wind, turbulence (air wake), aircraft dynamic equations, and ship's forward motion were incorporated. The effect of using the MLS beam information for rate information versus using accelerometer derived data were evaluated with various information update rates. The results indicate that the MLS concept can be configured to provide highly accurate and safe automatic landings onboard a moving aircraft carrier. A more complete simulation which will include the effects of pitch, roll, and yaw with an updated MLS error model, is proposed as a necessary effort during Phase II.

LEAR SIEGLER, INC.

ASTRONICS DIVISION

3171 SOUTH BUNDY DRIVE
SANTA MONICA, CALIF. 90406
AREA CODE 213 391-7211

Prepared for
Texas Instruments
Equipment Group
Austin, Texas
Under TI Purchase Order 531402

ADR-770

REPORT
MICROWAVE LANDING SYSTEM STUDY
TASK 4 – CARRIER LANDING
(TI REPORT KEY III C12)

18 August 1972

TABLE OF CONTENTS

		Page
	REFERENCES	iii
1.	INTRODUCTION	1-1
2.	STATEMENT OF PROBLEM	2-1
3.	STUDY OBJECTIVES	3-1
4.	SUMMARY AND RECOMMENDATIONS	4-1
5.	SIMULATION AND SYSTEM MODELING	5-1
5.1	Aircraft Dynamics and Geometry	5-1
5.2	Ship Geometry and Dynamics	5-1
5.3	Aerodynamic Disturbances (Air Wake)	5-5
5.4	MLS Models and Simulation	5-5
5.5	Control System	5-13
5.6	Simulation Diagrams	5-13
6.	EVALUATION TECHNIQUES	6-1
7.	STUDY RESULTS AND DISCUSSION	7-1
7.1	General	7-1
7.2	MLS Derived Altitude Rate	7-4
7.3	MLS Filtering	7-4
7.4	MLS Scan Rates	7-5
7.5	MLS Computational Requirements	7-5

APPENDIX A: Stochastic Landing Results
APPENDIX B: Activity Traces

LIST OF ILLUSTRATIONS

Figure		Page
5-1	Carrier Geometry (CVA-64)	5-4
5-2	Power Spectral Density of Horizontal Velocity Turbulence Astern the Carrier.	5-8
5-3	Power Spectral Density of Vertical Velocity Turbulence Astern the Carrier.	5-9
5-4	Variation of Horizontal Velocity Turbulence Power Spectral Density Parameters with Distance Aft of Ramp	5-10
5-5	MLS Receiver Beam Error Models	5-11
5-6	MLS Receiver Sampling and Computational Delay Simulation.	5-12
5-7	MLS Carrier Landing Block Diagram -- Configuration 1	5-14
5-8	MLS Carrier Landing Block Diagram -- Configuration 2	5-15
5-9	Autothrottle Block Diagram	5-16
5-10	Overall Simulation Diagram	5-17

REFERENCES

a) "An Analysis of Navy Approach Power Compensator Problems and Requirements," STI Report No. 197-1, March 1971.

b) "Environmental Conditions of Ship Motions and Vibrations for Design of Radar Systems on Destroyers and Aircraft Carriers," David Taylor Model Basin Report No. 1298, July 1959.

c) "An Experimental Study of the Dynamics and Steady-State Flow Disturbances Encountered by Aircraft During a Carrier Landing Approach," Oceanics, Inc., Report No. 65-21, March 1965.

d) "Proposal to Perform Studies in Support of MLS Program," ASD 72-014/1, Lear Siegler, Inc., 24 February 1972.

e) "Purchase Order 531402 Task Revision," TWX, 3 August 1972, TI, Austin, Texas, to LSI Astronics Division.

f) "U.S. Navy Aircraft Accident Statistics," U.S. Naval Aviation Safety Center, 29 October 1964.

1. INTRODUCTION

An international group of government and industry landing system experts have spent several years formulating requirements and developing specifications for a system to replace the present VHF/UHF Instrument Landing System (ILS). The culmination of their effort was "A New Guidance System for Approach and Landing," Document No. -148, 18 December 1970, prepared by SC-117 of the Radio Technical Commission for Aeronautics (RTCA). Based on this work, the Federal Aviation Administration (FAA) prepared a "National Plan for Development of the Microwave Landing System" and subsequently issued, on 21 June 1971, a request for proposal, No. WA 4M-2-0021, for the development of a Microwave Landing System (MLS). It is FAA's intent to fund development, over a 5-year period, of an MLS based upon SC-117's report.

One of the six Phase 1 contractor teams selected by FAA is Texas Instruments/Thomson CSF who have selected the Astronics Division of Lear Siegler, Inc. (LSI) to perform studies in support of TI's effort during the Techniques Analysis and Contract Definition Phase.

LSI's studies in support of this effort consist of several tasks intended to provide the TI team with technical expertise in the airborne portion of the MLS as it would interface with aircraft systems such as cockpit instrumentation and flight control systems.

The results of Task 4.0, "Carrier Landing Study," are documented in this report. The A-7E aircraft and USS Constellation, CVA-64, were used for this study. Originally, "Pilot Factors Study" was intended for this task (Reference d). However, it was redirected by TI to accomplish a simplified carrier landing study (Reference e).

2. STATEMENT OF PROBLEM

Carrier landings are regarded as one of the most exacting airplane operations. The small dimensions of the carrier deck, its heaving, pitching, and rolling motions, and the rapid closure rates associated with high landing speeds of high performance aircraft combine to require exceptional intelligence, integrity and response from the autopilot. This is evident from the available operational data (Reference f). The accident rate for carrier landings is excessive, about two order of magnitude higher compared to operations on fixed fields.

To predict carrier landing performance and safety accurately, a simulation should include proper modeling of all the sensitive parameters, particularly disturbances which are external or internal to the aircraft itself. The latter includes variations due to weight, center of gravity, component tolerances, sensor errors, etc. The external parameters are broadly classified as:

- Atmospheric Conditions
- Ship Motion and Geometry
- MLS Characteristics
- Data Stabilization

Each group includes several parameters which are either random or deterministic in nature. Many of them are independent, but a few are statistically dependent on others. The models to be used for simulation should be based on the spectral characteristics, distribution functions and joint densities where required.

The carrier landing safety should be demonstrated with a risk factor of less than one in 10^5 or better. The very nature of this requirement and the random characteristics of the disturbances indicate a need for statistical performance study. The study should include a large number of simulated landings in the presence of these disturbances.

For realistic results all the hardware limitations, such as scaling limits, control surface authority and rate limits, and nonlinearities such as hysteresis should also be included.

Due to these complexities, a detailed carrier landing study which can accurately predict landing performance is beyond the scope of this task. The basic objective is to investigate the suitability of MLS for carrier landing application; hence, to simplify the study, only the ship heave motion (Reference e) was utilized for a carrier disturbance. The winds, horizontal and vertical turbulence (air wake), MLS characteristics, and ship geometry were included in the study since they have a significant effect. Other variables were not included for this study.

It may be noted that, as per Reference f, ≈ 80 percent of carrier landing fatalities are due to hard landings and undershoots and these are largely caused by heave motion. Hence this study, though simplified, provides an understanding of the most important aspect of the carrier landing problem.

To summarize, the following steps are necessary for carrier landing study:

a) Formulation of mathematical models for the landing system and related disturbances.

b) Computation of performance and touchdown landing dispersions, mainly the longitudinal distance and sink rate of touchdown.

c) Integration of measured dispersions into performance and safety indices.

3. STUDY OBJECTIVES

The primary requirement for this study is to examine suitability, capability and limitations of the MLS system for providing the intelligence and integrity required by the aircraft to safely land on the carrier with an acceptably low risk rate. Hence the study was aimed at meeting the following objectives:

a) Establish performance and safety criteria.

b) Define a carrier landing system which provides good performance under nominal conditions.

c) Examine effect of MLS noise on performance and activity.

d) Evaluate filters for minimizing the effect of MLS noise.

e) Investigate the possibility of complementing or replacing the output of other sensors with MLS derived information.

f) Examine effect of MLS sampling rate, filters and blenders on system stability, performance and activity.

g) Conduct sensitivity study to identify the parameter which affects the performance most. Future studies should be oriented to minimize the effect of this parameter.

h) Define problem areas which require further studies.

4. SUMMARY AND RECOMMENDATIONS

The major problem in automatic carrier landing is to develop a landing control system which is sufficiently precise to meet the stringent performance and safety requirements in the presence of ship's motion, air wake, guidance signal noise and irregularities. Two configurations were developed; both use MLS information for position error. Configuration 1 uses rate information derived from MLS, whereas Configuration 2 uses the rate information derived from accelerometer.

The performance evaluation was based on stability, control activity, flow rate requirement, sensitivity to MLS sampling rate, and landing performance/safety. The safety criteria is defined by allowable sink rate at touchdown (-21 fps maximum) and landing zone (between 0 feet and 460 feet beyond the ramp). Based on available statistical accident data (Reference f) a goal of 10^{-5} was established for landing hard or for landing short. The risk factor for longer landings, which result in aircraft bolter, cannot be established because the risk factor associated with the resulting go-around mode is not known.

To minimize the effect of MLS noise and sampling rate, a 0.5-second rate limited filter was used. Configuration 1 uses lower gain, but still has high position and rate activity due to rate information derived from MLS. Attempts to reduce activity by reducing the filter rate limit resulted in poor stability. The activity results are summarized in Table 4-1.

The nominal (1σ, 2σ) and safety performance with and without ship motion, and for various sampling rates, is summarized in Tables 4-1 and 4-2. In the absence of ship motion, but with all other disturbances present, Configuration 2 provides considerably better nominal safety performance. With the ship motion included, the nominal performance with both the configurations is comparable; however, Configuration 2 shows lower risk due to landing short, whereas Configuration 1 shows lower risk due to hard landing. In either case the safety performance is an order of magnitude lower than desired.

The results also indicate that the safety performance can be improved by using higher sampling rate, such as 20 per second, rather than limiting it to 10 per second. In any case, the performance degradation caused by MLS noise is negligible.

Table 4-1. Safety Data

Config.		$P(\dot{h}_{TD}>21 fps)$	P(X<0)	P(Bolter)
1	10 Hz No Heave	$<10^{-6}$	$<10^{-6}$	0.0065
1	10 Hz With Heave	$5. \times 10^{-6}$	10^{-3}	0.11
2	10 Hz No Heave	$<10^{-6}$	$<10^{-6}$	$9. \times 10^{-5}$
2	5 Hz With Heave	$2. \times 10^{-4}$	7.5×10^{-3}	0.16
2	10 Hz With Heave	$5. \times 10^{-5}$	1.9×10^{-4}	0.17
2	20 Hz With Heave	$<10^{-6}$	$2. \times 10^{-4}$	0.12

Based on these results, the following recommendations can be made:

a) Develop better control laws which can utilize position, rate and acceleration activity associated with ship motion. This intelligence is necessary to minimize the effect of ship motion on performance.

b) Devise improved MLS noise filters and complimentary blenders to minimize activity due to use of rate and acceleration information. For this purpose, a detailed investigation of MLS noise frequency content should be conducted.

c) For this study the MLS computational time delay was assumed to be 25 percent of the sampling period. This estimate is conservative and the effect of this time delay should be examined in detail.

d) The future studies should include the disturbances such as ship's roll and pitch motion, aircraft variations, etc., which were not included in this study. The aircraft limitations, such as position and rate authority limits, etc., should be also included.

e) A literature search should be made to establish:

1) Better models for air wake turbulence and ship motion.

2) Safety levels achievable with the existing carrier landing systems.

Table 4-2. Performance Data

Configuration		$\dot{h}_{TD}$ (fps)			X_{TD} (ft beyond ramp)			Gear Clearance (ft)		
		Mean	1σ	2σ	Mean	1σ	2σ	Mean	1σ	2σ
1	10 Hz No Heave	-8.8	+1.22	+2.30	244	-30	-82	14.7	+2.2	+4.50
			-1.0	-2.20		+24	+66		-2.2	-4.50
1	10 Hz With Heave	-9.7	+2.80	+5.60	235	-76	-150	14.7	+4.90	+9.70
			-2.66	-5.70		+78	+160		-4.30	-8.10
2	10 Hz No Heave	-8.6	+0.60	+1.22	238	+10	-20	15.	+0.74	+1.50
			-0.66	-1.30		-10	+34		-0.74	-1.50
2	5 Hz With Heave	-9.7	+2.60	+6.00	230	-78	-170	14.5	+4.30	+8.70
			-2.90	-5.40		+100	+204		-4.50	-9.10
2	10 Hz With Heave	-9.7	+2.50	+5.40	233	-74	-152	14.7	+4.50	+9.0
			-2.90	-5.80		+102	+216		-4.0	-8.0
2	20 Hz With Heave	-9.8	+2.90	+4.80	235	-66	-160	15.	+4.8	+9.8
			-3.0	-5.10		+80	+170		-4.6	-8.4

5. SIMULATION AND SYSTEM MODELING

The simulation studies were conducted by using the special purpose simulation facility developed by LSI for L-1011 statistical Category III certification studies. All the dynamics and control laws were simulated on analog computers. The statistical performance data was obtained by using counters which registered exceedence levels for various parameters. Independent white noise sources were used to generate random disturbances.

The mathematical models used for the study, the simulation diagrams, and particularly the technique used for simulating MLS information, are described. The MLS filters are described in detail in Section 7.

5.1 AIRCRAFT DYNAMICS AND GEOMETRY

The A-7E aircraft was used for this study. The longitudinal dynamics were represented by three-degree-of-freedom perturbation equations of motion. The aircraft geometry and aerodynamic derivatives for power approach are summarized in Table 5-1. The sensor and aircraft equations, including the gust input, are summarized in Table 5-2.

The estimated aerodynamic derivative increment due to ground effect was introduced exponentially as a function of aircraft cg height below 50 feet of altitude.

5.2 SHIP GEOMETRY AND DYNAMICS

The carrier USS Constellation, CVA-64, was used for this study. Its geometry is shown in Figure 5-1. It defines the intended touchdown point and the touchdown zone.

The motion of the carrier deck results from the ship's response to sea wave and swell wave excitations. The motion affects the commanded glideslope and directly contributes to touchdown dispersions.

Table 5.1 A-7E Geometry and Aerodynamic Derivatives for Power Approach

Note: Data for body-fixed stability axes

$S = 375\ ft^2$, $\bar{c} = 10.84$ ft , $z_j = 0.271$ ft , $\alpha_{TL} = 10.73$ deg

$W = 24{,}000$ lb , $m = 746$ slugs , c.g. at 28.6% MAC

$I_{yy} = 68{,}000$ slug-ft^2

$h = 0$ ft , $M = 0.1953$, $U_o = 218$ ft/sec , $\alpha_o = 12$ deg

$\rho = 0.002378$ slugs/ft^3 , $a = 1{,}117$ ft/sec

Nondimensional Derivatives		Dimensional Derivatives	
C_L	1.105	X_u^*	-0.054534
C_{L_α}	3.870	X_w	0.064327
$C_{L_{\dot\alpha}}$	0	T_u	-0.005376
C_{L_M}	0	Z_u^*	-0.286953
C_{M_α}	-0.514	$Z_{\dot w}$	0
$C_{M_{\dot\alpha}}$	-0.750	Z_w	-0.528871
C_{M_q}	-3.900	M_u^*	-0.000165
C_{M_M}	0	$M_{\dot w}$	-0.000289
C_D	0.189	M_w	-0.007964
C_{D_α}	0.6113	$M_{\dot\alpha}$	-0.062987
C_{D_M}	0	M_α	-1.736239
T_M	-4480.0	M_q	-0.327532
$C_{L_{\delta_e}}$	0.518	X_{δ_e}	0.732836
$C_{M_{\delta_e}}$	-0.648	Z_{δ_e}	-14.713536
$C_{D_{\delta_e}}$	-0.0258	M_{δ_e}	-2.188878
		$X_{\Delta T}$	0.001317
		$Z_{\Delta T}$	-0.000250
		$M_{\Delta T}$	0.000004

*The starred derivatives are used to designate that thrust variations with speed (sometimes not available) have been included.

Table 5.2 Aircraft Equations of Motion

Longitudinal Equations of Motion

$$\dot{U} = X_u^* \cdot U_A + \frac{Uo}{57.3} Xw \cdot \alpha_A - \frac{g}{57.3} \cdot \Theta + \frac{X_{\delta e}}{57.3} \cdot \delta_e + \frac{X_{th}}{57.3} \delta_{th} + X_{GE} \cdot HF$$

$$(1 - Z\dot{w})\dot{\alpha} = \frac{57.3}{Uo} Z_u^* \cdot U_A + Zw \cdot \alpha_A + (1 + \frac{Zq}{Uo}) \cdot q - \frac{g\sin \Theta o}{Uo} \cdot \Theta + \frac{Z_{\delta e}}{Uo} \cdot \delta_e + \frac{Z_{th}}{Uo} \cdot \delta_{th}$$

$$+ \frac{Z_{GE}}{Uo} \cdot HF$$

$$\dot{q} = 57.3\, M_u^* \cdot U_A + UoM\dot{w} \cdot \dot{\alpha} + UoMw \cdot \alpha_A + Mq \cdot q + M_{\delta e} \cdot \delta e + M_{th} \cdot \delta_{th}$$

$$+ M_{GE} \cdot HF$$

$$HF = \text{ground effect height factor} = e^{-\frac{hgear}{25}}$$

$$U_A = U_I + U_{WIND}$$

$$\alpha_A = \alpha_I + \alpha\, WIND$$

Angles in degrees
Velocities in fps

Assuming $\cos \phi = 1.$, $\sin \phi \simeq 0$

$$\dot{\Theta} = q$$

$$\Theta_T = \Theta o + \Delta\Theta$$

$$\alpha_T = \alpha_o + \Delta\alpha_I$$

$$\dot{h} = \frac{Uo}{57.3} (\Theta_T - \alpha_T)$$

$$N_{zcg} = \frac{U_o}{57.3\, g} (q - \dot{\alpha}) - \frac{\sin\Theta o}{57.3} \Theta \qquad (+\text{ve up})$$

$$N_{zx} = N_{zcg} + \frac{lx}{57.3} \dot{q} - \frac{\dot{U}}{g} \sin\alpha_T$$

$$A_x = \frac{\dot{U}}{g} \cos \alpha_T + \frac{\Theta}{57.3} + N_{zcg} \sin \alpha_T \qquad (+\text{ve fwd})$$

Geometry

$h\,(gear) = h_{cg} - Z_G \cos \Theta_T + X_G \sin \Theta_T \qquad X_G = -4.7' \qquad X_R = 17.7'$

$h_{(ANTENNA)} = h_{cg} - Z_R \cos \Theta_T + X_R \sin \Theta_T \qquad Z_G = 7.36' \qquad Z_R = 0$

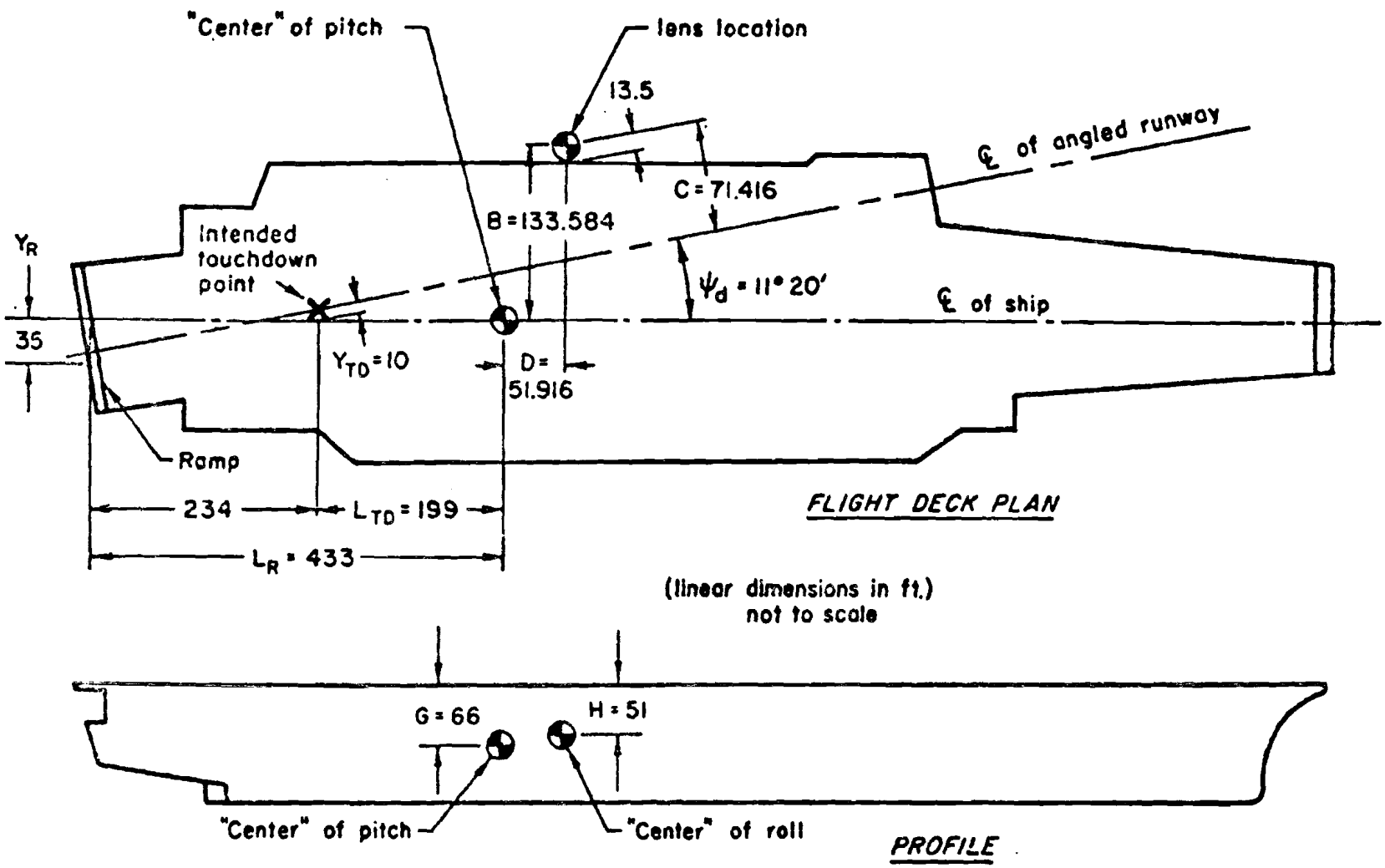

Figure 5-1. Carrier Geometry (CVA-64)

The result of the wave input acting through the ship's dynamic characteristics is represented by power spectral densities of ship pitch, roll and heave. The statistics for the Sea State 6 conditions (References a and b) are summarized in Table 5-3. For this study only the heave motion was used. The 2 percent condition was simulated to obtain low probability touchdown safety data with high confidence level.

White noise source output, through a filter to obtain proper frequency spectrum, was used as shown in Table 5-4. The ship's heave motion (h_s) was included in the simulation by using the following equations. All the altitude related terms in the simulation were referenced with respect to the level deck ($h_s = 0$).

Glideslope altitude $\overline{h_b} = h_b + h_s$

Hook position with respect to deck $\overline{h_g} = h_g - h_s$

Touchdown occurs when $\overline{h_g} = 0$

Sink rate with respect to deck $\dot{\overline{h_g}} = \dot{h}_g - \dot{h}_s$

5.3 AERODYNAMIC DISTURBANCES (AIR WAKE)

The modeling of the carrier's air wake is discussed in several industry reports such as References b and c. For this study, wind over the deck (WOD) and horizontal and vertical turbulence were simulated.

The power spectral densities and magnitude, as a function of WOD and distance aft of ramp are summarized in Figures 5-2, 5-3, and 5-4. To simplify the simulation and as a conservative approach, worst case turbulence level and spectral densities were used. Also, independent white noise sources were used. The RMS magnitude and filters are described in Table 5-4. A conservative value of 30 knots was used for WOD.

5.4 MLS MODELS AND SIMULATION

The MLS receiver signal beam error models used for this study were provided by TI. These are summarized in Figure 5-5. The elevation and DME information were used to generate altitude information. The noise models were simulated by using white noise sources that were inserted before the sample and hold circuits which simulated the MLS beam input. Since DME sampling occurs at 40 Hz, it was considered as continuous (compared to elevation signal) for this study.

The MLS was simulated by using a sample and hold circuit which sampled and held the MLS receiver input beam signal, simulating the beam passing over the aircraft each sample and hold period. The sample and hold circuit also contained a circuit which delayed the receiver input beam signal by one-fourth the sample and hold period. This was done to simulate the computation period following the receipt of new data. Also included in the MLS simulation was the simulation of the random variations of the MLS receiver input beam signals. These variations are due to such things as skewness of the MLS beam and variations of the 3 dB points.

Table 5-3. Ship Motion Environment

Motion Parameter		Pitch	Roll	Heave
Maximum Frequency Range (rad/sec)		0.4 - 1.0	0.2 - 0.9	0.45 - 1.0
Nominal Peak Frequency (rad/sec)		0.60	0.45	0.60
Maximum Expected Value		$\lvert\theta_s\rvert \leq 5$ deg	$\lvert\phi_s\rvert \leq 10$ deg	$\lvert\ddot{h}_s\rvert \leq 5$ ft/sec^2
Sea State 6 RMS Value		$\sigma_{\theta_s} = 1.25$ deg	$\sigma_{\phi_s} = 2.80$ deg	$\sigma_{\ddot{h}_s} = 1.35$ ft/sec^2
Long-Term Statistics: Values Exceeded Given Percentage of the Time	10%	± 0.65 deg	± 1.40 deg	± 1.30 ft/sec^2
	5%	± 0.95 deg	± 1.85 deg	± 1.85 ft/sec^2
	2%	± 1.50 deg	± 2.65 deg	± 2.75 ft/sec^2
	1%	± 2.10 deg	± 3.40 deg	± 3.40 ft/sec^2

The simulation drawing of the sample and hold with time delay circuit is shown in Figure 5-6. Also in the figure is a sketch of the sawtooth generator output with various symbols to describe the operation of the circuit. At the point where the sawtooth output reaches 25 percent of its peak value, the first sample gate is turned on, allowing input signals to reach the amplifier and capacitor and remains gated on until the sawtooth reaches 35 percent of its peak value. At this point the first sample gate is turned off and the value on the capacitor is held. At the point where the sawtooth reaches 85 percent of its peak value, the second sample gate is turned on, allowing the signal that is stored on the first amplifier to be transferred to the second amplifier. When the sawtooth reaches its peak value and drops to zero, the second sample gate is turned off, causing the second amplifier to hold the value which has been stored at that time. The period between the first sample and hold and the second sample and hold equals one-fourth of the total sample period which represents the computational delay of the receiver. It is understood that the actual delay will be less than this and consequently the MLS simulation is conservative.

The time constant of the sampler is equal to the RC product which is:

$$\tau = RC$$

$$\tau = 10^4 \times 10^{-9}$$

$$\tau = 10^{-5} \text{ sec.}$$

or 0.01 millisecond.

Table 5.4 Disturbance Models

Ship Heave

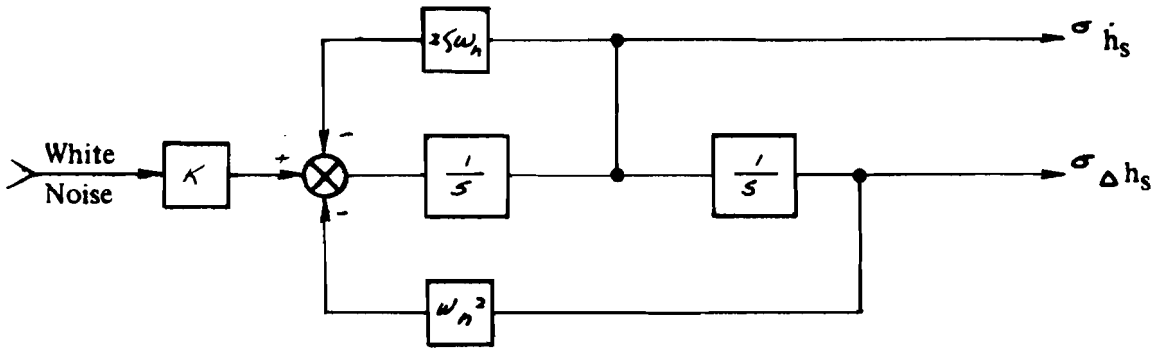

ω_n = 0.6 rad/sec
ζ = 0.42
$\sigma_{\Delta h}$ = 3.75 ft RMS
$\sigma_{\dot{h}}$ = 2.25 fps RMS

Horizontal Turbulence

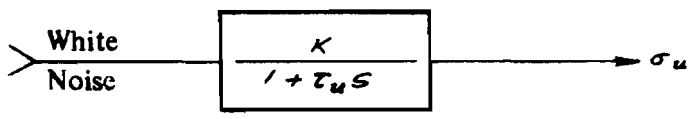

τ_u = 0.5 sec
σ_u = 0.0334 WOD
W.O.D. = Wind over deck
= 30 knots

Vertical Turbulence

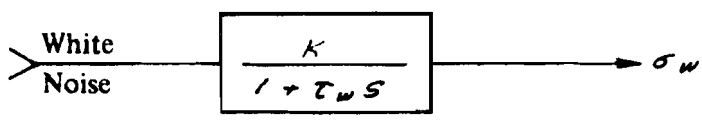

τ_w = 2.5 sec
σ_w = 0.0446 WOD

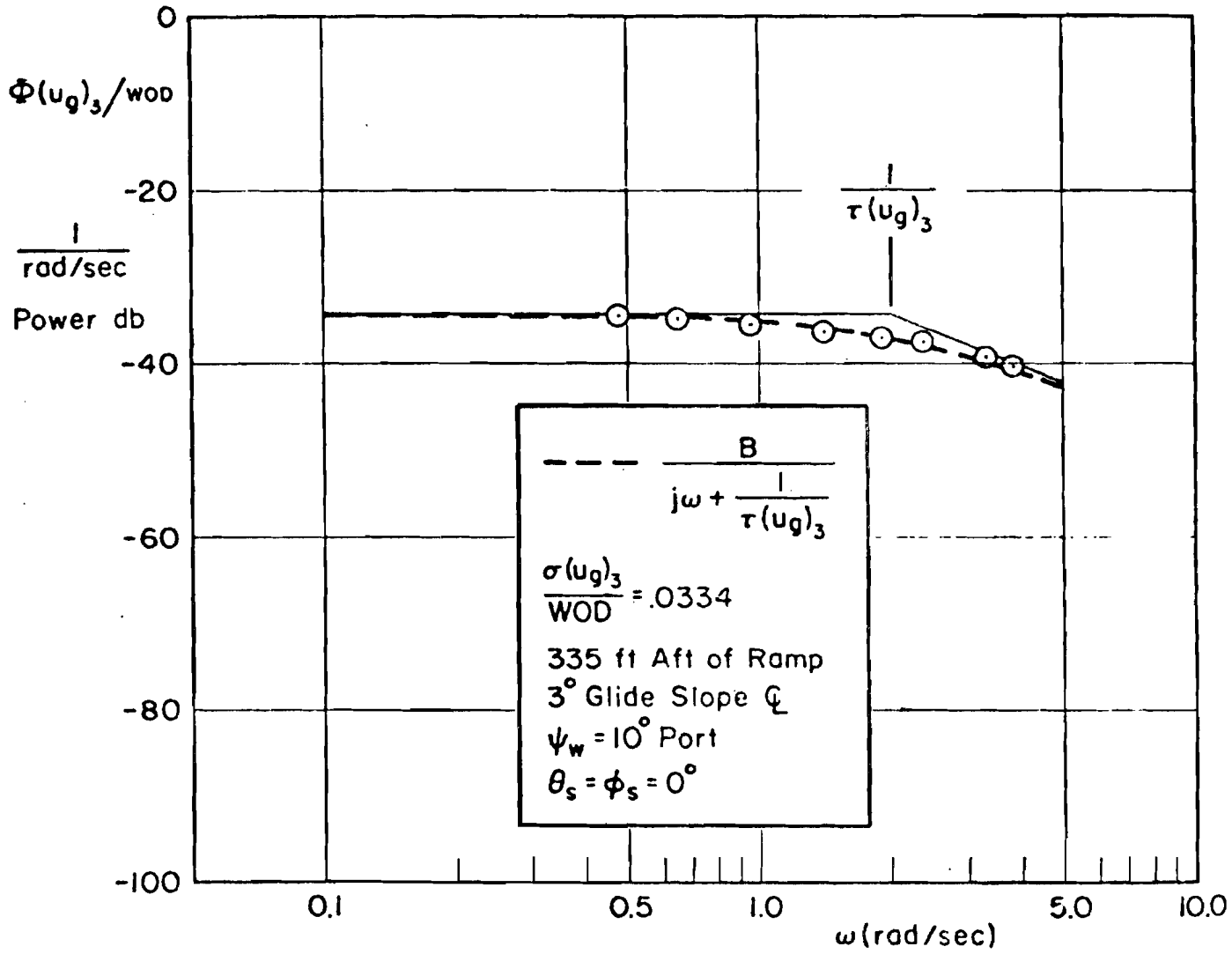

Figure 5-2. Power Spectral Density of Horizontal Velocity Turbulence Astern the Carrier

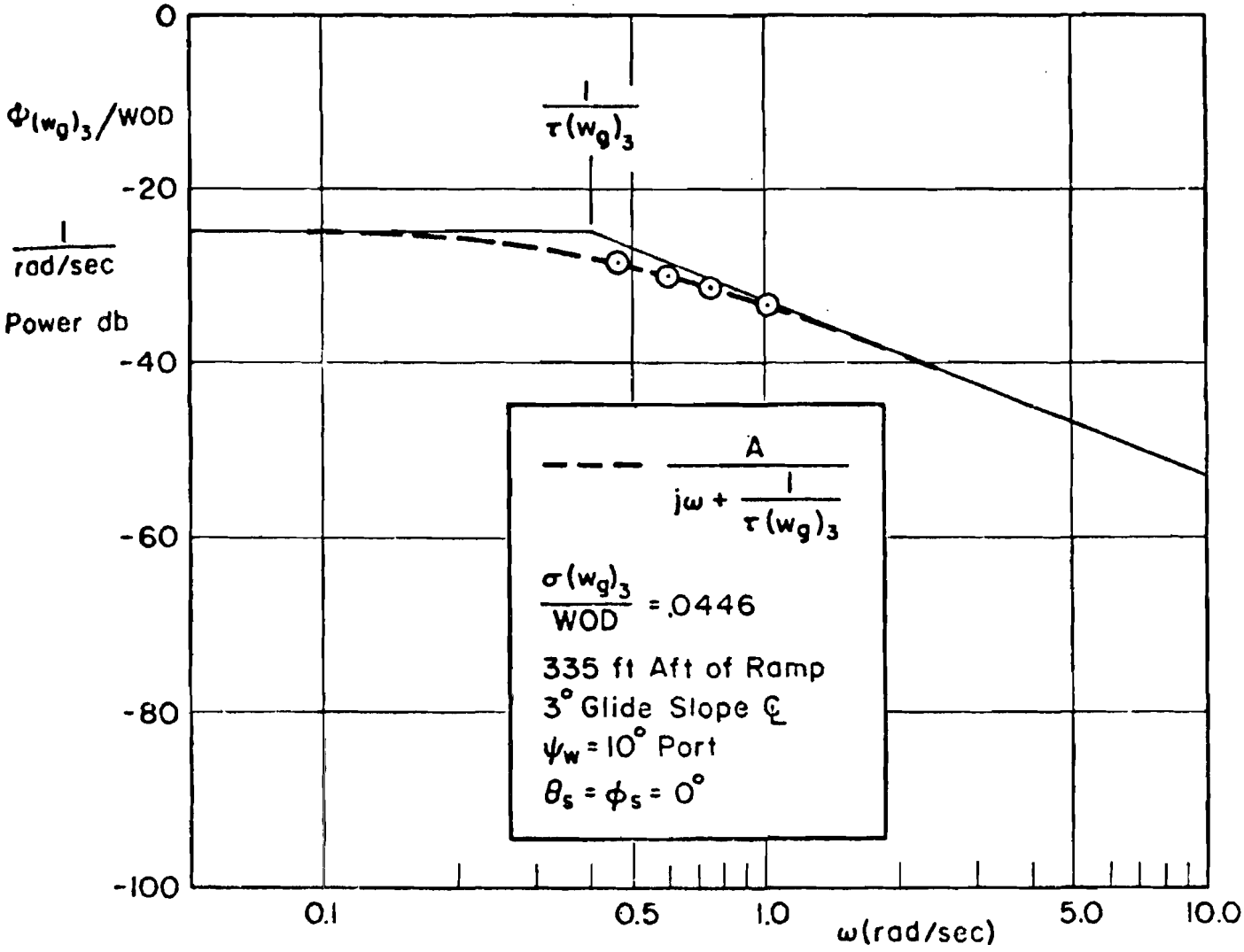

Figure 5-3. Power Spectral Density of Vertical Velocity Turbulence Astern the Carrier

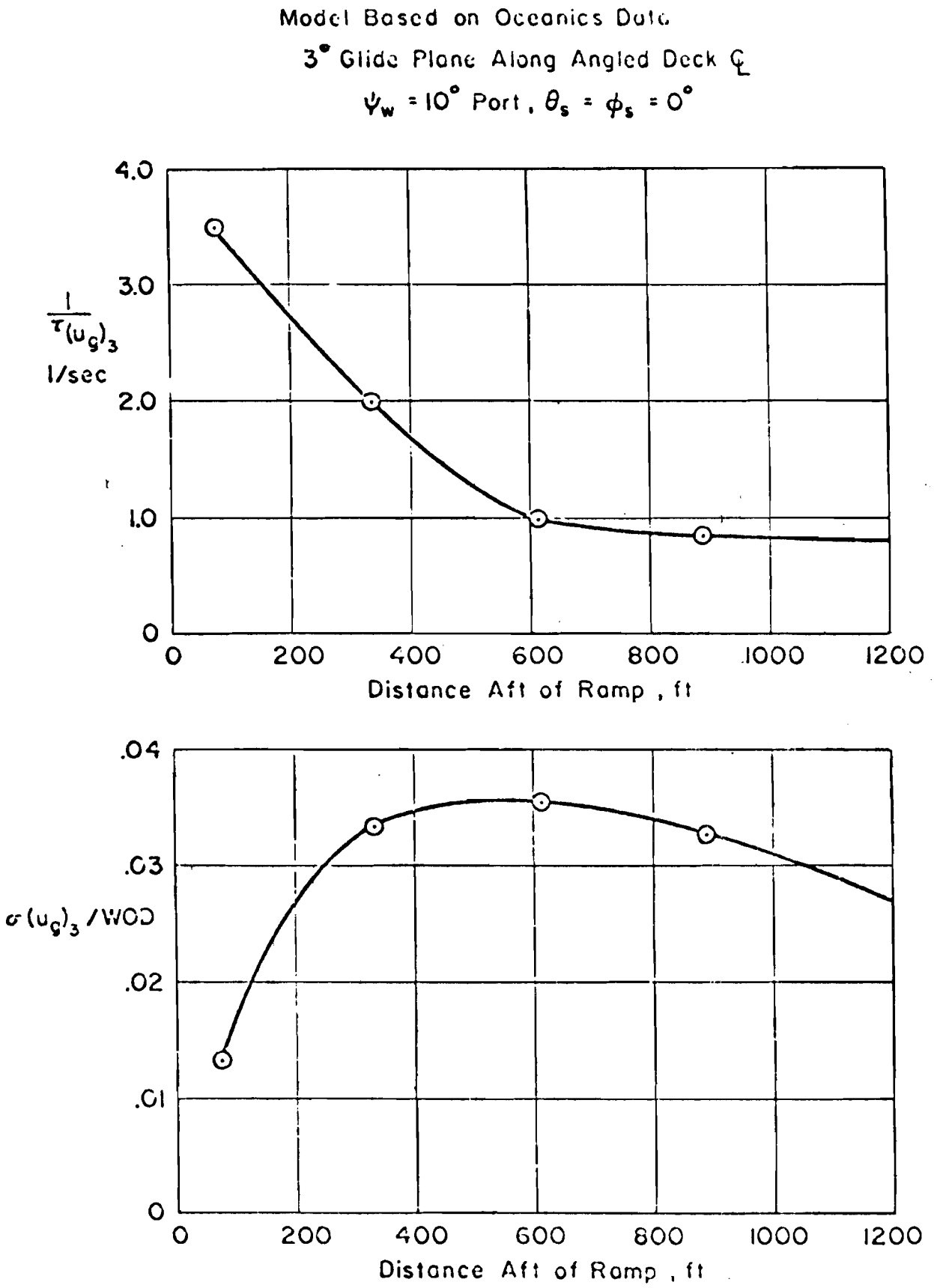

Figure 5-4. Variation of Horizontal Velocity Turbulence Power Spectral Density Parameters with Distance Aft of Ramp

AZIMUTH ERROR

Worst case bias error - .04°

Noise error - white Gaussian with standard deviation given by:

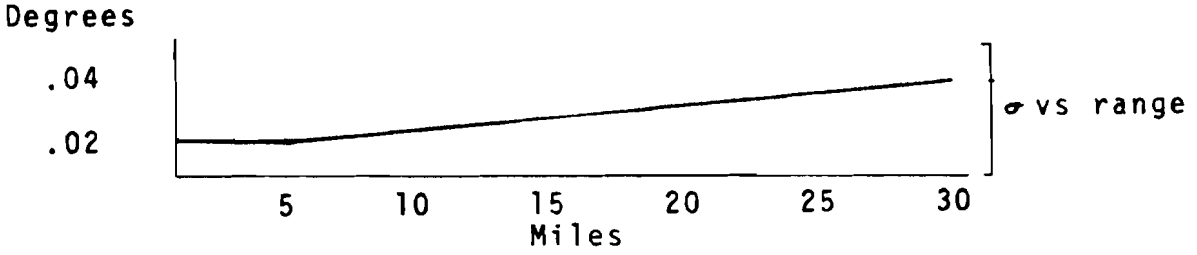

ELEVATION

Worst case bias error - .05°

Noise error - Gaussian white with:

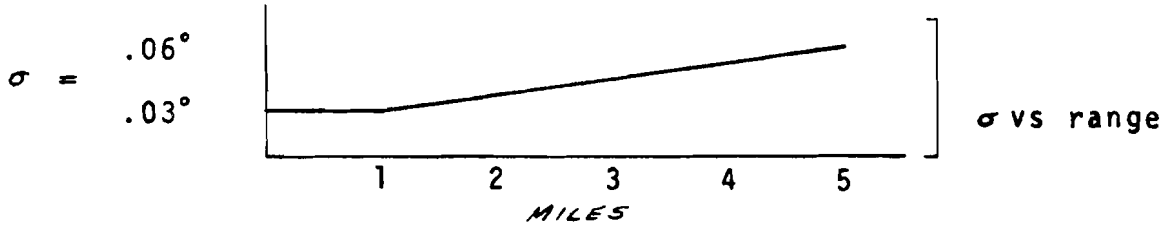

DME ERROR

Worst case bias error - ±20 ft.

Noise error - σ = ± 6ft. (all distances)

Figure 5-5. MLS Beam Error Models Summary

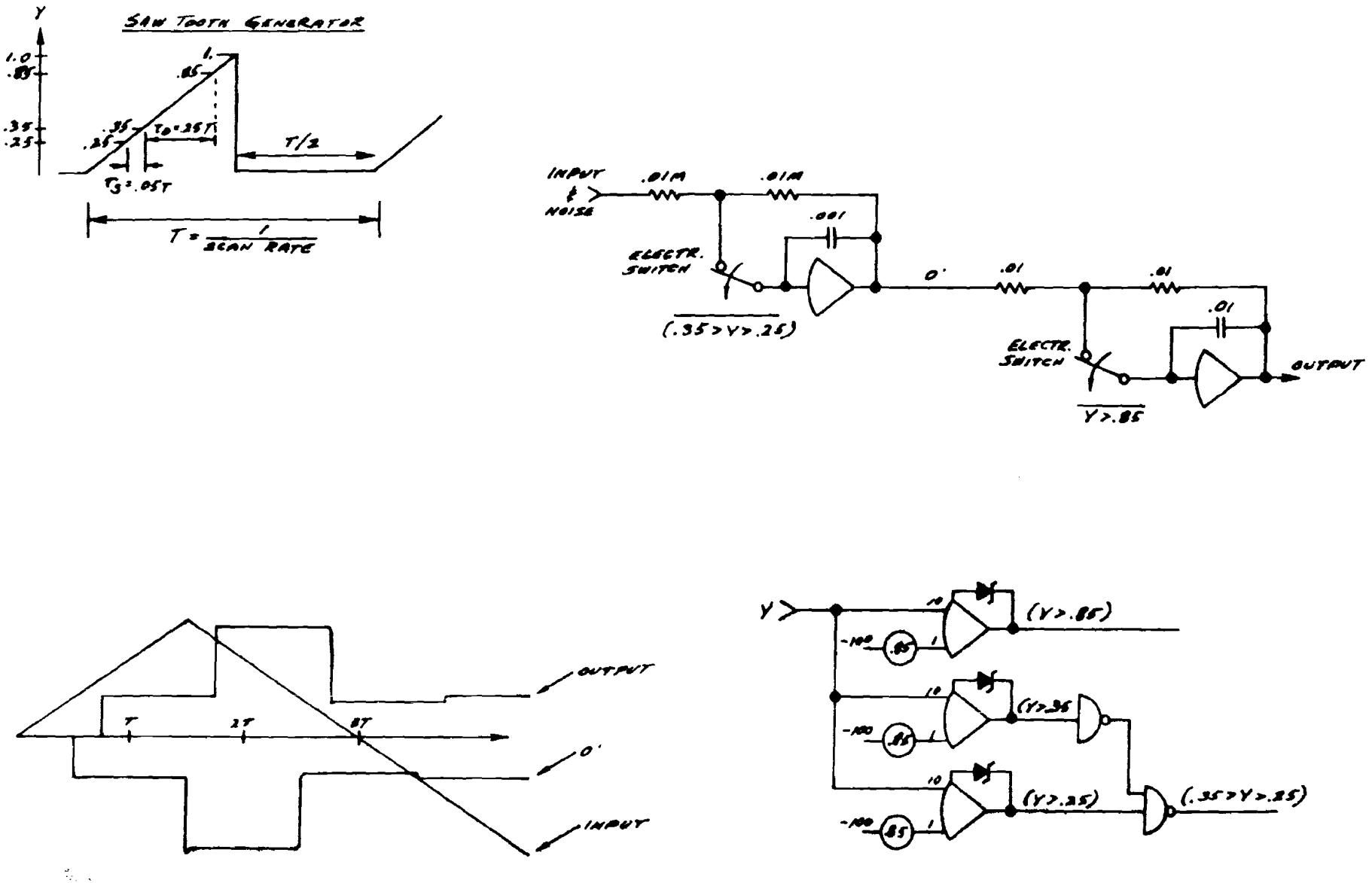

Figure 5-6. MLS Receiver Sampling and Computational Delay Simulation

Although this time constant is very small it is recognized that a perfect simulation would have a time constant of zero in order to be pure gaussian. This time constant difference will cause the large narrow noise spikes which have a low probability of occurrence to be averaged to some lower value. However, in spite of this difference, it is believed that the simulation is valid for two reasons. The flight control laws contain a 0.5-second time constant filter with a rate limit of 5 ft/sec. From this it can be seen that the maximum change that can pass through the rate limited filter in 0.2 second (assuming 5 receiver inputs/second) is 1 foot, which is quite small as compared to a large spike error. The second reason that the simulation is considered valid is that the probability of occurrence of a large narrow spike is so small that its effect would probably not be seen in any case.

5.5 CONTROL SYSTEM

The control laws used are similar to the beam tracking mode used in the L-1011. No major control system changes were considered for this study.

Based on optimization studies, two configurations, 1 and 2, were selected for detailed statistical studies. The configuration A1, shown in Figure 5-7, uses relatively lower gain and both position and rate information derived from MLS. The other one, shown in Figure 5-8, uses higher gains and only position information from MLS. The altitude rate information is obtained by integrating the normal accelerometer output. In each case the accelerometer output is also used for gust sensing and/or for complementary filtering. Rate gyro and derived pitch rate was used for damping. Rate limited position filtering is recommended, as shown in Figures 5-7 and 5-8, to minimize the effect of noise on MLS signals. The gain on MLS altitude signal is increased below 500 feet to obtain tighter tracking and to take advantage of reduction in MLS noise (in terms of Δh) with altitude.

An airspeed autothrottle, shown in Figure 5-9, was used for this study. No attempts were made to optimize it by including gust compensations. Only longitudinal accelerometer is used for feedback and it is possible that it can be replaced with range information available from MLS.

5.6 SIMULATION DIAGRAMS

The detailed simulation diagrams are shown in Figure 5-10. These diagrams were generated for use with SD-80 computers which have a 100-volt scaling limit. The gains shown are for ten times real time scale.

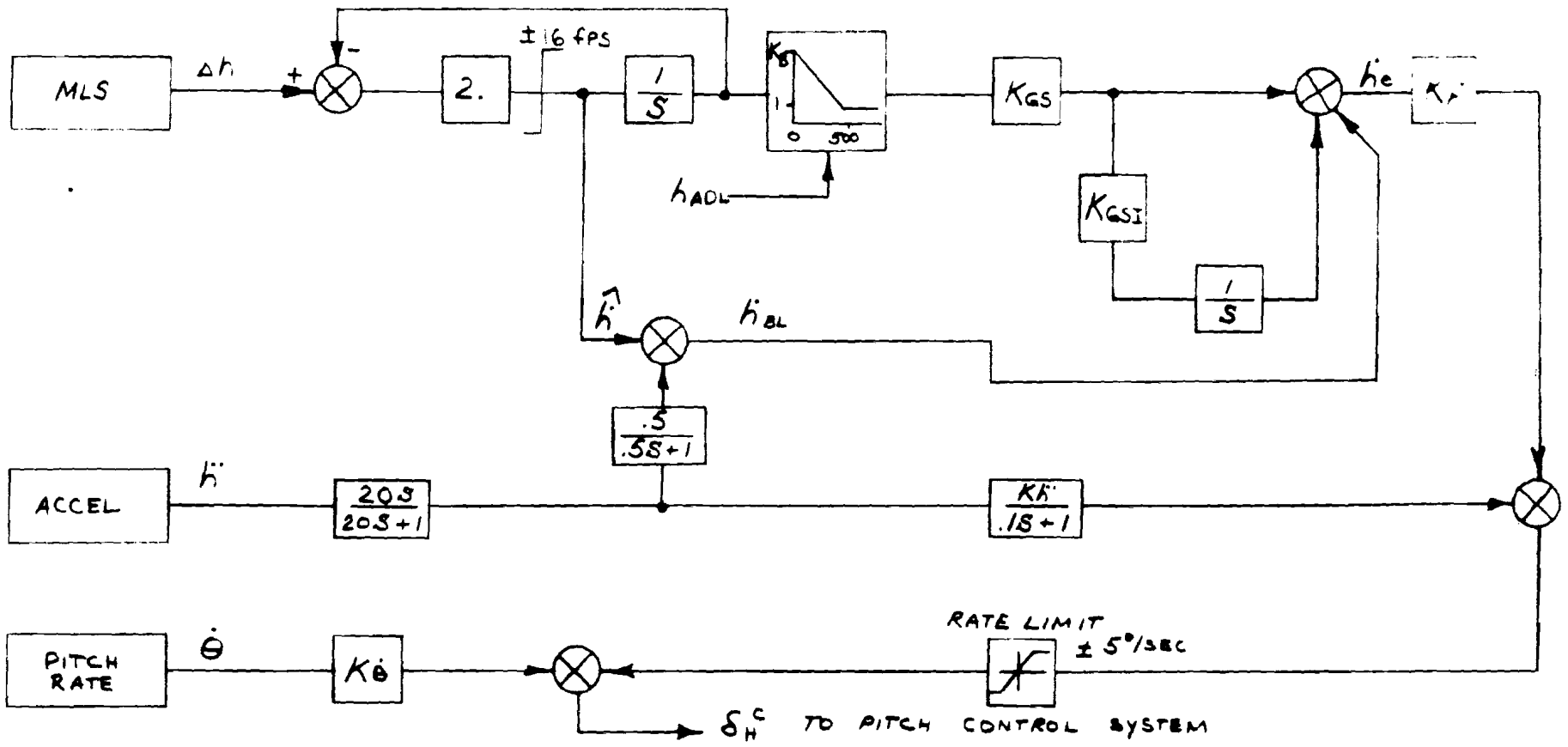

K_{GS} = .25
K_{GSI} = .50
$K_{\dot{h}}$ = .75
$K_{\ddot{h}}$ = .2
$K_{\dot{\theta}}$ = .5
K_B = 2

Figure 5-7. MLS Carrier Landing Block Diagram – Configuration 1

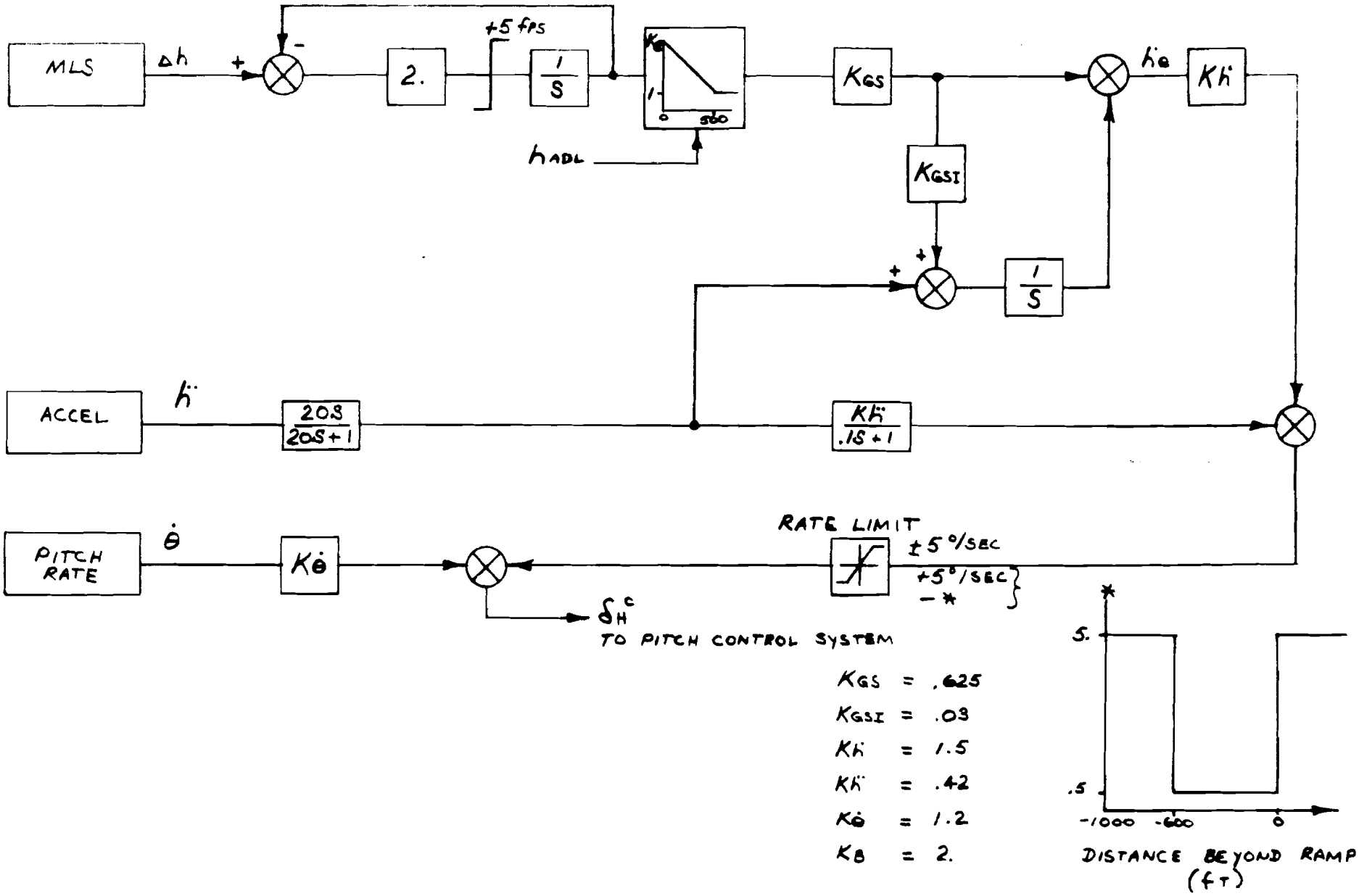

Figure 5-8. MLS Carrier Landing Block Diagram – Configuration 2

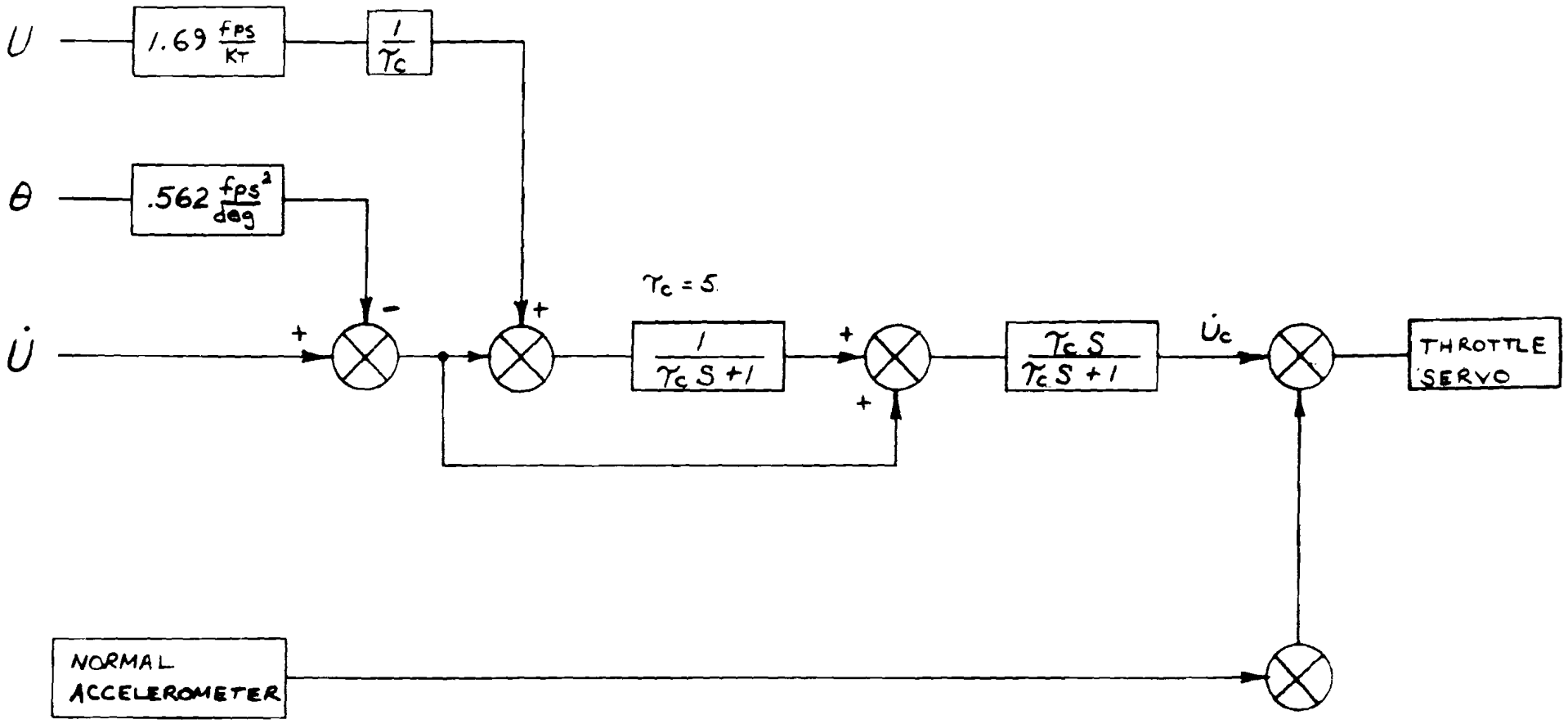

Figure 5-9. Autothrottle Block Diagram

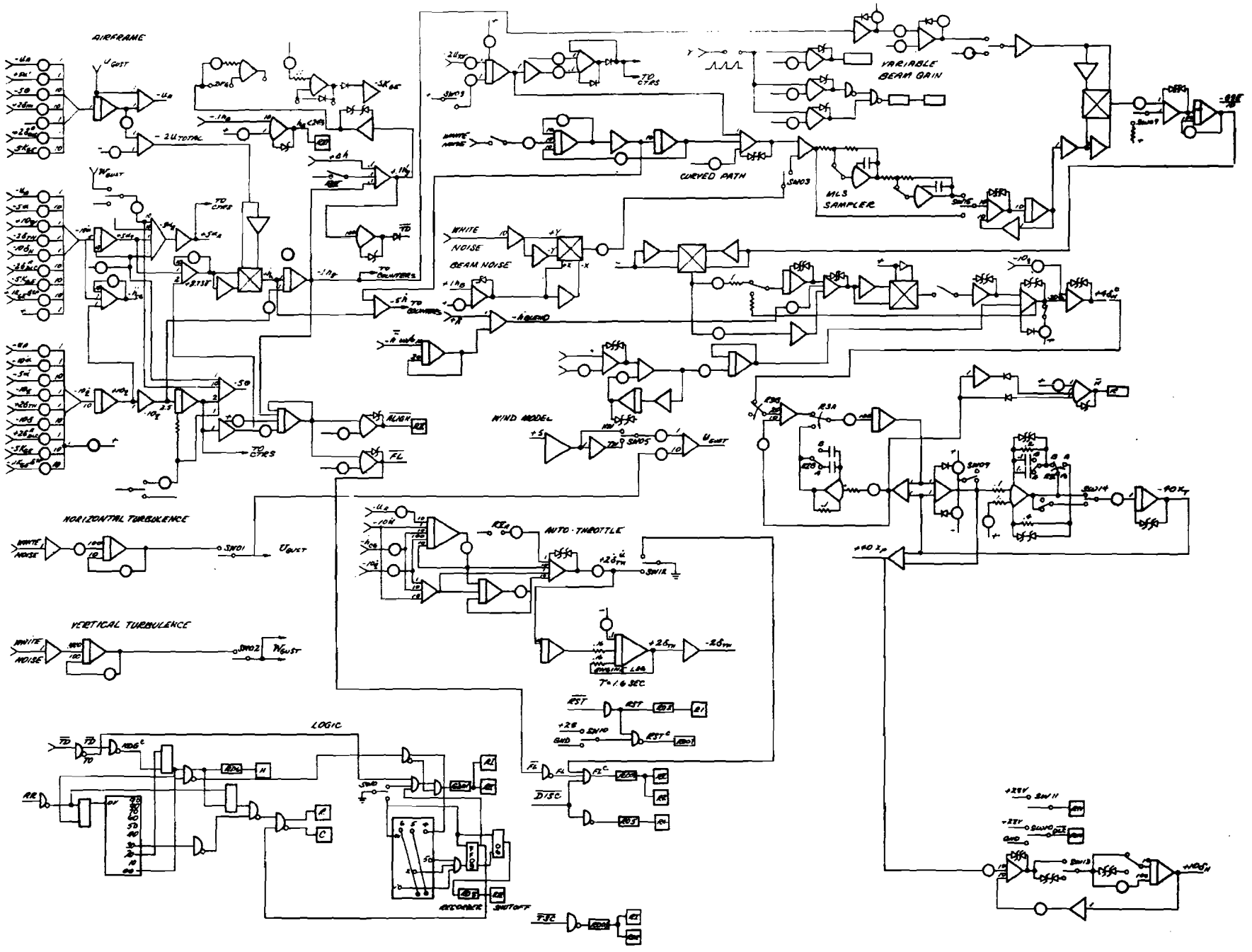

Figure 5-10. Overall Simulation Diagram

6. EVALUATION TECHNIQUES

Within the scope of the MLS carrier landing task, trade studies were performed to define the best control system. The various configurations were evaluated in four major areas:

- Stability
- Control activity
- Sensitivity to MLS sampling rate
- Landing performance

To evaluate stability margins of the various configurations, the simulated airplane was flown at constant altitude and responses to step beam, ship and gust disturbances were examined. For good landing control, it is desirable to have a tight, fast responding beam loop, while maintaining maximum insensitivity to gust disturbances.

While flying at constant altitude, the airplane was subjected to horizontal and vertical gusts, MLS beam disturbances, and ship heave motion, and activity data was obtained. Typical traces are shown in Appendix B, with activity due to each disturbance noted, and then the disturbances combined to yield an indication of overall variations. Minimized altitude and altitude rate excursions, when subjected to these disturbances, are indicative of tight control, and such a control law normally yields superior landing performance. Reduced stabilizer position activity ensures pilot acceptance of control column activity, while stabilizer rate activity must be compatible with aircraft hydraulic system flow capabilities. Lower pitch attitude, attitude rate, and acceleration excursions are representative indicators of ride comfort.

Based on the results of these tradeoffs, two configurations, 1 and 2, were chosen for further performance evaluation. First landing performance data was obtained without ship heave motion, with gusts and beam disturbances only. Then both cases were evaluated with stochastic disturbances and a 10 Hz scan rate. Then the landing performance sensitivity to MLS sampling rate was determined for the better case, which was Configuration 2.

For stochastic performance evaluation, limiting levels of beam noise, ship heave in Sea State 6, horizontal and vertical turbulence, and steady wind were included. Electro-mechanical counters were used to record exceedances of several levels for the parameters of interest ($\dot{h}_{TD}$, X_{TD}, θ_{TD}, α peak, and gear clearance at ramp). A minimum of 1,000 landings was made for each case in order to plot the exceedance probability distributions included in Appendix A.

All touchdown range measurements were referenced to the carrier ramp position. The closed loop simulation model is shown below.

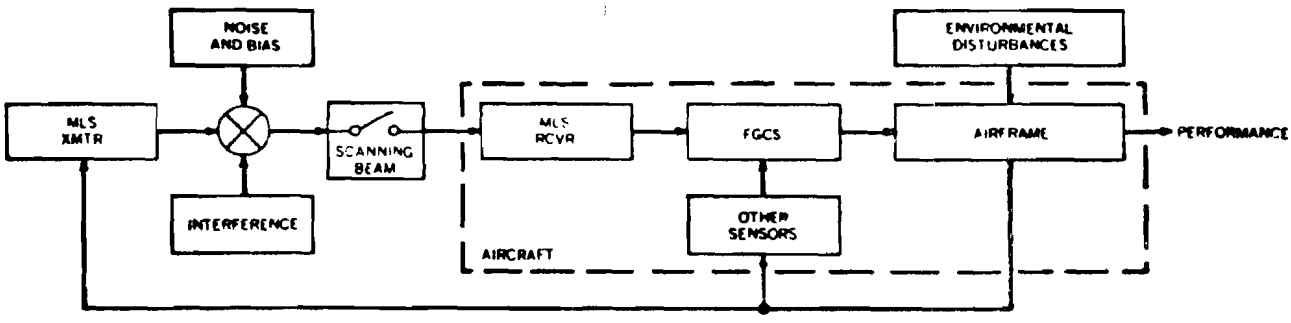

From this stochastic landing data, the performance capability of each control law configuration was obtained, as shown in Table 4-2. By extrapolation, the landing hazard probabilities were also obtained as shown in Table 4-1. The results indicate improved touchdown range dispersion with Configuration 2.

The important parameters for carrier landing are touchdown sink rate and position, with gear clearance at ramp giving an indication of safety margin. Gear design strength of 21 fps was used, with acceptable touchdown ranges between 0 and 460 feet beyond the ramp. Longer landings result in aircraft bolter, where the pilot would initiate a go-around.

7. STUDY RESULTS AND DISCUSSION

7.1 GENERAL

The carrier approach was simulated, using the A-7E aircraft, with a 3 degree nominal glide path to touchdown. The elevation (equivalent to elevation 2 transmitter) and DME information was used to compute aircraft altitude, as shown below, enabling an output from the MLS receiver of altitude error from the derived path, and this error signal became the control input to the pitch autoland system.

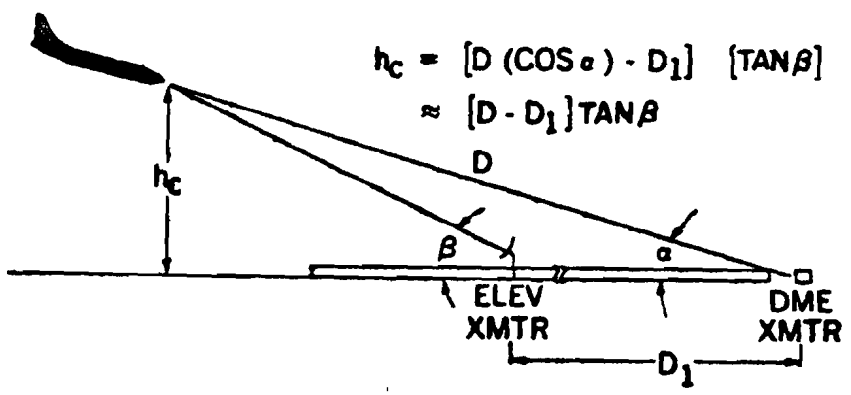

To minimize path tracking errors, the beam gain is gradually doubled from 500 feet Above Deck Level (ADL) to touchdown. Note that only ship heave motion was included during this preliminary carrier landing study.

During landing control law optimization studies, two configurations were selected as candidates for further performance evaluation: Configuration 1, using relatively lower gains with derived altitude rate to compensate for ship heave motion, and Configuration 2, with higher gains to give improved beam tracking but with inertial $\dot{h}$ used instead of

MLS derived information (see Figures 5-7 and 5-8). The exceedance probability plots for the landing parameters, obtained with limiting stochastic wind, beam, and ship disturbances, are included in Appendix A, with a summary of results given in Tables 4-1 and 4-2. Activity traces due to horizontal and vertical gusts, MLS disturbances and ship heave motion were also obtained, and Appendix B consists of these time histories, with a summary given in Table 7-1. The landing performance obtained with each control law configuration is briefly discussed below, using a 10 Hz scan rate for comparison purposes.

The first landing configuration is somewhat similar to the L-1011 beam tracking control system. Higher $\dot{h}$ error and pitch rate gains are used to obtain tighter control with good stability. MLS beam gain is gradually doubled below 500 feet ADL to improve beam tracking and take advantage of the reduced MLS noise (in both $\Delta\theta$ and Δh) with altitude. A 0.5-second blended altitude rate signal is used, derived from MLS position information, to compensate for ship heave motions. The MLS filter is rate limited to 16 fps to avoid extended saturation during severe disturbances. With no ship heave motion, landing performance is excellent; the probability of landing hard or short is acceptably remote ($< 10^{-6}$), with low bolter probability (< 0.01). With heave included, landing performance is unacceptable. The probability of landing short (hitting the ramp) is 0.001, even though hard landings are remote. As shown in the activity traces of Appendix B, altitude rate variations due to MLS and heave disturbances are very large, indicating poor beam control. Also, surface position and rate activity is quite large. The rate limit on the MLS filter was reduced to 10 and 5 fps to attempt to reduce this activity, but both of these changes resulted in marginally or totally unstable systems due to the extended saturation of the rate limit with these limiting disturbance levels. With the beam disturbance models used, it appeared unlikely that suitable performance could be obtained while using derived altitude rate with respect to the ship's deck. Thus, the second configuration was investigated further.

For Configuration 2 (Figure 5-8), inertial altitude rate is obtained by integrating the accelerometer output. Higher gains are used, with a 5 fps rate limited 0.5-second beam filter to minimize activity despite the increased gains. A large improvement in $\dot{h}$ variations was obtained (from 3.9 fps RMS to less than 0.5 fps RMS) with acceptable surface activity, thus indicating good beam tracking. To minimize landing short probability, a 0.5 deg/sec nose-down pitch rate command limit was used below 30 feet ADL, but this resulted in a higher bolter rate. The nose-down limit was opened up when the aircraft passed over the ramp, thus minimizing bolter probability. This resulted in excellent performance without heave motion, less than 30 feet 2σ range dispersion and $< 10^{-4}$ probability of landing beyond the arresting cables. Again, when ship heave motions were simulated, performance was noticeably degraded, but seems acceptable for a preliminary carrier landing study. Short and hard landing probabilities are remote (5×10^{-5} for landing hard, 2×10^{-4} for landing short), even though they do not satisfy the 10^{-5} design goal. However, bolter rate is quite high, in the order of 17 percent.

Thus, further optimizing studies are required to meet the 1 in 10^5 hazard probability design goal.

Table 7-1. Activity Data

		Configuration I (10 S/S)					Configuration II (10 S/S)					Configuration II (5 S/S)				
		HT	VT	MLS	Heave	All	HT	VT	MLS	Heave	All	HT	VT	MLS	Heave	All
Δh (ft)	*			1.9	0.9	2.8										
	+	0.1	0.3	2.1	0.7	2.8	0.2	0.4	0.9	2.1	3.7	0.1	0.4	1.4	2.4	3.0
	**		unstable		1.3											
$\dot{h}$ (fps)	*			3.3	1.5	4.2										
	+	0.2	0.4	3.9	1.0	4.5	0.2	0.4	0.2	0.6	1.1	0.2	0.3	0.3	0.6	1.1
	**		unstable		1.9											
$\ddot{h}$ (fps^2)	*			4.0	0.6	3.9										
	+	0.3	0.4	4.0	0.8	4.1	0.5	0.8	0.3	0.3	1.0	0.4	0.5	0.3	0.4	0.9
	**			4.0	1.1											
$\Delta\theta$ (deg)	*			2.4	0.7	2.6										
	+	0.2	0.5	2.4	0.4	3.0	0.1	0.4	0.1	0.2	1.9	0.2	0.3	0.1	0.2	0.7
	**		unstable		1.0											
δe (deg)	*			2.4	0.6	2.5										
	+	0.3	0.3	2.4	0.4	2.6	0.5	0.4	0.4	0.1	0.8	0.5	0.4	0.5	0.2	1.0
	**		unstable		0.6											
$\dot{\delta}_e$ (deg/sec)	*			>3.0	1.7	>3.0										
	+	1.9	1.9	>3.0	1.6	>3.0	2.2	2.0	1.7	0.2	2.7	2.2	2.0	2.1	0.2	2.7
	**			>3.0	2.5											

Note: For Configuration I: + denotes 15 fps rate limit
* denotes 10 fps rate limit
** denotes 5 fps rate limit

7.2 MLS DERIVED ALTITUDE RATE

It was felt at the start of this study that derived altitude rate, with respect to the carrier deck, would be beneficial to performance since it would provide additional intelligence to the autopilot about ship motion. Configuration 1 was designed from this viewpoint, using a half-second complementary filter to obtain a good altitude rate signal. No stringent rate limited filtering could be used, however, since this resulted in $\dot{h}$ saturation and total loss of damping signal in large disturbances, causing system instability and degraded performance. With the wide rate limit (15 fps), this problem was not in evidence (compare the traces shown for 5 and 10 fps limit in Appendix B), but activity was high mainly due to the MLS noise model used.

The stochastic landing results, with ship heave motion, show an improved 2σ touchdown range variation compared to Configuration 2; however, the landing short probability is 10 times greater, with equivalent hard landing probability. The short landing probability would be improved by using the nose-down limit scheme of Configuration 2 in future studies.

From these results, it appears that derived altitude rate information would yield improved landing performance and safety if a good filter can be obtained to minimize the MLS noise effects. Thus, more effort should be expended to verify the MLS disturbance model, and to obtain better filtering; if this can be achieved, performance improvement should be substantial.

7.3 MLS FILTERING

The beam input signal for Configuration 2 consists of a half-second position filter, rate limited to 5 fps. This yielded excellent performance with acceptable surface activity, since it effectively reduces both low and high frequency noise signals and provides suppression of large input spikes.

For Configuration 1, with derived altitude rate, it was not possible to use a 5 fps rate limit since saturation of the limit due to large disturbances resulted in loss of damping signal and system instability. Thus, only the position filter could be tolerated. With the derived altitude rate, the high frequency MLS noise content was amplified by differentiation, resulting in very large activity levels, sufficient to exceed the autopilot authority limitations; thus, while 2σ performance showed some improvement, the "tail areas" of the exceedance distribution curves were significantly degraded. If the high frequency content is found to be lower than assumed in the noise model used in this study, and if better filtering techniques are found, it would be feasible to obtain a large performance improvement with this configuration.

7.4 MLS SCAN RATES

For the exacting task of carrier landings, a high scan rate is desired, with minimum computational delays. As shown in Tables 4-1 and 4-2, and in the probability plots in Appendix A, a data rate of 20 Hz shows some improvement in performance, compared to 10 Hz for Configuration 2. A reduction to 5 Hz shows a marked performance degradation. Thus, it appears that a data rate of 10 samples per second is the absolute minimum for good carrier landings, with a 20 Hz rate preferred. Configuration 1 was even more susceptible to MLS scan rate, since the rate information was derived from the beam.

Thus, while a 5 Hz MLS scan rate was found acceptable for all fixed field landing requirements, a minimum of 10 samples per second is required for carrier landings, based on this simplified study. A more detailed carrier landing study, with ship pitch and roll motion included, may indicate a need for even higher scan rates.

7.5 MLS COMPUTATIONAL REQUIREMENTS

The digital computation section of the MLS receiver computes aircraft position based on EL2 and DME signals. It is desirable that the output position signal be compensated for antenna geometry (using pitch attitude); this is especially true if higher order signals are derived from the position information.

In this study, gain schedules and logic trip points were based on altitude ADL. These could have been programmed with DME range with some differences in landing performance. No attempt was made to choose between these two methods during this task.

Good touchdown control necessitates accurate MLS guidance information very near the ground. It was assumed that the EL2 noise model remained accurate to touchdown; this should be verified by actual tests, since the impact on performance may not be trivial.

APPENDIX A

STOCHASTIC LANDING RESULTS

Figure	Configuration	Scan Rate	Probability Plot
A-1	2	5, 10, 20	Touchdown Sink Rate - with heave
A-2	2	5, 10, 20	Touchdown range - long
A-3	2	5, 10, 20	Touchdown range - short
A-4	2	5, 10, 20	Touchdown attitude
A-5	2	5, 10, 20	Gear clearance at ramp
A-6	2	5, 10, 20	Peak angle-of-attack
A-7	2	10	Touchdown sink rate - with and without heave
A-8	2	10	Touchdown range - long - with and without heave
A-9	2	10	Touchdown range - short - with and without heave
A-10	2	10	Touchdown attitude - with and without heave
A-11	2	10	Gear clearance at ramp - with and without heave
A-12	2	10	Peak angle of attack - with and without heave
A-13	1	10	Touchdown sink rate - with and without heave
A-14	1	10	Touchdown range - long - with and without heave
A-15	1	10	Touchdown range - short - with and without heave
A-16	1	10	Touchdown attitude - with and without heave
A-17	1	10	Gear clearance at ramp - with and without heave
A-18	1	10	Peak angle of attack - with and without heave

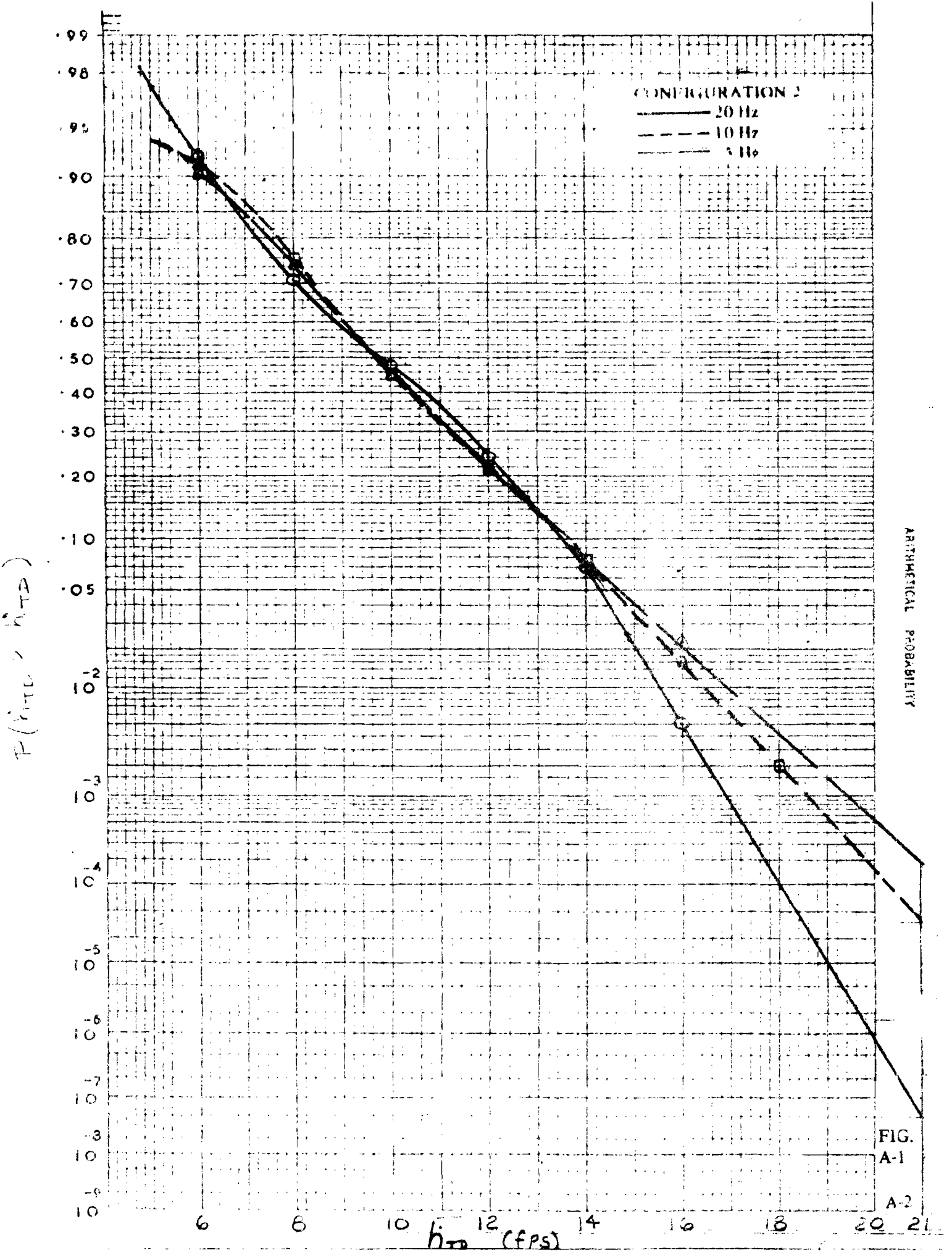
CONFIGURATION 2
20 Hz
10 Hz
5 Hz
·99
·98
·95
·90
·80
·70
·60
·50
·40
·30
·20
·10
·05
10^{-2}
10^{-3}
10^{-4}
10^{-5}
10^{-6}
10^{-7}
10^{-8}
10^{-9}
6
8
10
12
14
16
18
20
21
$\dot{h}_{TD}$ (fps)
$P(\dot{h}_{TL} > \dot{h}_{TD})$
ARITHMETICAL PROBABILITY

FIG. A-1

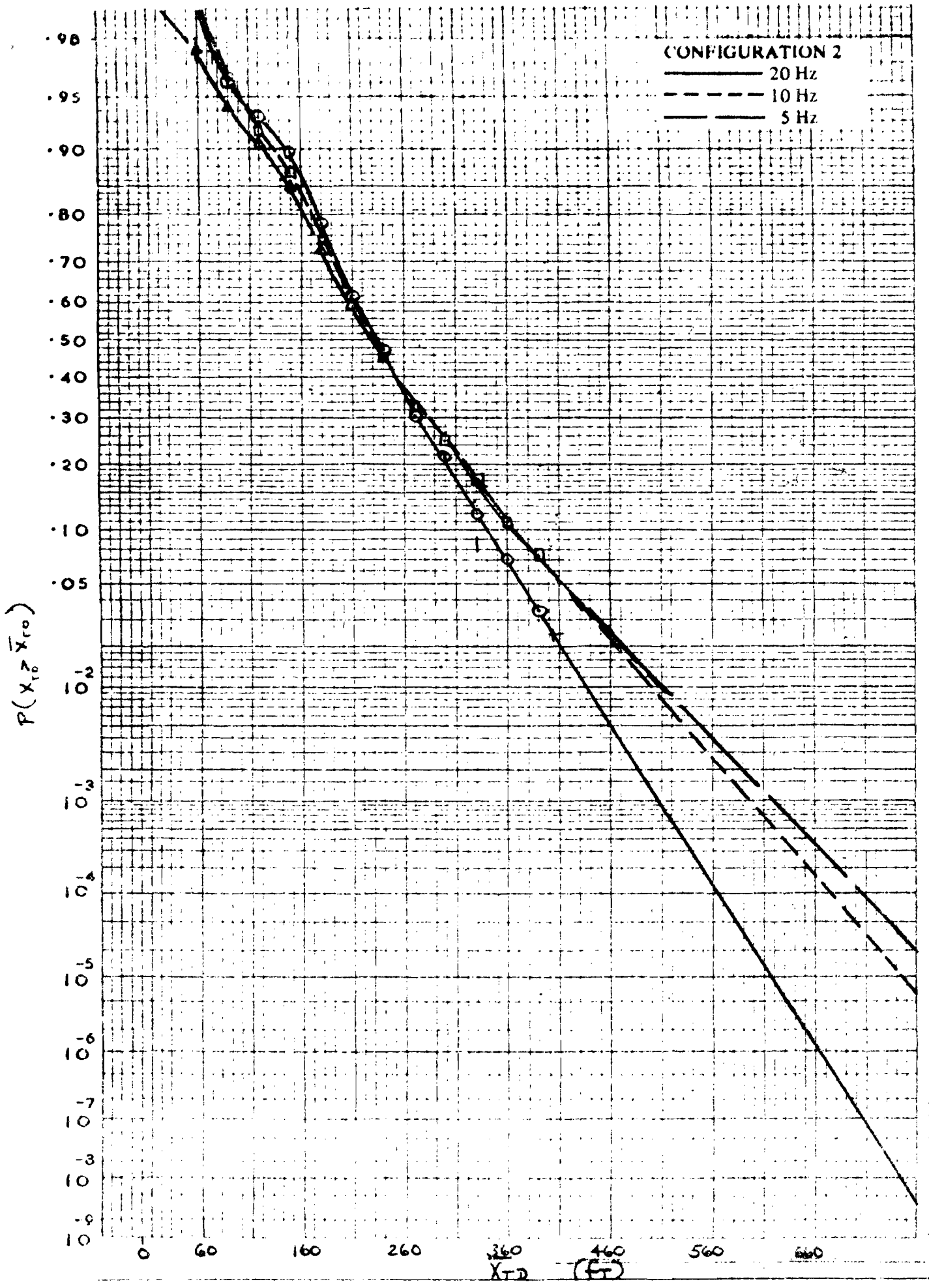

ARITHMETICAL PROBABILITY

FIG. A-2

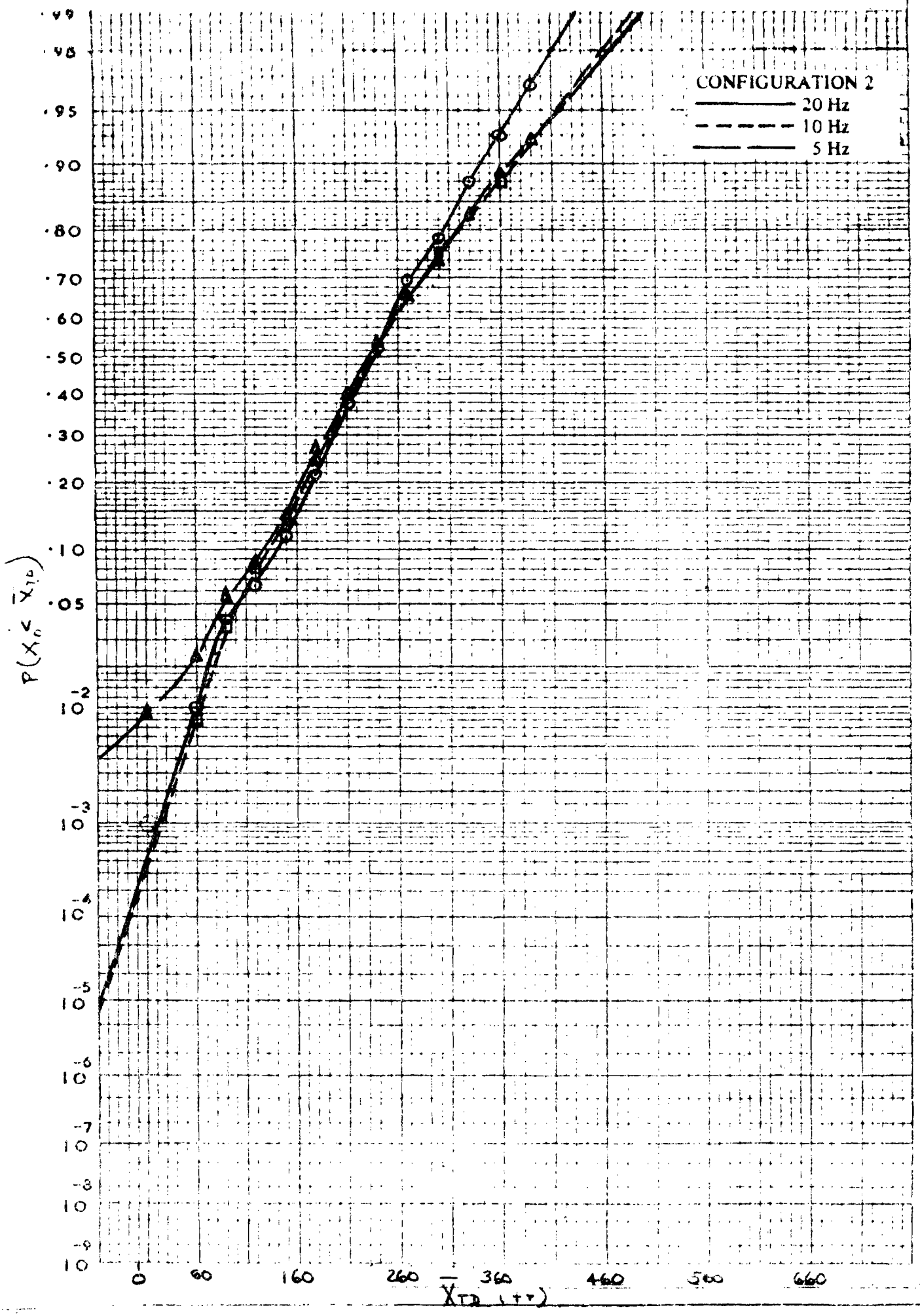

ARITHMETICAL PROBABILITY

FIG. A-3

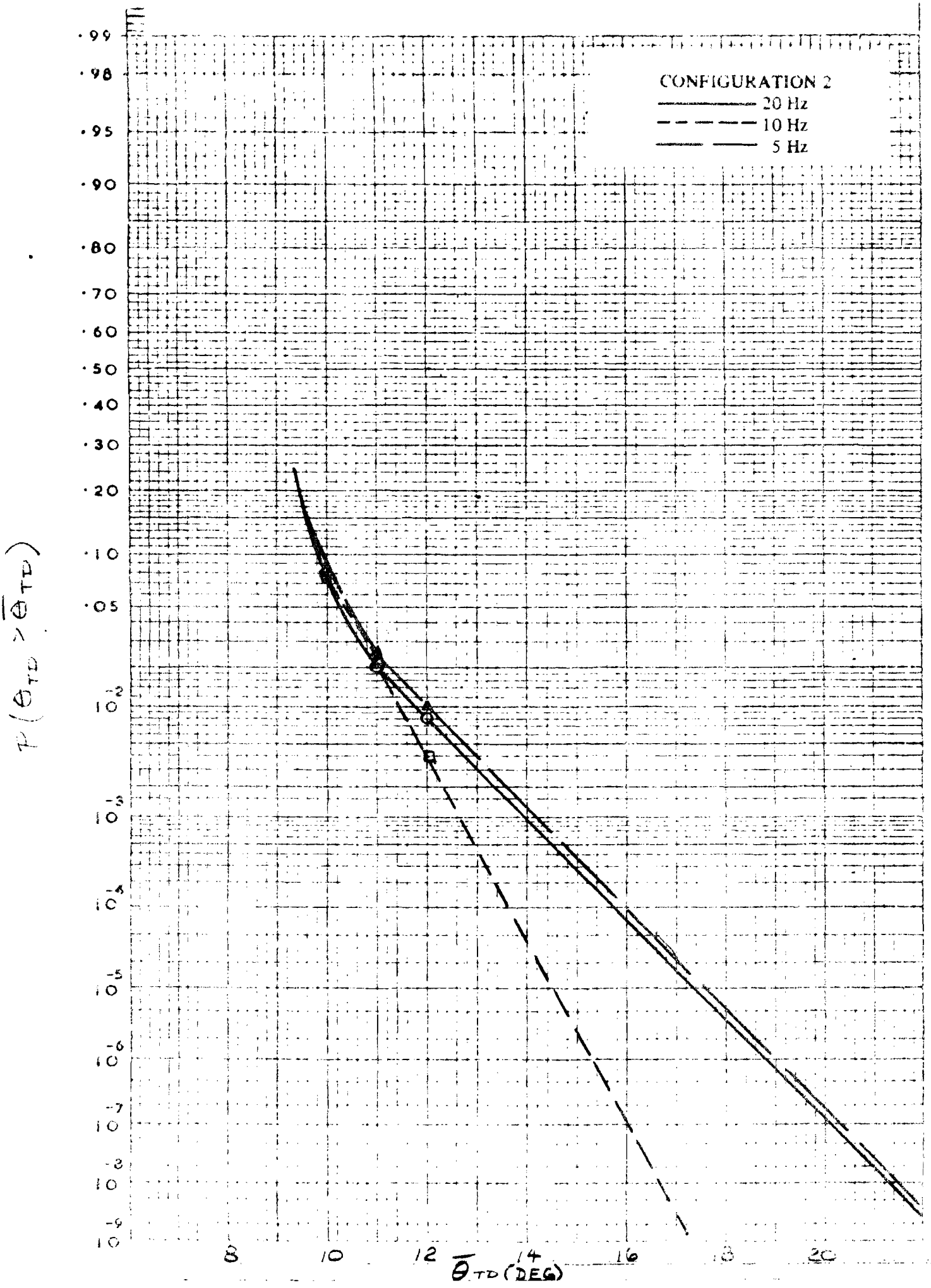

ARITHMETICAL PROBABILITY

FIG. A-4

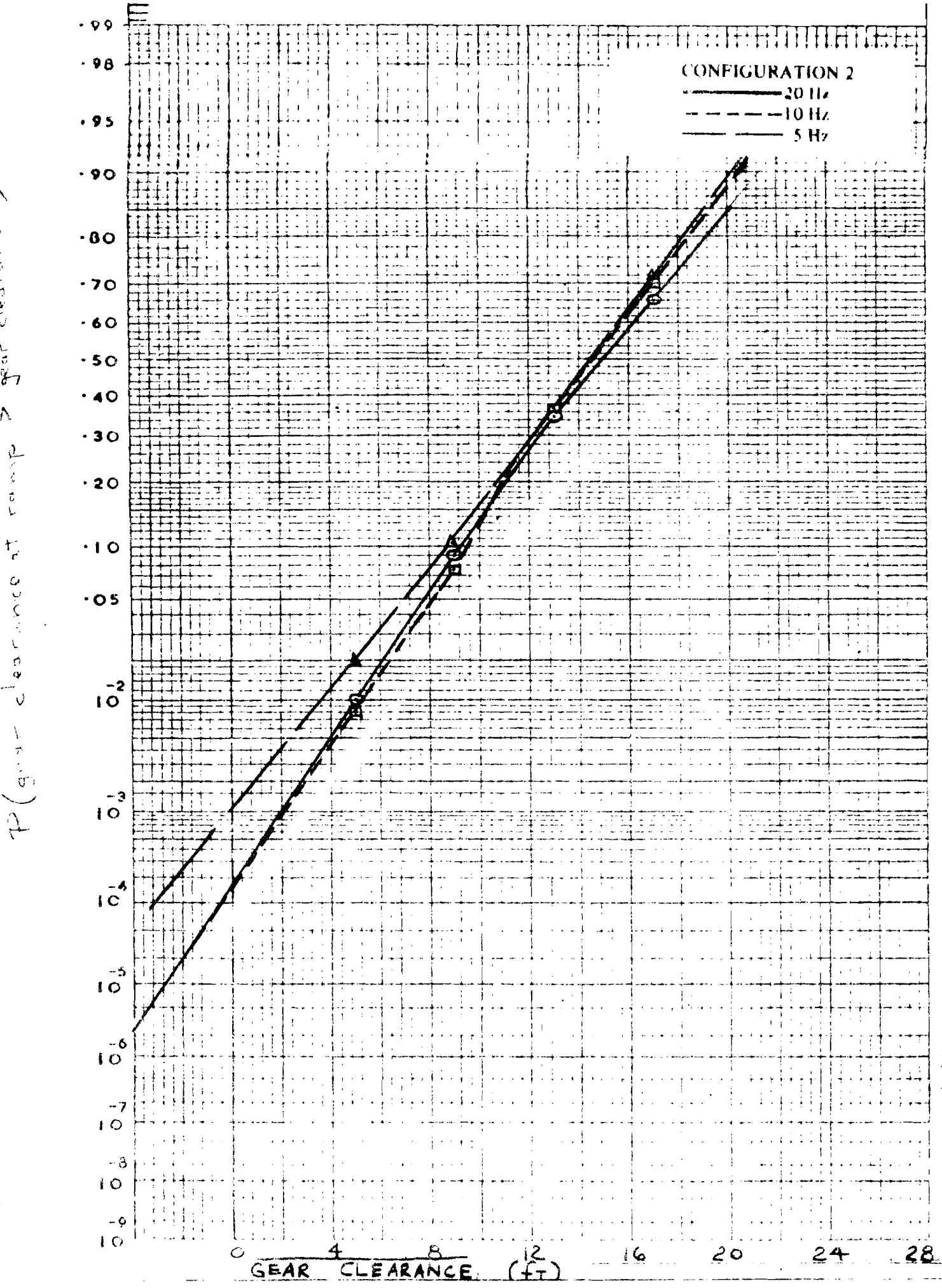
CONFIGURATION 2
20 Hz
10 Hz
5 Hz
·99
·98
·95
·90
·80
·70
·60
·50
·40
·30
·20
·10
·05
10^{-2}
10^{-3}
10^{-4}
10^{-5}
10^{-6}
10^{-7}
10^{-8}
10^{-9}
0
4
8
12
16
20
24
28
GEAR CLEARANCE (FT)
ARITHMETICAL PROBABILITY

FIG. A-5

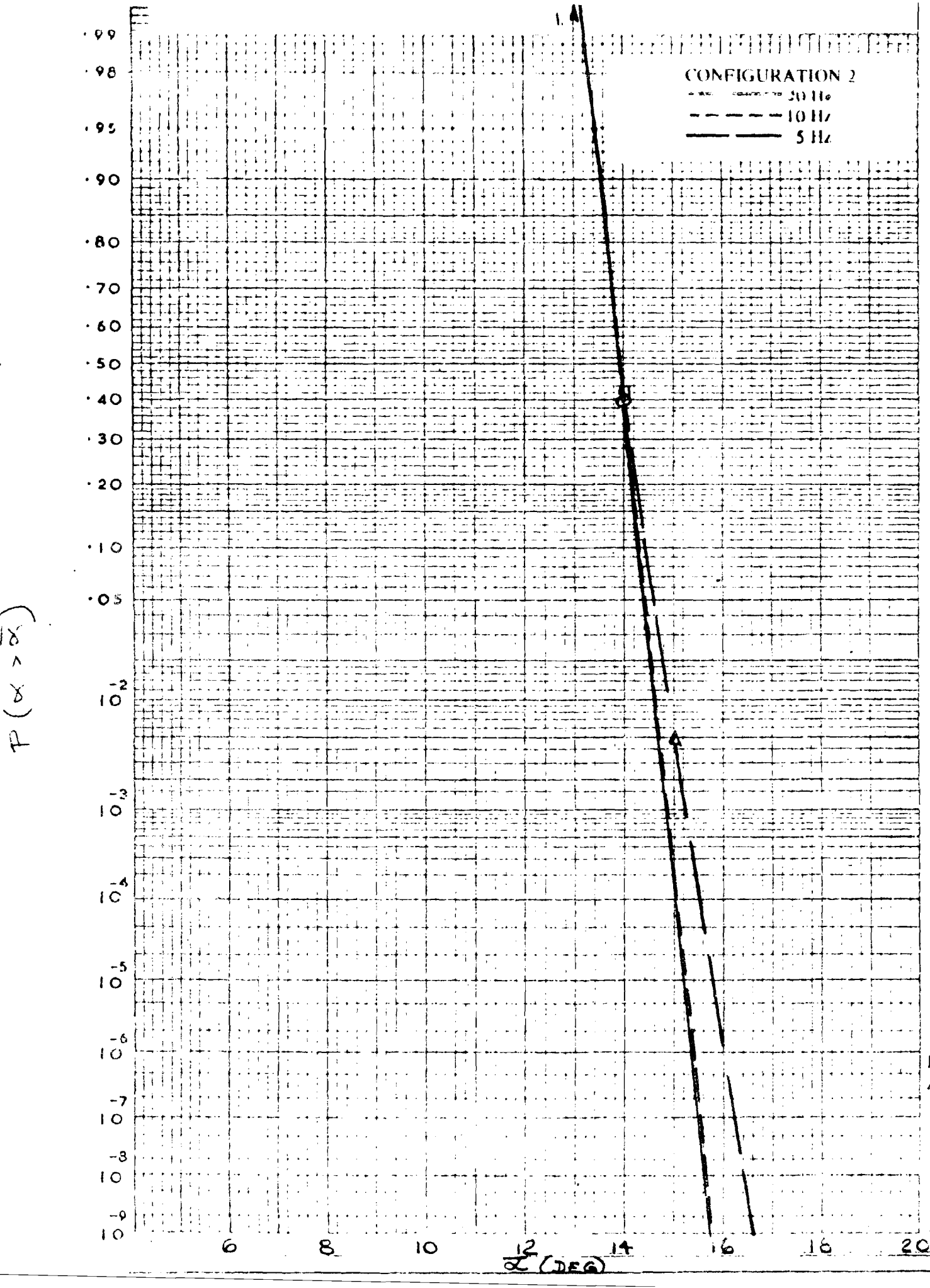

ARITHMETICAL PROBABILITY

FIG. A-6

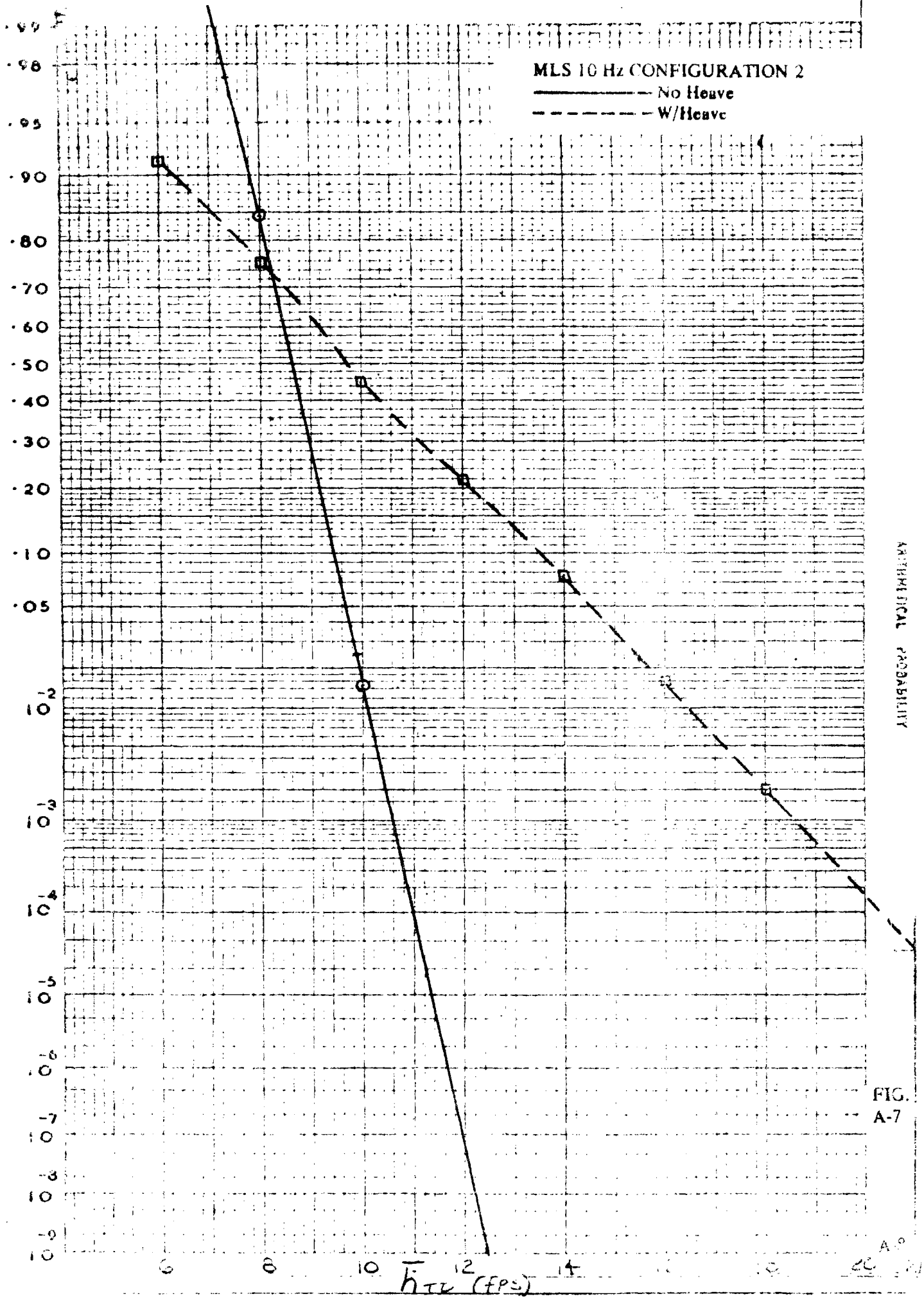

FIG. A-7

ARITHMETICAL PROBABILITY

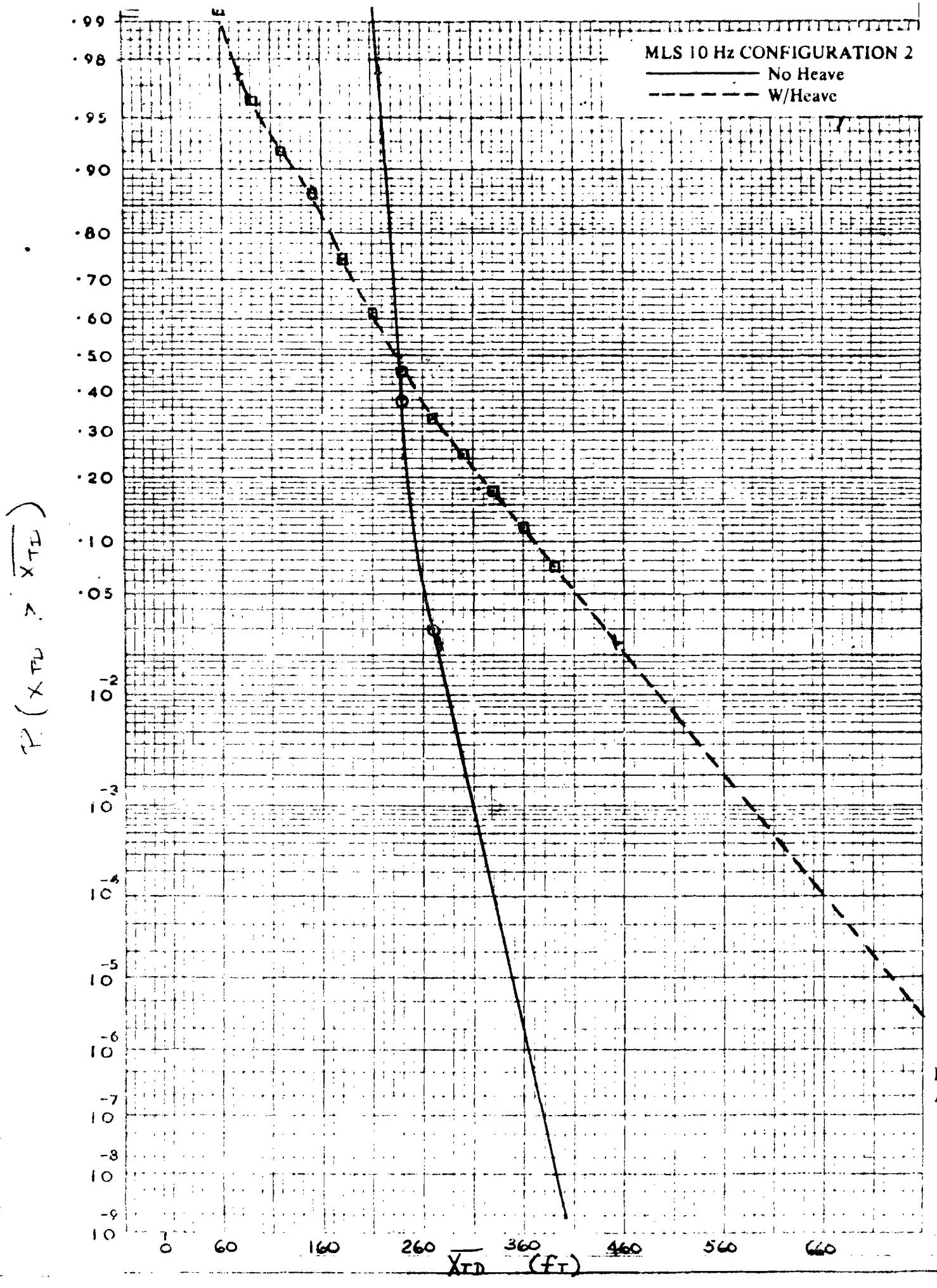

ARITHMETICAL PROBABILITY

FIG. A-8

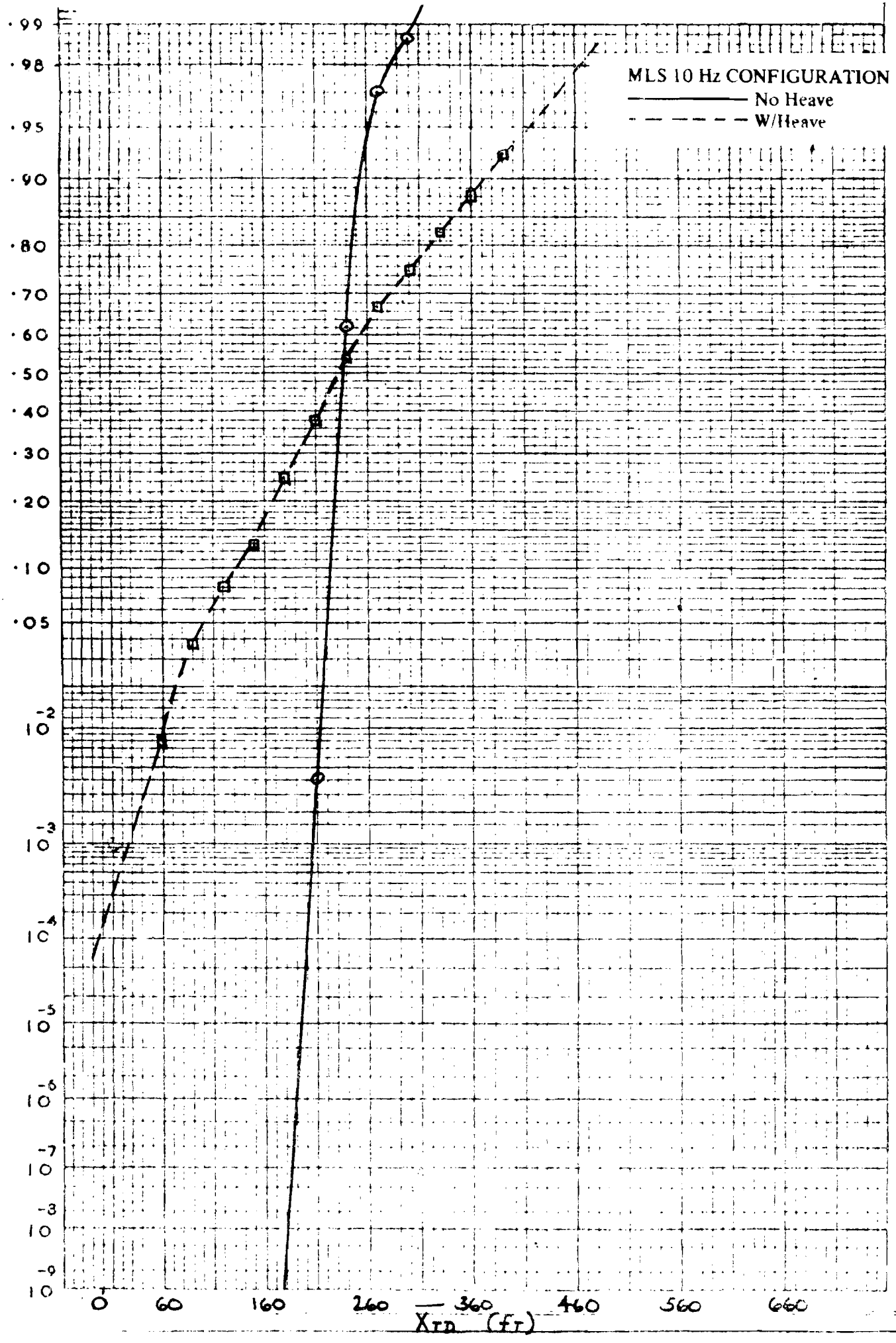

ARITHMETICAL PROBABILITY

FIG. A-9

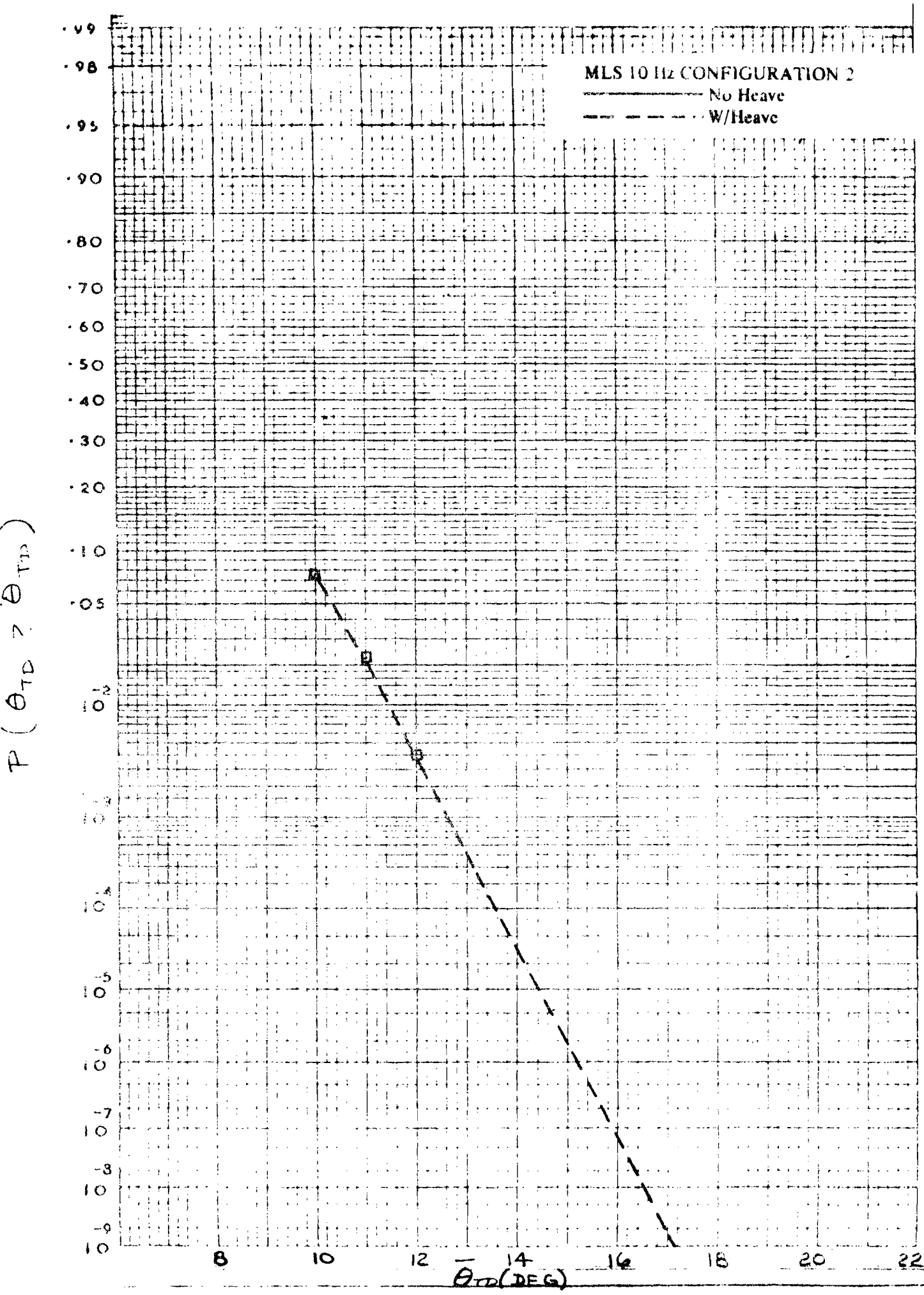

ARITHMETICAL PROBABILITY

FIG. A-10

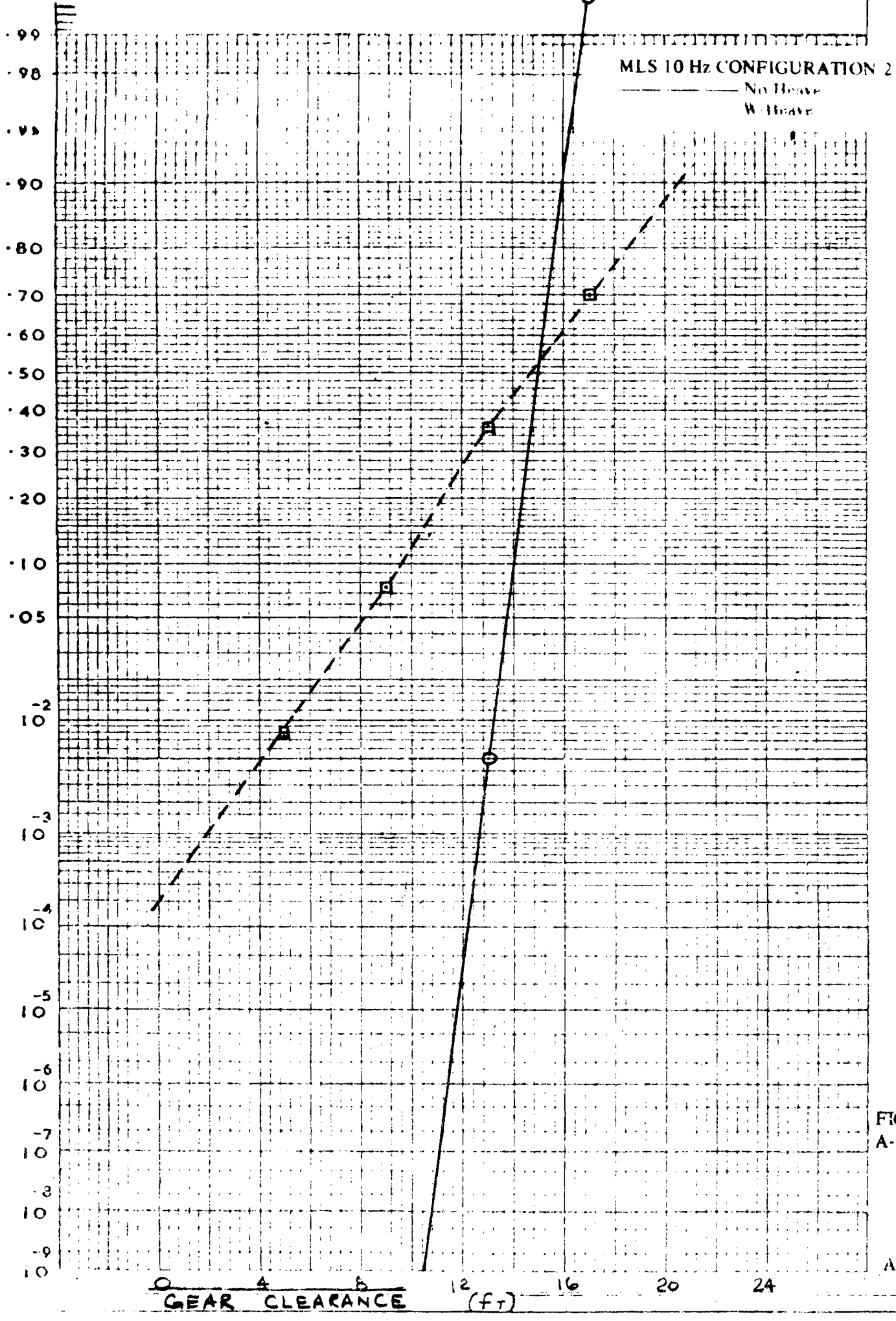

ARITHMETICAL PROBABILITY

FIG. A-11

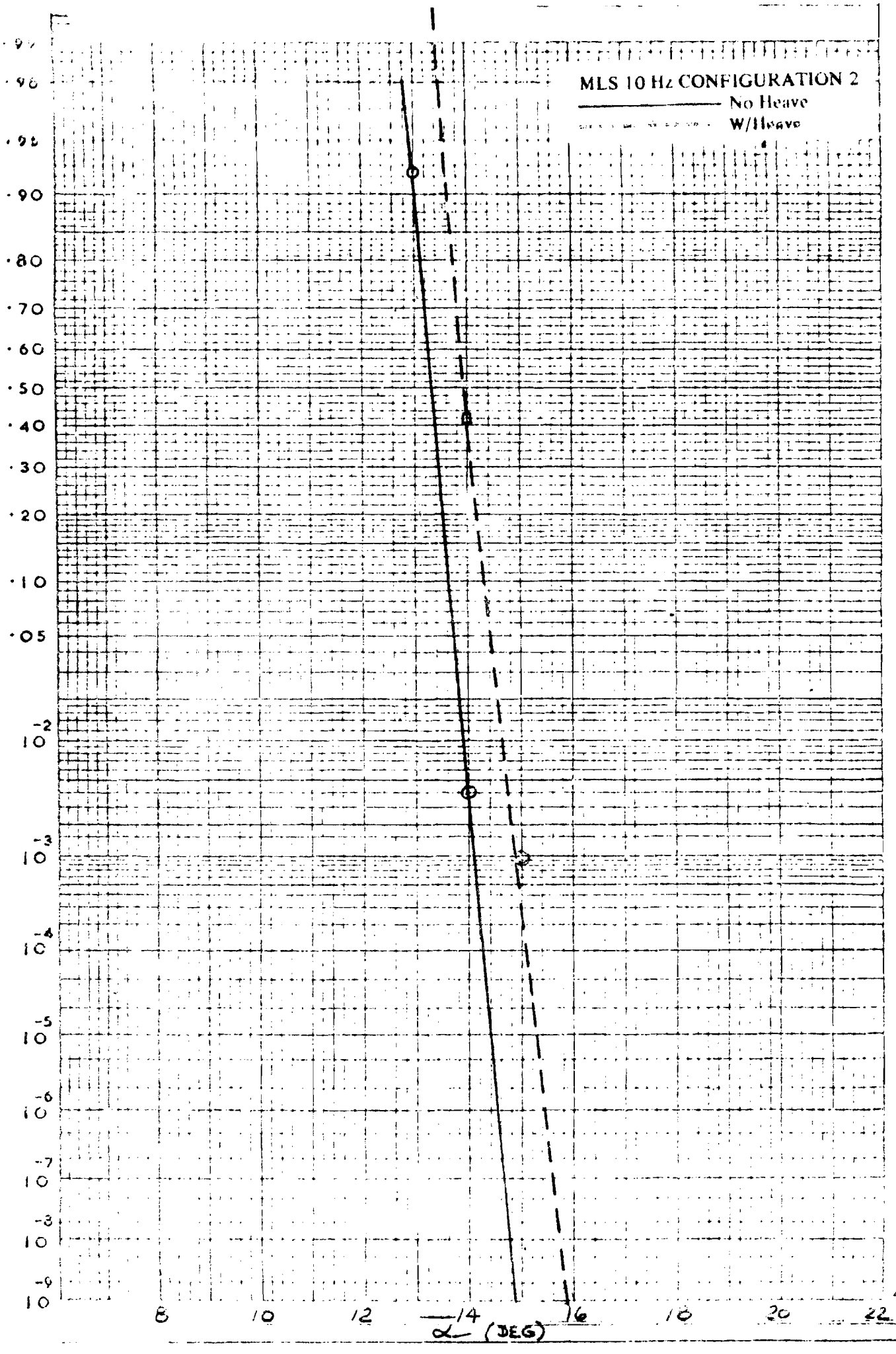
MLS 10 Hz CONFIGURATION 2
No Heave
W/Heave
.99
.98
.95
.90
.80
.70
.60
.50
.40
.30
.20
.10
.05
10^{-2}
10^{-3}
10^{-4}
10^{-5}
10^{-6}
10^{-7}
10^{-8}
10^{-9}
8
10
12
14
16
18
20
22
α (DEG)
ARITHMETICAL PROBABILITY

FIG. A-12

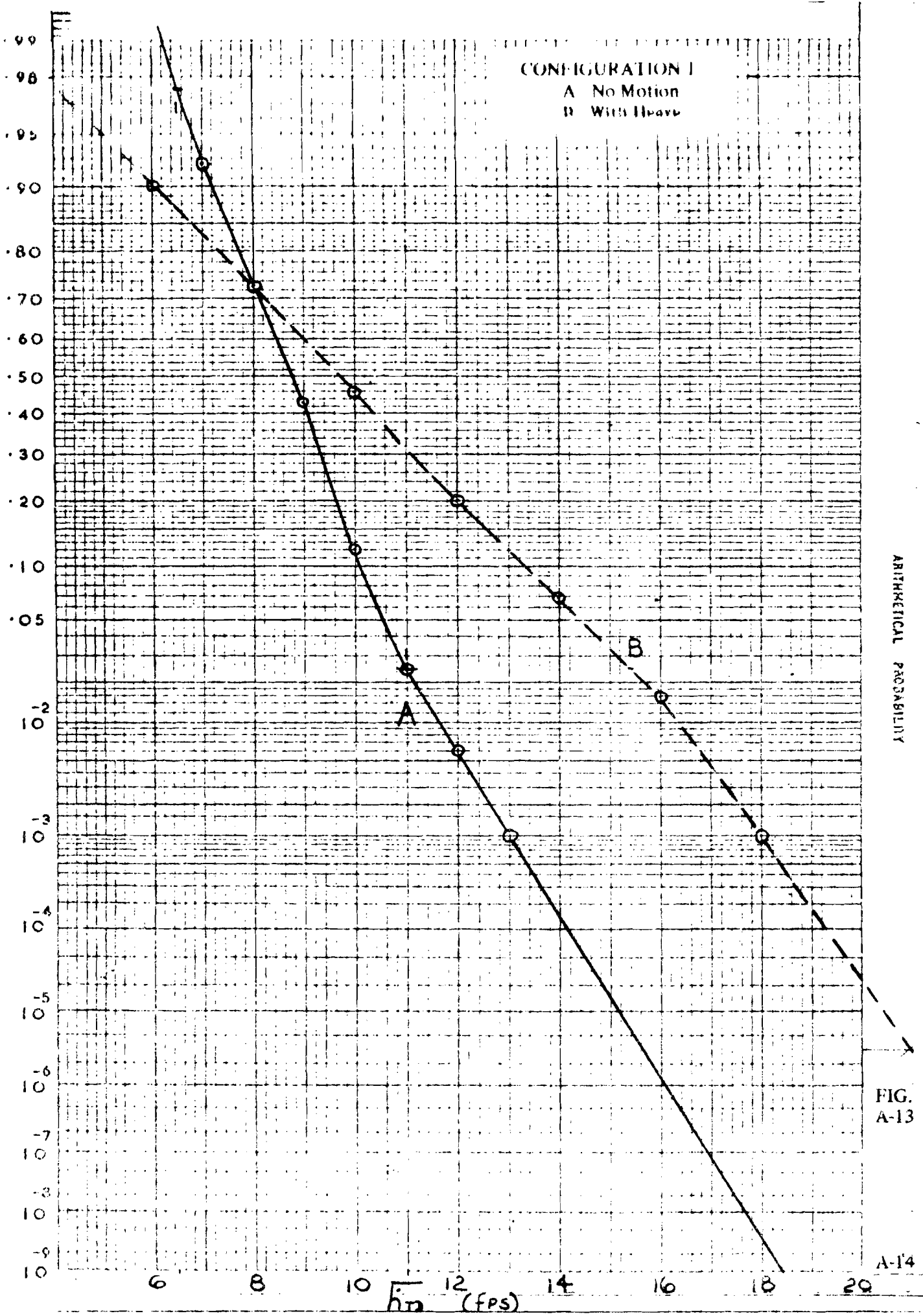
CONFIGURATION I
A No Motion
B With Heave
A
B
·99
·98
·95
·90
·80
·70
·60
·50
·40
·30
·20
·10
·05
10^{-2}
10^{-3}
10^{-4}
10^{-5}
10^{-6}
10^{-7}
10^{-8}
10^{-9}
6
8
10
12
14
16
18
20
$\overline{h_{1/3}}$ (FPS)
ARITHMETICAL PROBABILITY

FIG. A-13

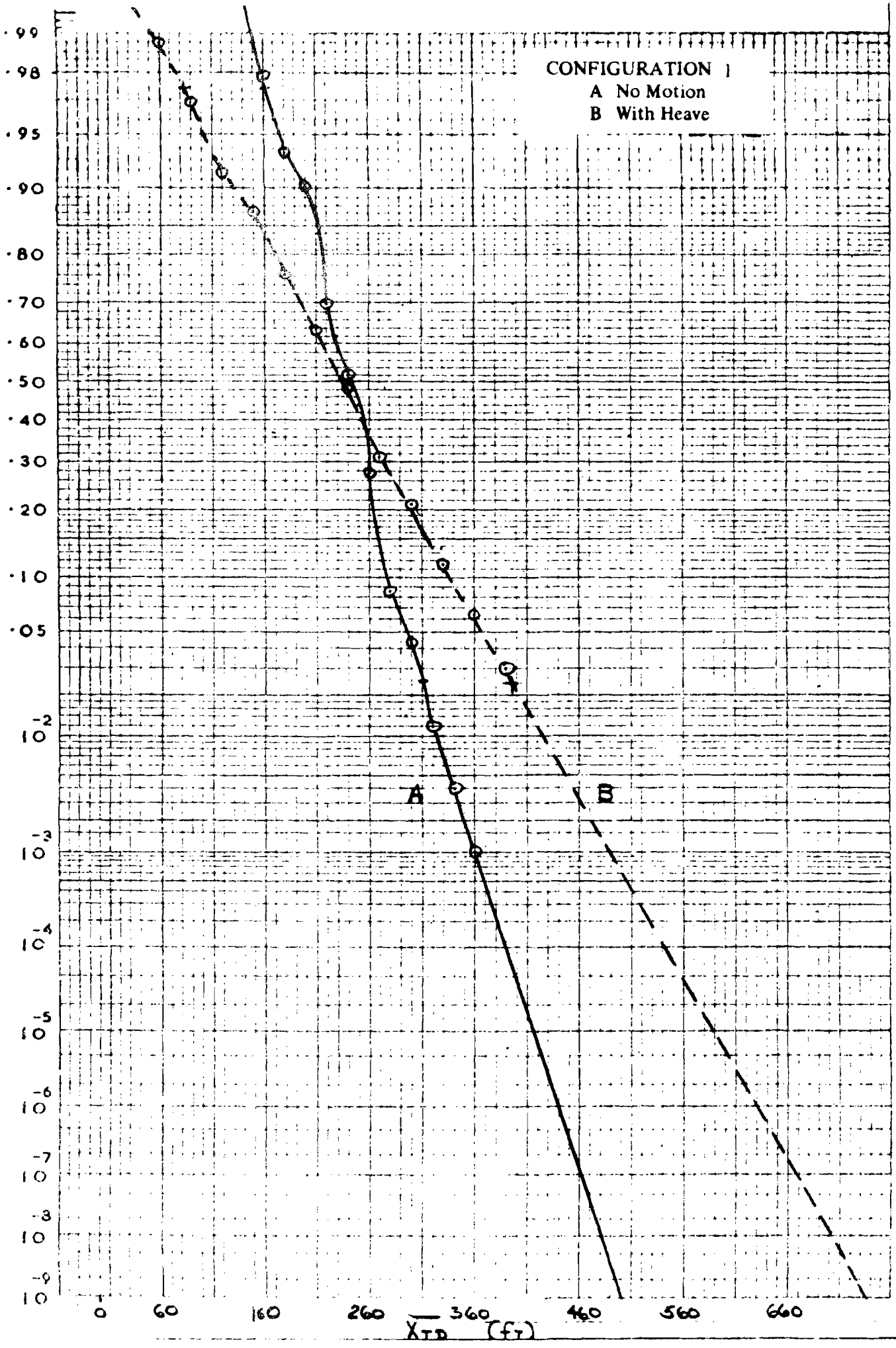

ARITHMETICAL PROBABILITY

FIG. A-14

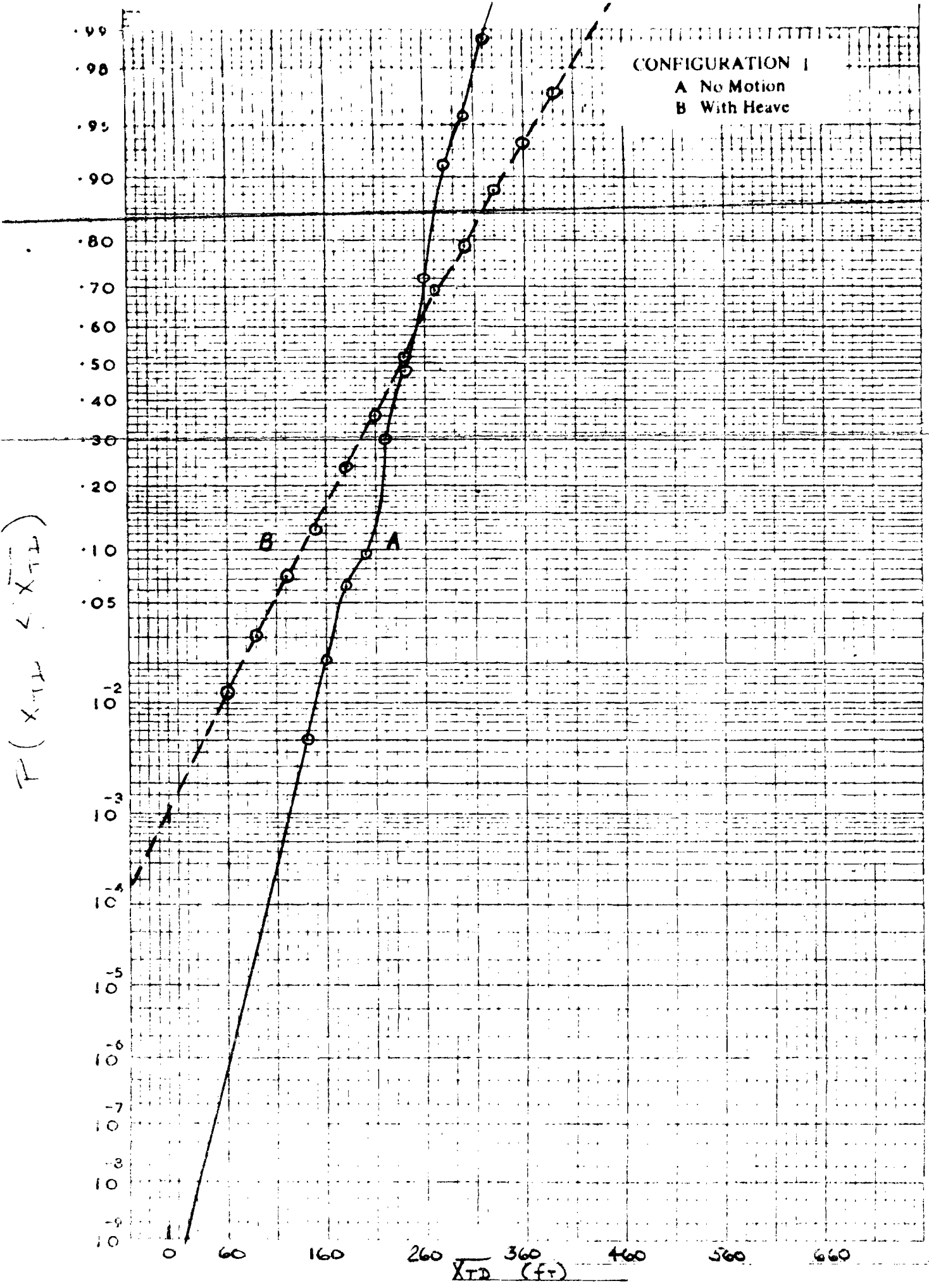

ARITHMETICAL PROBABILITY

FIG. A-15

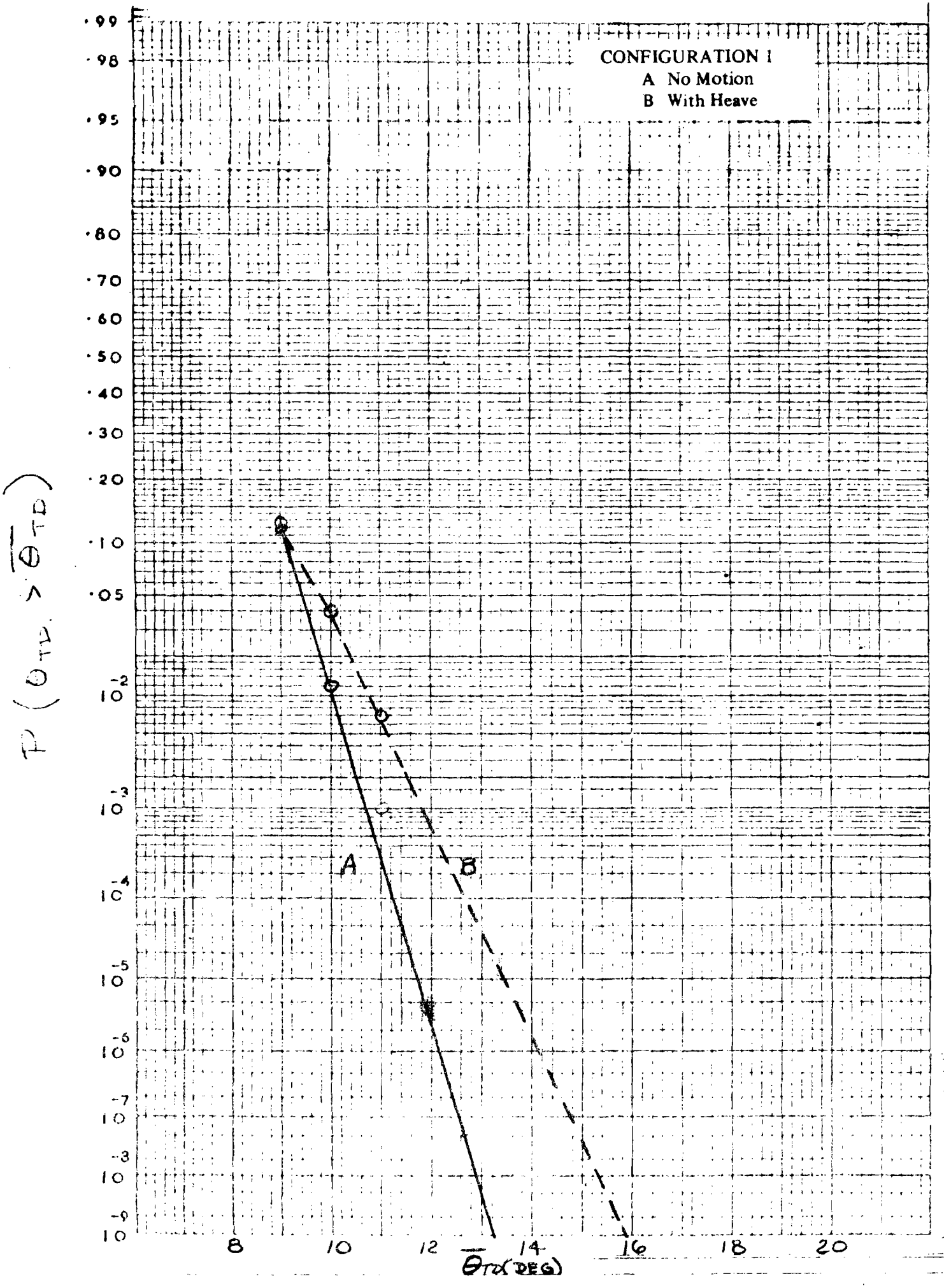

ARITHMETICAL PROBABILITY

FIG. A-16

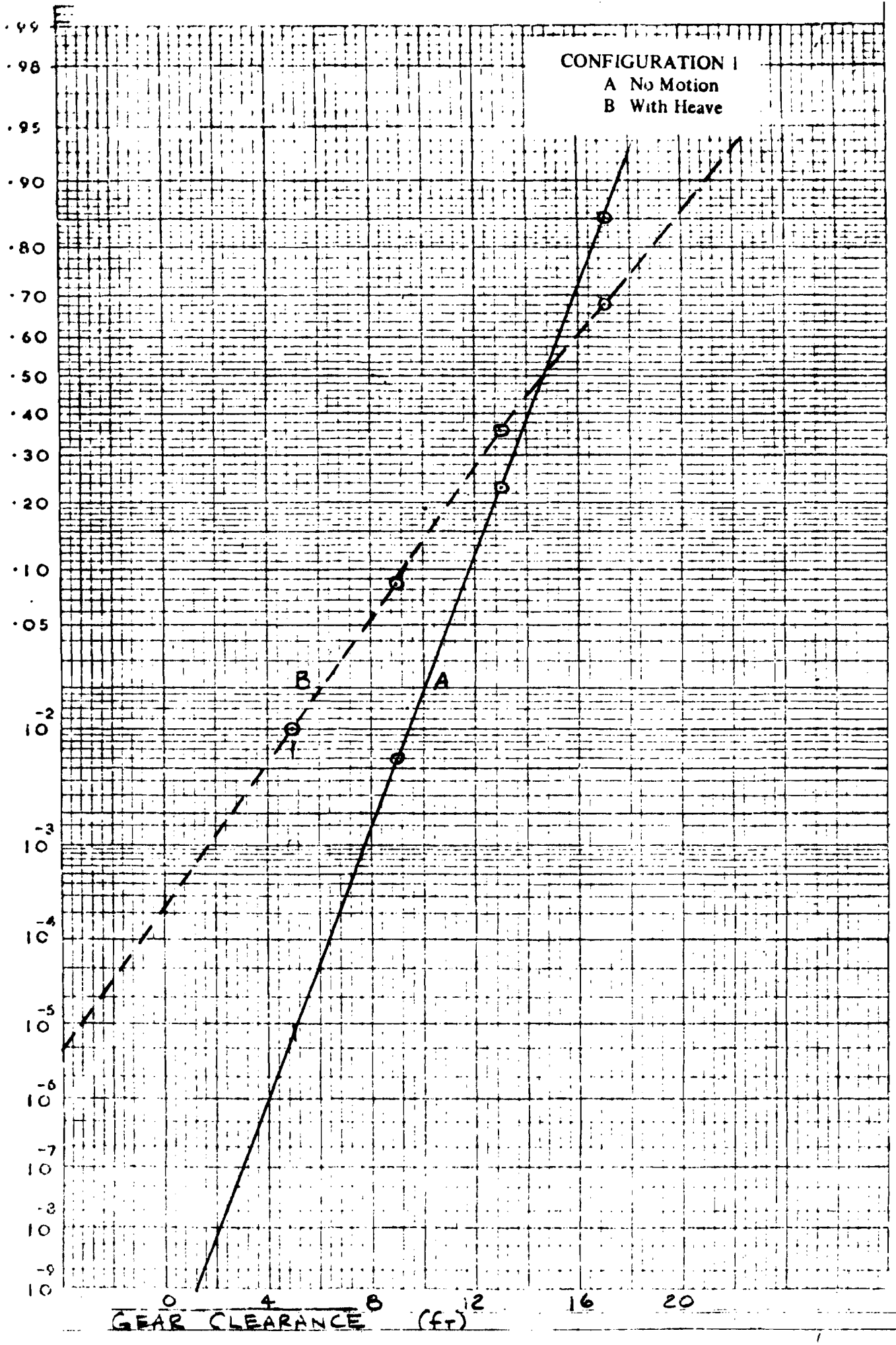

ARITHMETICAL PROBABILITY

FIG. A-17

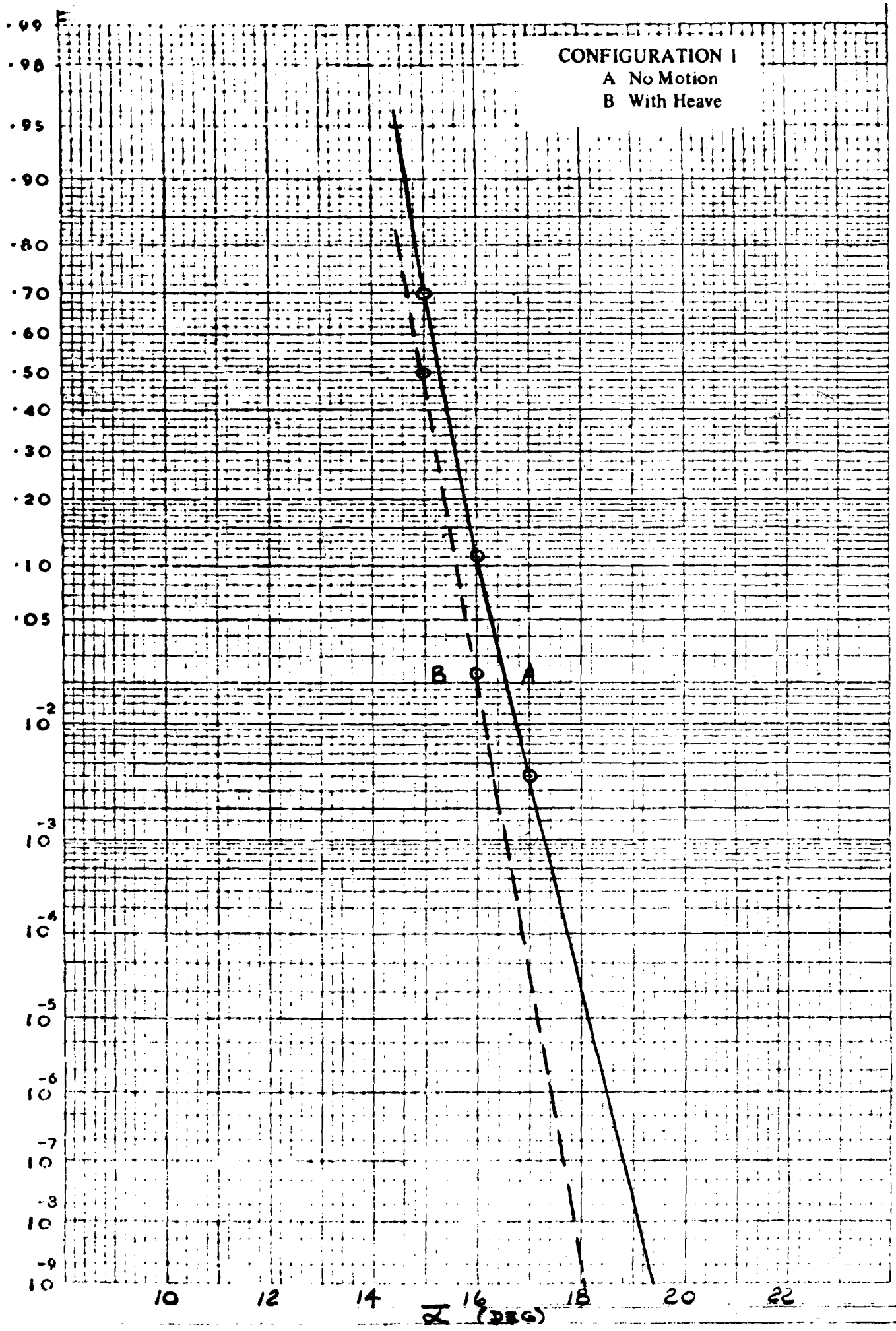

ARITHMETICAL PROBABILITY

FIG. A-18

APPENDIX B

ACTIVITY TRACES

Figure	Configuration	Scan Rate (Hz)	Title
B-1	1	10	Activity at 500 feet due to H.T., V.T., B.N., and Heave
B-2	1	10	Activity at 500 feet due to combined disturbances
B-3	1	10	Activity with 5 fps beam rate limit
B-4	1	10	Activity with 10 fps beam rate limit
B-5	2	10	Activity at 500 feet due to H.T. and V.T.
B-6	2	10	Activity at 500 feet due to B.N. and Heave
B-7	2	10	Activity at 500 feet due to combined disturbances
B-8	2	5	Activity at 500 feet due to H.T., V.T., B.N. and Heave
B-9	2	5	Activity at 500 feet due to combined disturbances

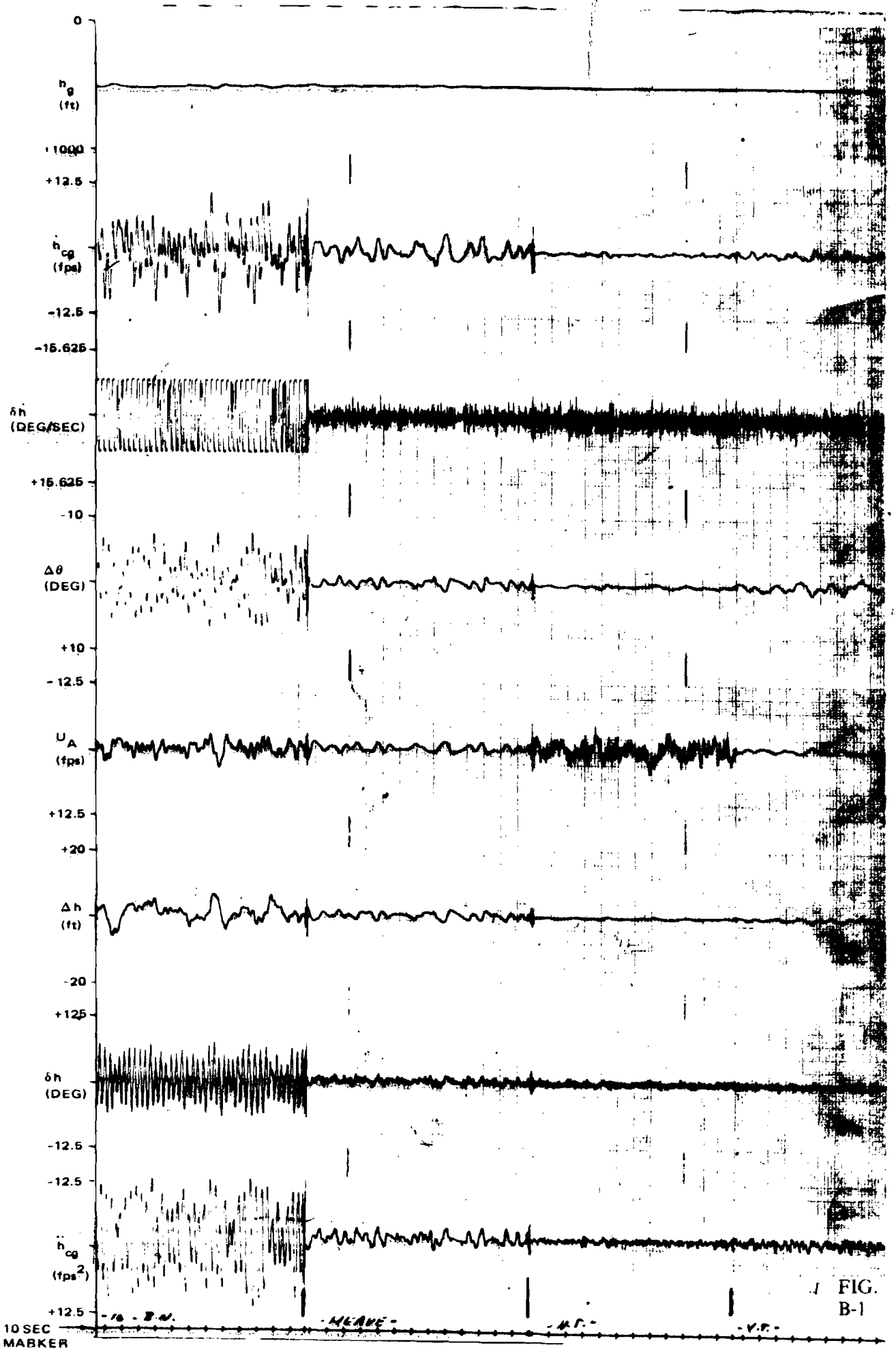
0
h_g (ft)
+1000
+12.5
$\dot{h}_{cg}$ (fps)
-12.5
-15.625
$\delta\dot{h}$ (DEG/SEC)
+15.625
-10
$\Delta\theta$ (DEG)
+10
-12.5
U_A (fps)
+12.5
+20
Δh (ft)
-20
+125
δh (DEG)
-12.5
-12.5
$\ddot{h}_{cg}$ (fps^2)
+12.5
10 SEC MARKER

FIG. B-1

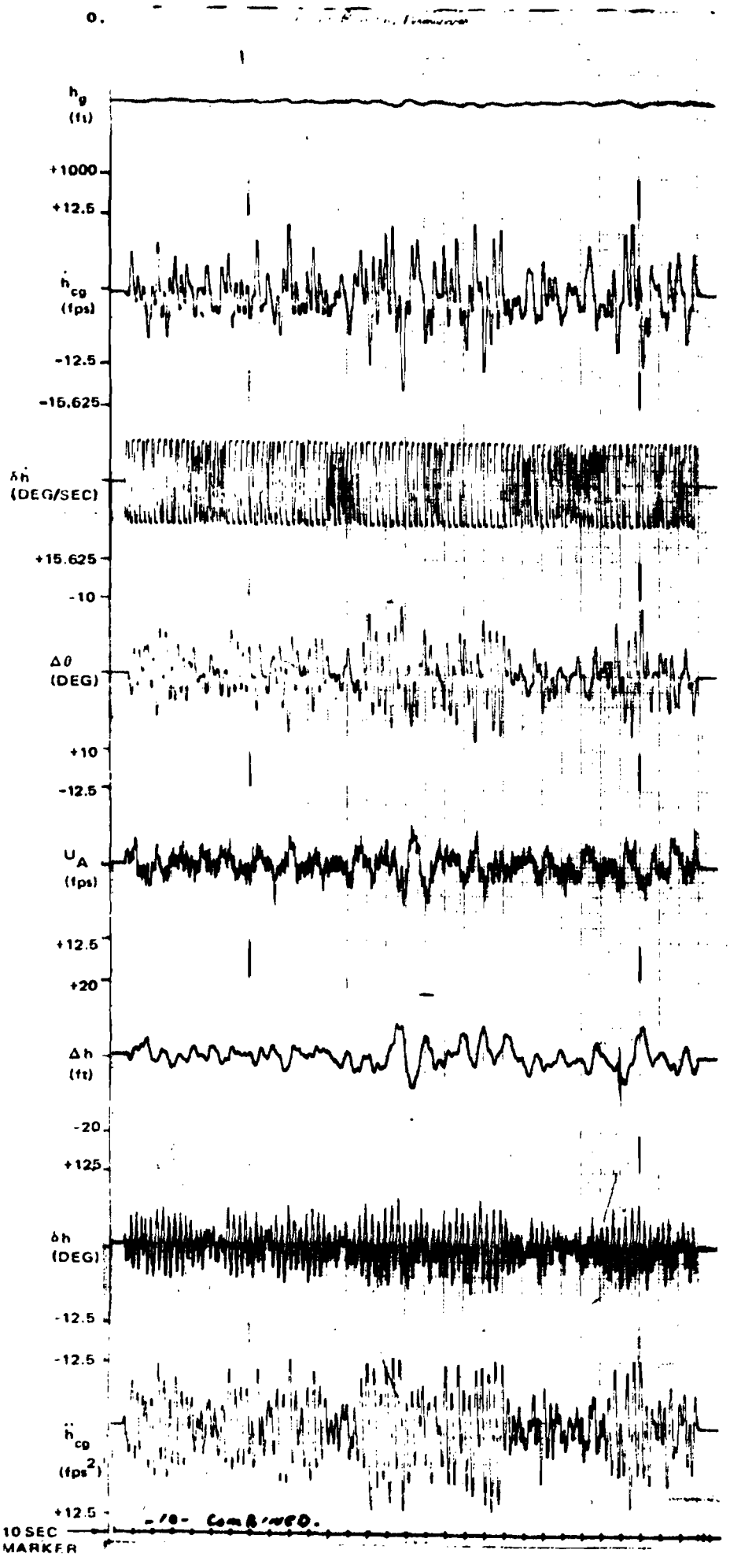
0.
h_g (ft)
+1000
+12.5
$\dot{h}_{cg}$ (fps)
-12.5
-15.625
$\delta\dot{h}$ (DEG/SEC)
+15.625
-10
$\Delta\theta$ (DEG)
+10
-12.5
U_A (fps)
+12.5
+20
Δh (ft)
-20
+12.5
δh (DEG)
-12.5
-12.5
$\ddot{h}_{cg}$ (fps^2)
+12.5
10 SEC MARKER

FIG. B-2

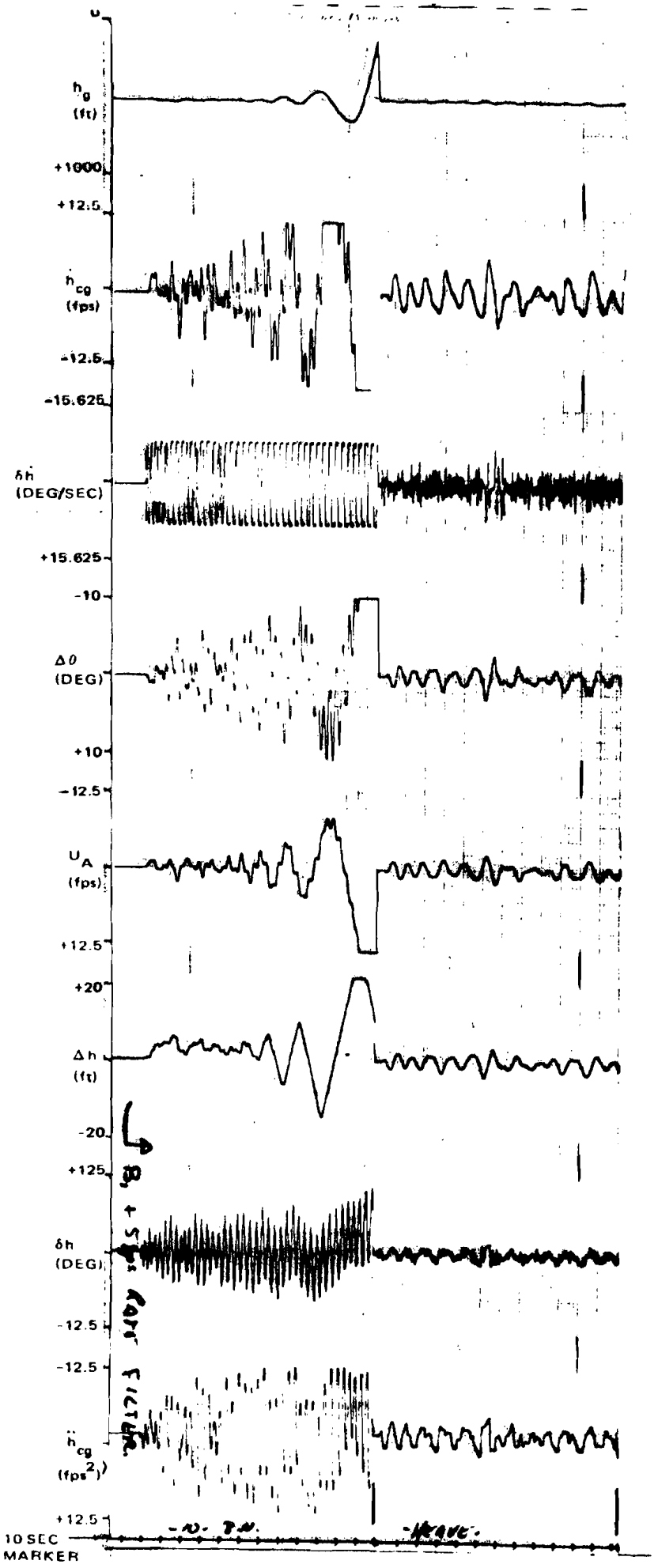
h_g (ft)
+1000
+12.5
$\dot{h}_{cg}$ (fps)
-12.5
-15.625
$\delta\dot{h}$ (DEG/SEC)
+15.625
-10
$\Delta\theta$ (DEG)
+10
-12.5
U_A (fps)
+12.5
+20
Δh (ft)
-20
+125
δh (DEG)
-12.5
-12.5
$\ddot{h}_{cg}$ (fps^2)
+12.5
10 SEC MARKER

FIG. B-3

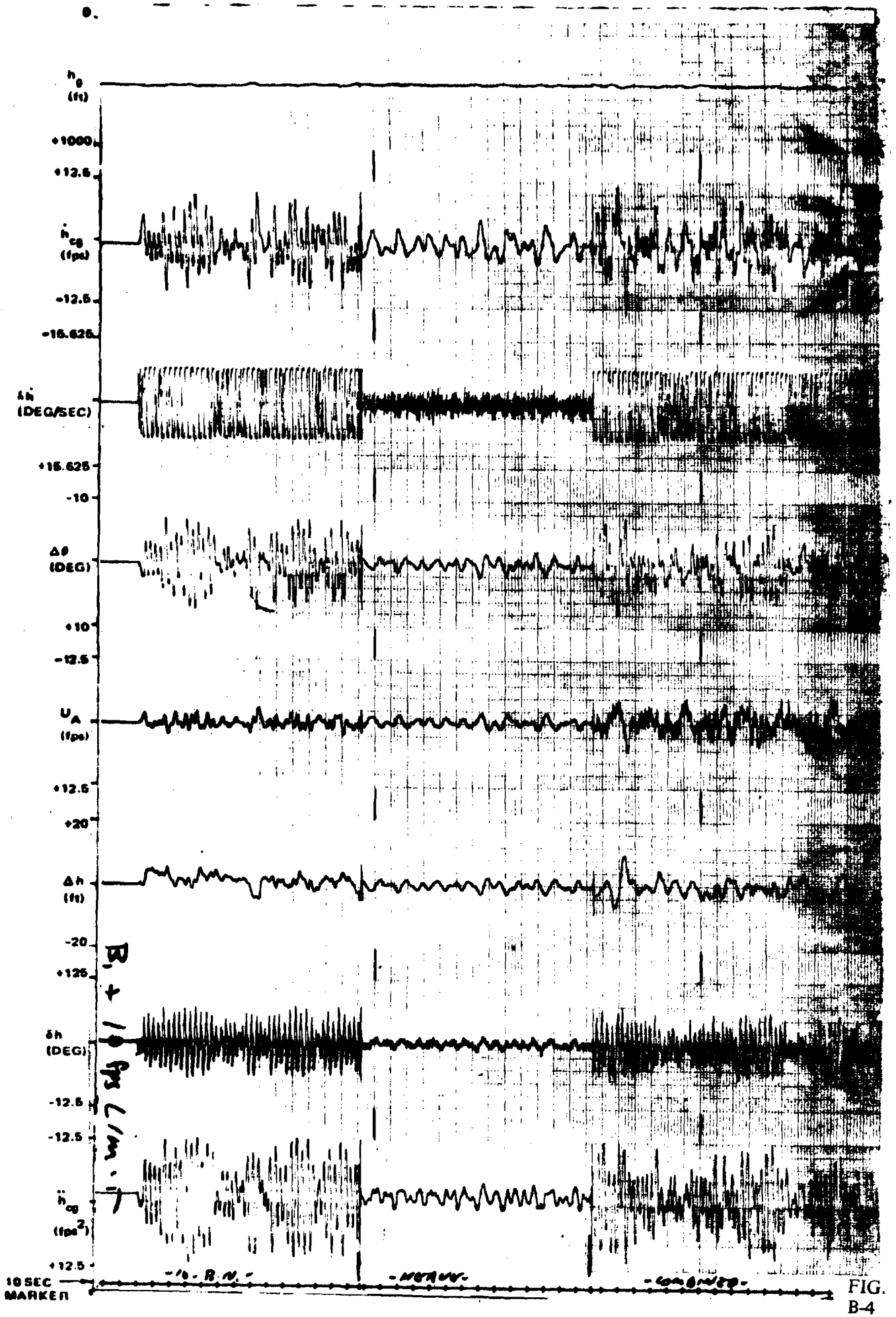
h_g (ft)
+1000
+12.5
$\dot{h}_{cg}$ (fps)
-12.5
-15.625
$\delta\dot{h}$ (DEG/SEC)
+15.625
-10
$\Delta\theta$ (DEG)
+10
-12.5
U_A (fps)
+12.5
+20
Δh (ft)
-20
+125
δh (DEG)
-12.5
-12.5
$\ddot{h}_{cg}$ (fps^2)
+12.5
10 SEC MARKER
-NORMAL-
-COMBINED-

FIG. B-4

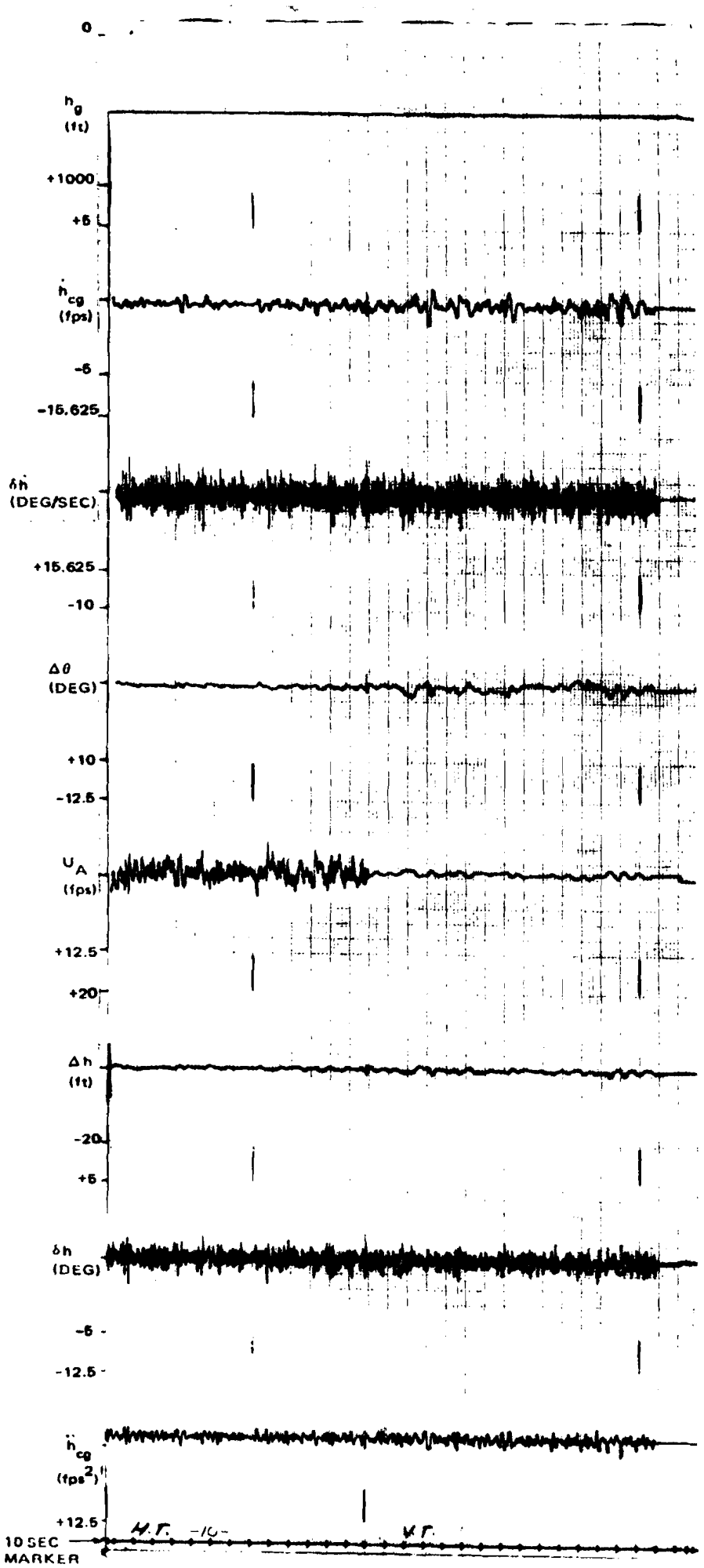
0
h_g (ft)
+1000
+5
$\dot{h}_{cg}$ (fps)
-5
-15.625
$\delta\dot{h}$ (DEG/SEC)
+15.625
-10
$\Delta\theta$ (DEG)
+10
-12.5
U_A (fps)
+12.5
+20
Δh (ft)
-20
+5
δh (DEG)
-5
-12.5
$\ddot{h}_{cg}$ (fps^2)
+12.5
10 SEC MARKER

FIG. B-5

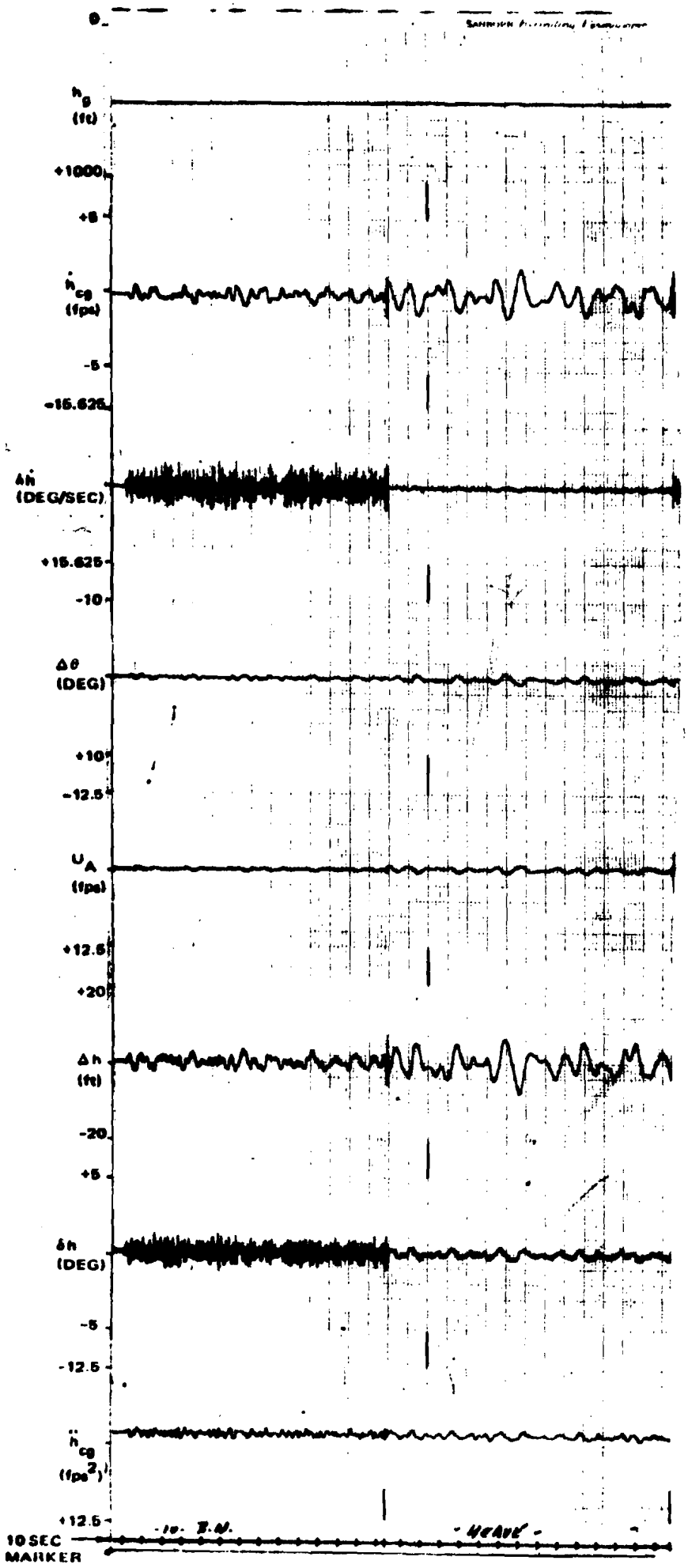
0
h_g (ft)
+1000
+5
$\dot{h}_{cg}$ (fps)
-5
-15.625
$\Delta\dot{h}$ (DEG/SEC)
+15.625
-10
$\Delta\theta$ (DEG)
+10
-12.5
U_A (fps)
+12.5
+20
Δh (ft)
-20
+5
δh (DEG)
-5
-12.5
$\ddot{h}_{cg}$ (fps^2)
+12.5
10 SEC MARKER
- HEAVE -

FIG. B-6

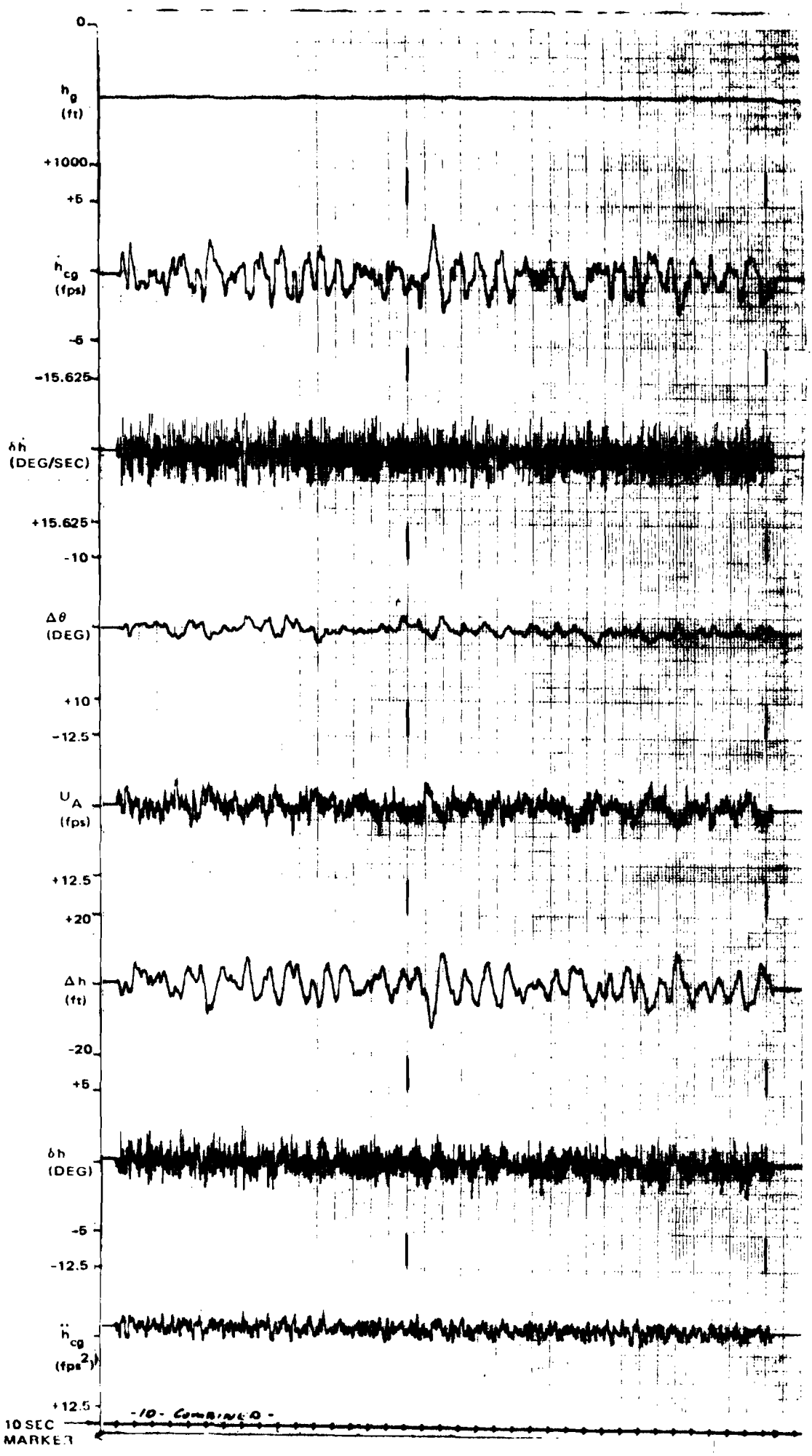
0
h_g (ft)
+1000
+5
$\dot{h}_{cg}$ (fps)
-5
-15.625
$\delta\dot{h}$ (DEG/SEC)
+15.625
-10
$\Delta\theta$ (DEG)
+10
-12.5
U_A (fps)
+12.5
+20
Δh (ft)
-20
+5
δh (DEG)
-5
-12.5
$\ddot{h}_{cg}$ (fps^2)
+12.5
10 SEC MARKER
-10- COMBINED -

FIG. B-7

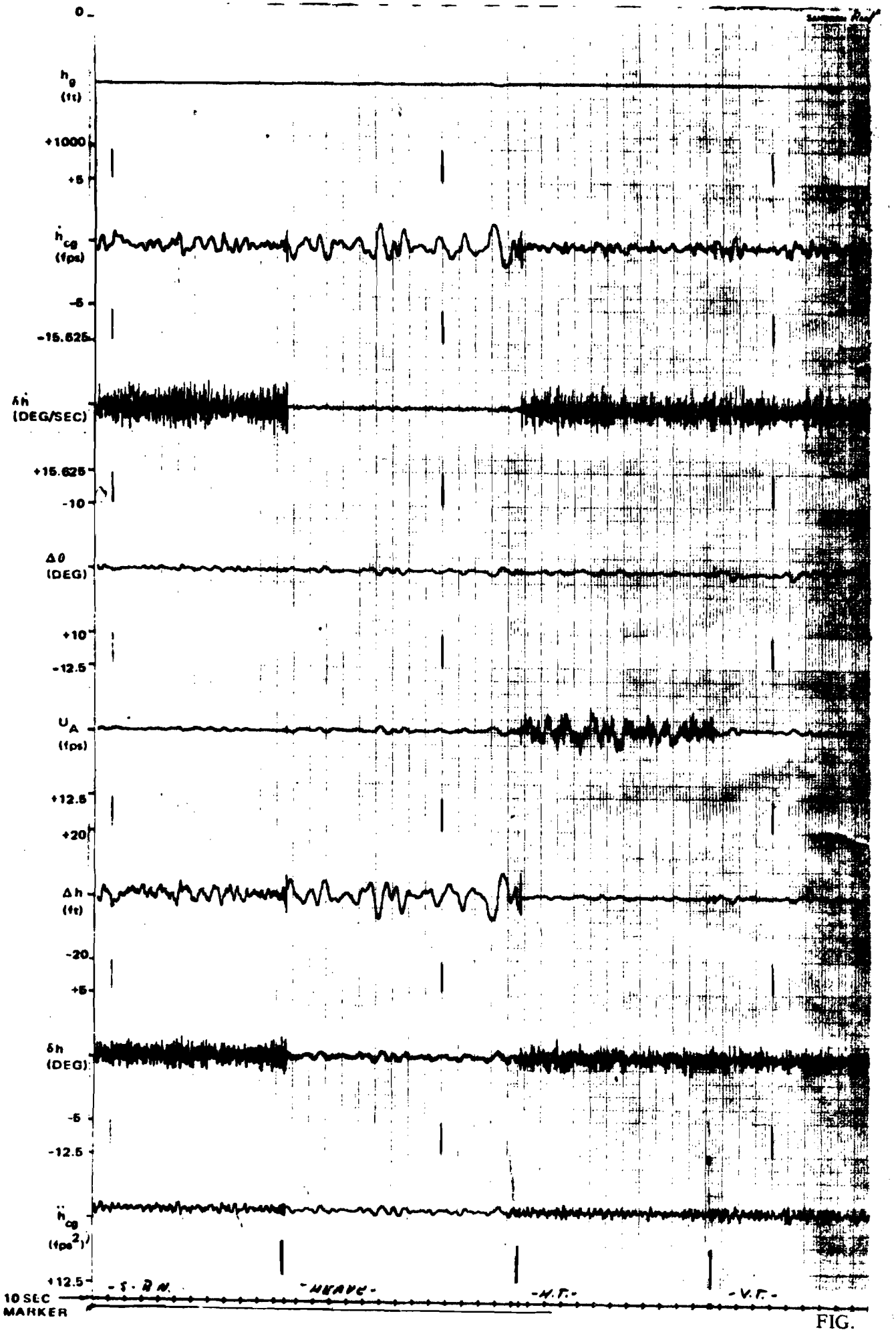
0
h_g (ft)
+1000
+5
$\dot{h}_{cg}$ (fps)
-5
-15.625
$\delta\dot{h}$ (DEG/SEC)
+15.625
-10
$\Delta\theta$ (DEG)
+10
-12.5
U_A (fps)
+12.5
+20
Δh (ft)
-20
+5
δh (DEG)
-5
-12.5
$\ddot{h}_{cg}$ (fps^2)
+12.5
10 SEC MARKER
-S.R.N.
-HEAVE-
-H.T.-
-V.T.-

FIG. B-8

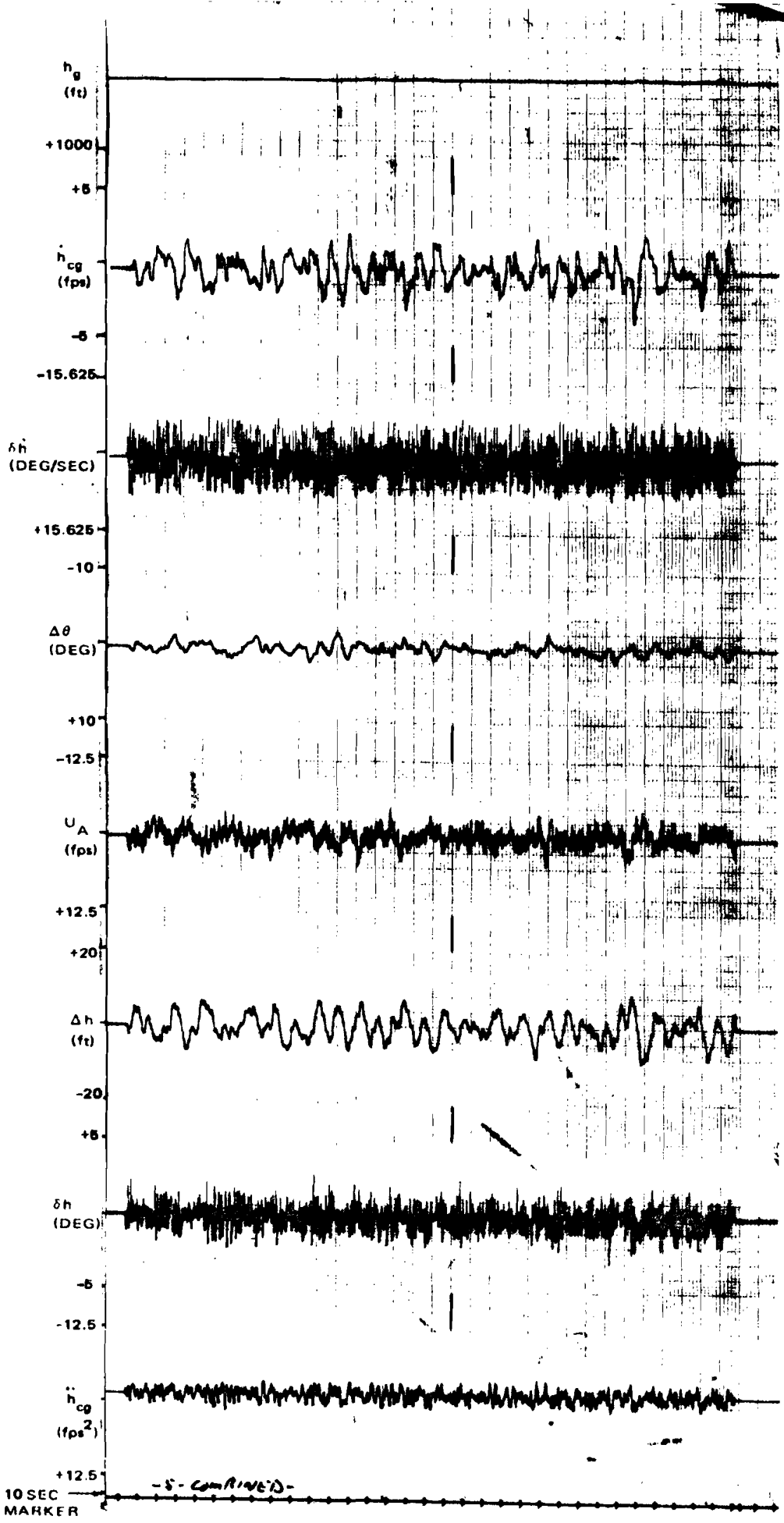
h_g (ft)
+1000
+5
$\dot{h}_{cg}$ (fps)
-5
-15.625
$\delta\dot{h}$ (DEG/SEC)
+15.625
-10
$\Delta\theta$ (DEG)
+10
-12.5
U_A (fps)
+12.5
+20
Δh (ft)
-20
+5
δh (DEG)
-5
-12.5
$\ddot{h}_{cg}$ (fps^2)
+12.5
10 SEC MARKER
-S- COMBINED-

FIG. B-9

IX. ECM/ECCM ANALYSIS

a. General

This section presents the results of an analysis conducted on the MLS military configurations to verify that the MLS concept can successfully perform in tactical ECM environment. The analysis basically shows that, although the MLS signals could be jammed at the airborne receiver, the normal deployment of the ground stations will prevent the enemy from detecting the MLS frequency and modulation characteristics necessary to concentrate his jamming power within the receiver bandwidths. Additionally, the airborne receiver does not radiate; thus the aircraft position is unknown to the jammer and the jammer cannot concentrate his antenna gain on the aircraft but would have to area or zone jam requiring broader jamming beamwidths with lower antenna gain and greater deployment ranges to cover larger areas. All of these requirements act to the advantage of the MLS. Some question also exists as to the enemy's desire to jam MLS operation with unknown (unobservable) results versus using his jammers more effectively for fighter air defense which normally has a high priority and observable results. These three factors: low probability of MLS signal detection, unknown aircraft location, and probable enemy ECM priorities indicate that the MLS concept should be effective in a sophisticated tactical ECM environment. The following sections present summary analyses of the ground-based (E_2-E_3-G_2-I_3) and shipboard (I_2) MLS configurations.

b. Ground Based Systems

1. General

The Army E_2/E_3 and the USMC G_2/I_3 configurations are normally tactically deployed in the vicinity of the forward edge of the battle area (FEBA). The E_2 and G_2 systems might also be deployed behind enemy lines during airmobile/assault operations. These environments result in operations within the range of both air defense and field multipurpose jammers. Two ground-based jammers were configured for analysis purposes. They employ noise jamming and represent what the enemy could have in his inventory. It is not expected that the enemy would develop jammers especially designed to jam or deceive MLS type equipment. Jammers 1 and 2 have the following characteristics:

	Jammer 1	Jammer 2
Frequency	15.4 - 15.6 GHz	15.4 - 15.6 GHz
Waveform	Noise	Noise
Power	1000 watts CW	100 watts CW
Antenna gain	20 dB	20 dB
Antenna beamwidth	≃17 degrees	≃ 17 degrees
Jamming bandwidth	2 and 10 MHz	2 and 10 MHz
Sensitivity	-98 dBm	-98 dBm

The analysis is divided into two basic areas; detection and jamming. A hypothetical deployment of the E_2/G_2 configuration is depicted which should be representative of the expected tactical situation; however, the data is presented such that it may be extrapolated to other deployment situations.

2. Detection

The operation of the MLS differs somewhat from the normal radar ECM analysis in that the radiating element is ground based without a reception capability and the airborne receiver is non-radiating. The enemy must thus detect the ground emitted radiation to determine frequency and modulation characteristics and then direct the jamming signal at some aircraft position (which he cannot determine and, therefore, must zone or area jam). Therefore, without adequate detection of the ground station characteristics, the enemy cannot jam the aircraft receiver to prevent MLS operations. The detection of the ground system is affected by range, propagation effects, and terrain shadowing, each of which is discussed below.

Assuming that line of sight could exist between the MLS ground system and the jammer unit and that the peak gain of the MLS antenna (the azimuth antenna in this case since it has higher gain) is directed at the jammer, the curves of Figure D-21 give the absolute maximum detection ranges for clear air and with intervening rainfall at a rate of 15mm/hr. Considering that the MLS could be in use at night without precipitation, the maximum detected range would be 52 nmi. Using the standard equation of $R = 1.23\sqrt{h}$

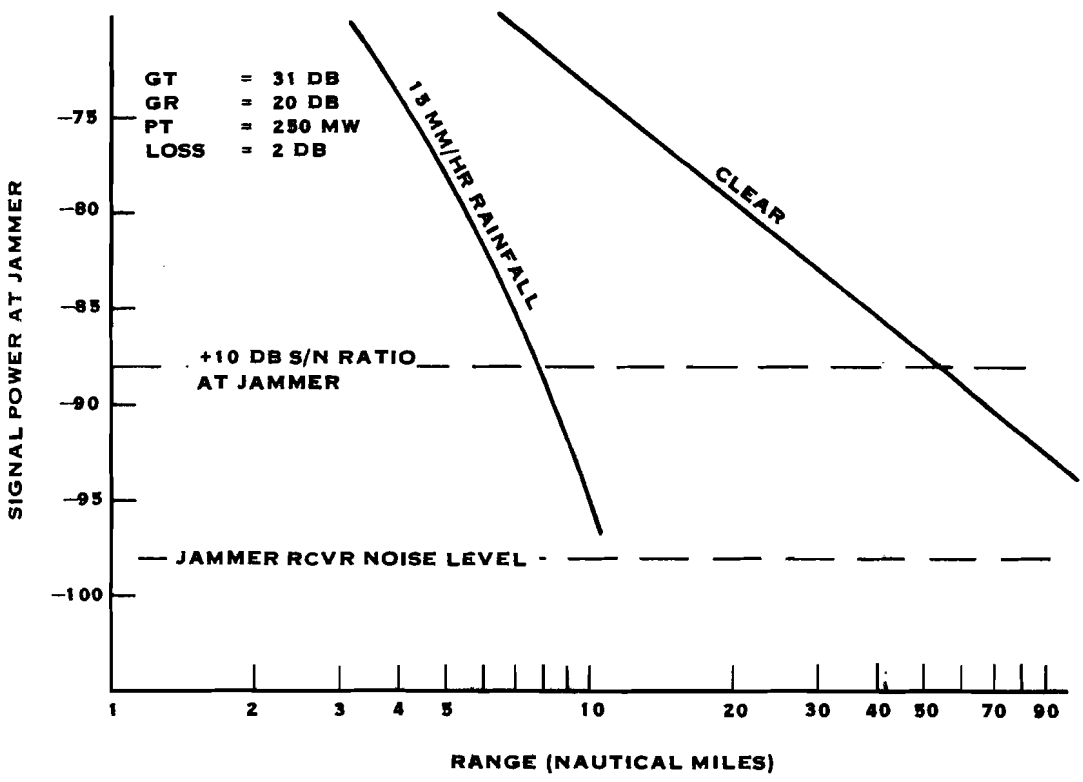

Figure D-21. MLS Jammer Detection Range

for curvature of the earth, the jammer would have to be located at a relative height of ≃ 1800 feet above the MLS site elevation. An altitude of approximately 400 feet would probably be more realistic for a situation of a jammer placed on a high-terrain feature and the landing site in a valley. This situation would limit the detected line-of-sight range to approximately 25 nmi. This range must be additionally modified by terrain masking, such as trees surrounding the landing zone, the fact that the gain of the MLS beam at low angles is at least 12 dB down (reducing the 25-nmi range to 6.25 nmi), and the probability that the MLS scan sector may not face the jammer (from 0.167 to 0.95 assuming uniform probability of facing any direction and using the various MLS sector widths). All of these factors indicate that with reasonable care in MLS deployment, maximizing the use of surrounding vegetation and terrain features, the enemy would have to be extremely close to the MLS for effective detection. This exposure would reduce the physical security of his jammers. The short ranges would also limit his ability to zone or area jam since his 17-degree beamwidth would cover a smaller area at closer ranges.

The propagation effects of concern are reflection, refraction, and attenuation. The effects of reflection are dependent on the environment but, in general can be neglected in the ECM case since most terrain surrounding the MLS would be absorptive (i.e., by vegetation) rather than reflective. Refraction will be very small at the Ku-band frequencies and the radio horizon will be the geometric horizon of the earth as discussed in the previous section. Attenuation at Ku-band will be approximately 0.02 dB/nmi in clear air and greater for increasing rainfall. More attenuation of course acts in favor of the MLS for ECM purposes since the detection ranges are reduced (Figure D-21) and the enemy's jamming power is also attenuated. The Ku-band frequencies have very poor foliage penetration for even small amounts of vegetation which is additionally in favor of the MLS.

In summary, there must be reasonably short ranges, clear line of sight, and direct illumination of the jammer by the MLS scan sector for sufficient detection by an enemy ECM receiver. Reasonable deployment tactics by the MLS can further reduce the probability of detection.

3. Jamming

Assuming that, even in light of the previous detection analysis, the enemy can detect the MLS signal, an analysis of the jamming powers at the airborne MLS receiver offers further proof of the low probability that the enemy can negate MLS operations through ECM.

The depth of penetration into enemy territory of the air mobile operation will affect the geometry of the placement of ECM equipment in relation to the MLS. If the air mobile penetration is deep into enemy territory, the enemy ECM can be placed at any point about the periphery of the landing zone (LZ) where line of sight exists. Depending on the terrain, the enemy will select the site which will give him the best jamming capability, and also at the same time ensure that his ECM is protected from destruction by the air mobile forces. Figure D-22 presents two possible geometries which might apply in a tactical situation.

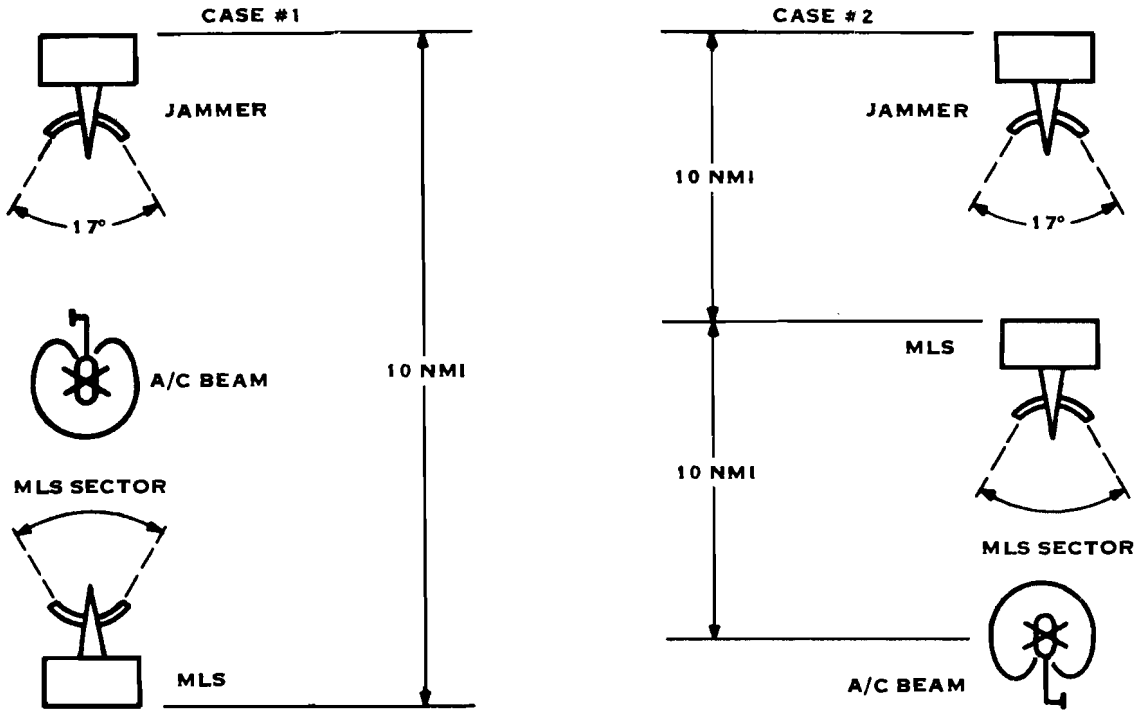

Figure D-22. Possible Deployment Geometries

In Case 1 the jammer would be approximately 10 nmi from, and directly in, the scan coverage of the MLS. The aircraft can be assumed to be 5 nmi from the MLS. The airborne antenna gain in the direction of the jammer is -8 dB relative to isotropic. The airborne antenna gain in the direction of the MLS is +4 dB. Figure D-23 can be used to determine the received signal power from the MLS. For a 5-nmi range this power is -77 dBm. By subtracting 11 dB for the difference between the jammer and MLS antenna gain, and an additional 12 dB for the difference in airborne antenna gain, plus adding 29 dB for the increased jammer power (1 kW) and receiver bandwidth, yields the second curve of Figure D-23. For the ranges shown the S/J input ratio will be -6 dB, effectively jamming the MLS airborne receiver. When the aircraft is 2.5 nmi from the MLS, the S/J input ratio will be +3.5 dB and, thus, still jammed.

For Case 2 the MLS ground antenna back radiation is nominally 30 dB down from peak or +1 dB isotropic and would not allow detection of the MLS by the jammer (see paragraph b.2 above).

In summary, for the noise jamming cases presented (Case 1 being absolute worst case), as long as the MLS ground system scan sector does not radiate toward the jammer or the jammer does not have clear line of sight within 10 nmi of the MLS transmitter, ECM-free operations are possible. With care in siting to take advantage of terrain masking even Case 1 type operation is feasible.

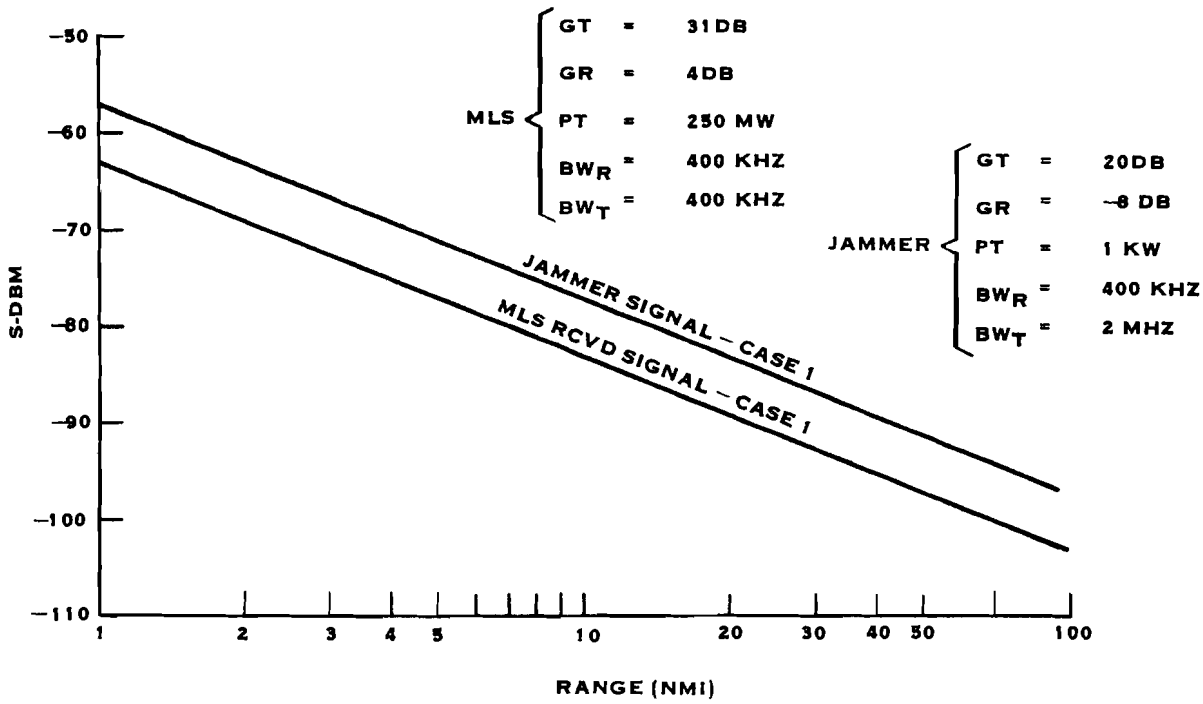

Figure D-23. Jamming Power Levels

4. Deception Jamming

The azimuth and elevation MLS signals do not lend themselves to deception techniques. The C-band DME system of the MLS could be deceived by a repeater-type jammer by heterodyning the signal from the DME to a lower frequency, use a short delay line to introduce a delay, heterodyne backup in frequency, then transmit. This repeater could repeat both the airborne DME transmitted signals and the ground-based DME transmitted signals. In one instance, the ECM repeater could cause saturation of the ground DME equipment and confuse the airborne equipment as to the distance to the landing zone. Line of sight is a requirement between the ECM equipment as well as the ground-based and airborne DME equipment.

5. Conclusions

The Army Configuration "E" and Marine Configuration "G" MLS systems cannot be classed as lucrative victims of ECM signals by the enemy. Practically all of the deployment initiative is on the side of the MLS when a qualitative analysis is performed of the effects of the use of ECM on the systems. The choice of system frequencies, signal bandwidths, RF powers, antenna directivities, antenna sector scan capabilities, and postulated deployment tactics all contribute to this MLS initiative. The MLS cannot be jammed by expendable type jammers. A noise waveform would be the best choice waveform to jam the azimuth and elevation MLS, should jamming be attempted. A deception repeater would be best against the DME.

c. Navy/Shipboard System

The Navy I_2 system usually operates in an open sea. The previous analysis of the ground-based systems is also valid for the shipboard system with minor exceptions. The open sea environment reduces the terrain shadowing effects to that of radar horizon and and the deployment of the enemy jammers is changed because fleet deployment. The I_2 antenna gains are greater than the E_2/G_2 configurations, resulting in slightly higher detection signal levels and the MLS system will normally be used for all aircraft recovery operations rather than only low visibility typical of the ground-based MLS.

The antennas for the transmission of the MLS signals will usually be sited approximately 100 feet above the waterline. This places the horizon at Ku-band and C-band at approximately 11-nmi range. If an enemy tried to deploy his ECM equipment using a surface vessel or a surfaced submarine, his vessel would be in the midst of the fleet which provides protection to the MLS-equipped carrier. This immediately requires that the ECM equipment must be deployed via aircraft, and must be at some distance from the fleet to enable a chance of survival of the ECM carrying aircraft.

There are many formations used by naval task forces which include attack carriers or air-capable ships. When a threat axis can be identified, the preponderance of appropriate covering vessels are deployed on that axis, however, the other directions are not abandoned. There are still covering ships or aircraft deployed in the directions other than the threat axis. For air defense, an all-around deployment is assumed with the ships of the fleet mutually supporting each other. In any case, the fleet defense is in great depth. An example of this depth is the deployment of airborne early warning (AEW) aircraft. This aircraft with its very powerful radar can be on station as far as 200 nmi from fleet center. The radar aboard the AEW could have a range coverage of 200 nmi. Furthermore, for the ECM carrying aircraft to be able to jam or deceive the MLS it must have line of sight to not only the MLS transmitted signal sources for frequency acquisition, but the airborne receivers to accomplish the jamming or deception function. With the ECM carrying aircraft having line of sight to the fleet, the fleet also has line of sight to the jamming aircraft and can accomplish detection.

In conclusion, in the light of the previous considerations, it is deemed that the MLS as used by the Navy will not be a lucrative target for the use of ECM. Jamming or deceiving the radars of the AEW aircraft on station and the radars of the ships of the fleet will provide greater payoff in accomplishing a successful attack. The defense in depth, the multiplicity of sensors available to the fleet, the nature of the MLS signals, as well as the alertness of the fleet make it highly improbable that the shipboard MLS could be successfully jammed or deceived.

X. CARRIER-BASED MICROWAVE LANDING SYSTEM-ALTERNATE DESIGNS (AUTOMATIC CARRIER LANDING SYSTEMS CORP.)

This section presents the results of a subcontracted study by ACLS Corporation directed at a carrier-based MLS design. The two system configurations described in this study report were parallel design efforts to those conducted internally by Texas Instruments and were used in the system tradeoff analysis before selecting the proposed configuration described in section 1.1.4.4.3.3.2 of the main report body. The two ACLS described configurations are viable solutions and indicate the design flexibility of MLS concept.

REPORT

on

CARRIER BASED MICROWAVE LANDING SYSTEM

for

TEXAS INSTRUMENTS, Inc.
Austin, Texas

PURCHASE ORDER No. 531405

August 1972

Volume 2

ACLS
CORPORATION

ACLS CORPORATION
6900 WISCONSIN AVENUE • CHEVY CHASE, MARYLAND 20015 • (301) 656-5432

21 August 1972

PREFACE

This volume of our report on Carrier Based Microwave Landing System concludes our fulfillment of Subtask 1.3 of the Statement of Work for Texas Instruments Purchase Order No. 531405.

Section 5 (the entirety of Volume 2) contains our views and recommendations for two possible configurations of MLS for Aircraft Carriers and their assigned aircraft. Supporting rationale and computational requirements are provided.

John L. Loeb,
President

TABLE OF CONTENTS

Preface..... i
List of Tables..... iii
List of Figures..... iii
V. Subtask 1.3 Specification for Carrier Based MLS.... 5.1
A. General..... 5.1
1. System A..... 5.1
2. System B..... 5.2
B. Ship's Motion..... 5.4
1. Antenna Stabilization..... 5.4
2. Deck Motion..... 5.10
C. Antenna Locations..... 5.15
1. System A..... 5.15
2. System B..... 5.18
D. Computations and Data Transmissions..... 5.20
1. Definition of Terms..... 5.20
2. System A..... 5.23
a. Shipboard Computations..... 5.23
b. Aircraft Computations..... 5.26
3. System B..... 5.29
a. Shipboard Computations..... 5.29
b. Airborne Computations..... 5.31
E. Approach Monitoring..... 5.36
F. Compatability..... 5.38

LIST OF TABLES

5.1 Effects of Ship's Motion on MLS Beams..... 5.9
5.2 Definition of Symbols..... 5.21

LIST OF FIGURES

5.1 Pictorial Diagram of AN/SPN-42 Operational Program, OPS-II..... 5.5
5.2 Geometry of Ship's Motion, Antenna to Touchdown Point..... 5.12
5.3 Geometry of Ship's Motion, Antennas Space Stabilized..... 5.13
5.4 Antenna Locations, System A..... 5.16
5.5 Antenna Locations, System B..... 5.17
5.6 Block Diagram, System A, Ship's Computer Program..... 5.24
5.7 Geometry of the Airborne Problem..... 5.27
5.8 Block Diagram, System A, Airborne Computer Program..... 5.28
5.9 Block Diagram, System B, Ship's Computer Program..... 5.33

V. SUBTASK 1.3 SPECIFICATION FOR CARRIER BASED MLS

A. GENERAL

In making recommendations for a specification, certain requirements both operational and political should be assumed. Some of these are set forth here:

Not all aircraft will be equipped to make fully automatic Mode I landings. Mode II, manual approaches with the pilot flying a crosspointer, and Mode IA, automatic control of the aircraft to a point where the pilot can safely take over for a manual landing, will continue to be used.

The system specified will be installed aboard ASW carriers (CVS), Air Capable Ships and possibly other ships with V/STOL capability, as well as attack carriers (CVA) and combined ASW and attack carriers (CV).

Complexity of airborne equipment should be reduced to a minimum even at the expense of added complexity on the ship, with the possible exception of ships such as the Sea Control Ship where the Navy has stated a firm policy to put complexity in the aircraft. The final mix of shipboard and airborne installation must consider equipment operability reliability, flight safety, and to a lesser degree the safety of the ship from radiation seeking missiles.

The Navy has been installing MLS equipment aboard carriers and in aircraft for the past nine years. Much experience has been accumulated which should be used to the best advantage. Opinions of design engineers and pilots have hardened and will be difficult to change.

The requirement that the position of an approaching aircraft must be monitored in the Carrier Air Traffic Control Center (CATCC) during a landing must be considered. MLS (FAA style) does not provide this.

Under this task, two systems will be specified. A short description of these systems and the rationale in support of each is provided here:

1. SYSTEM A

This system consists of single azimuth and elevation transmitters plus DME and is installed on the carrier island in approximately the same position as the SPN-42. Offsets to the touchdown point will need to be computed in order to accurately provide Ze and Ye in the aircraft. The computations will be fairly complex although it may be possible to place part of the burden on the ship. (This is discussed in more detail below.)

RATIONALE--System A can profit from experience and acceptance attained for the SPN-42. Transfer equations and computations can be used almost without change. An unobstructed coverage pattern can be radiated from the shipboard equipment with the antennas located on the island. This is the most simple arrangement that will provide such coverage.

2. SYSTEM B

This system retains the elevation antenna on the island, relocates the azimuth antenna and provides additional azimuth and elevation transmissions. It is believed that System B would reduce considerably the computational requirements, particularly for ModeI in the aircraft, as will be discussed in more detail later.

RATIONALE--System B might provide a total cost benefit in that the aircraft computations for Mode I would be greatly reduced. The additional azimuth and elevation would provide a higher data rate for the last one-half mile, would not look into the water (which might pose problems for System A close-in), and would provide an independent source for cross-checking aircraft equipment at a critical flight stage.

B. SHIP'S MOTION

In the consideration of shipboard computations, it may be well to review the total computer program of the AN/SPN-42 as set forth in Figure 5.1 (same as Figure 4.2). In general, the left side of the diagram refers to ship's motion and the right side of the diagram are functions involving the aircraft dynamics. The notable exception to the above is that the elevation, azimuth and range information are air derived data and the polar to cartesian transformation (if required) is accomplished in the aircraft. The information transmitted from the ship to the aircraft consists of the guidance signals and such other information as is required to compensate for antenna to touchdown point offsets and ship's motion.

1. ANTENNA STABILIZATION

a. A discussion of antenna stabilization factors follows:

(1) KEEL AXIS--Ship's roll occurs about the keel axis although it is not safe to assume that it will swing equally. It is not unusual to have the ship list to port or starboard due to an unequal ballast. The MK-19 Stabilized Gyro Compass Equipment is roll stabilized about the keel axis.

(2) LANDING CENTERLINE AXIS--The landing centerline is canted from the keel axis approximately 10 degrees. It is possible to roll stabilize MLS antennas about either axis; however, it is advantageous to stabilize about the landing centerline axis as will be explained in more detail later. If a separate stable element is provided a direct readout can be provided for landing centerline stabilization. However, if the MK-19 is used, a correction must be applied to provide landing centerline stabilization.

NOTES:

1. The following definitions apply to symbols used in this figure:

R_s - Radar slant range

θ antenna - Radar vertical encoder angle

ϕ antenna - Radar horizontal encoder angle

X_{13}, Y_{13}, Z_{13} - Antenna to touchdown point offsets (in keel axis)

Z_{alt} - Aircraft altitude (in keel axis)

X_{range} - Aircraft range (in keel axis)

Y_{pos} - Aircraft lateral position (in keel axis)

X_3, Y_3, Z_3 - Center of motion to touchdown point offsets (in keel axis)

X_3', Y_3', Z_3' - Center of motion to touchdown point offsets (in cant axis)

Z_{stab} - Aircraft altitude (stabilized and in cant axis)

X_{stab} - Aircraft range (stabilized and in cant axis)

Y_{stab} - Aircraft lateral position (stabilized and in cant axis)

$\frac{d(X)}{dt}$ - Aircraft closing speed

True Airspeed = closing speed + wind velocity

θ_s - Ships pitch angle

ϕ_s - Ships roll angle

ψ - Ships yaw angle

Z_e - Altitude error

Y_e - Lateral error

X_5, Y_5, Z_5 - Accelerometer to touchdown point offsets (in keel axis)

X_f - Fantail to touchdown point distance (in cant axis)

θ_{TO} - Glideslope tip over command

Z_{11} - Vertical motion of accelerometer

Z_{10} - Vertical motion of touchdown point

ΔZ_c - Deck motion compensation command

ϕ_c - Additional bank command

$\frac{d(Z_c)}{dt}$ = Rate portion of θ_c

$\frac{d^2(Z_c)}{dt^2}$ = Acceleration portion of θ_c

$\frac{d(Y_c)}{dt}$ = Rate portion of ϕ_c

ψ_{mod} = Modified ships yaw

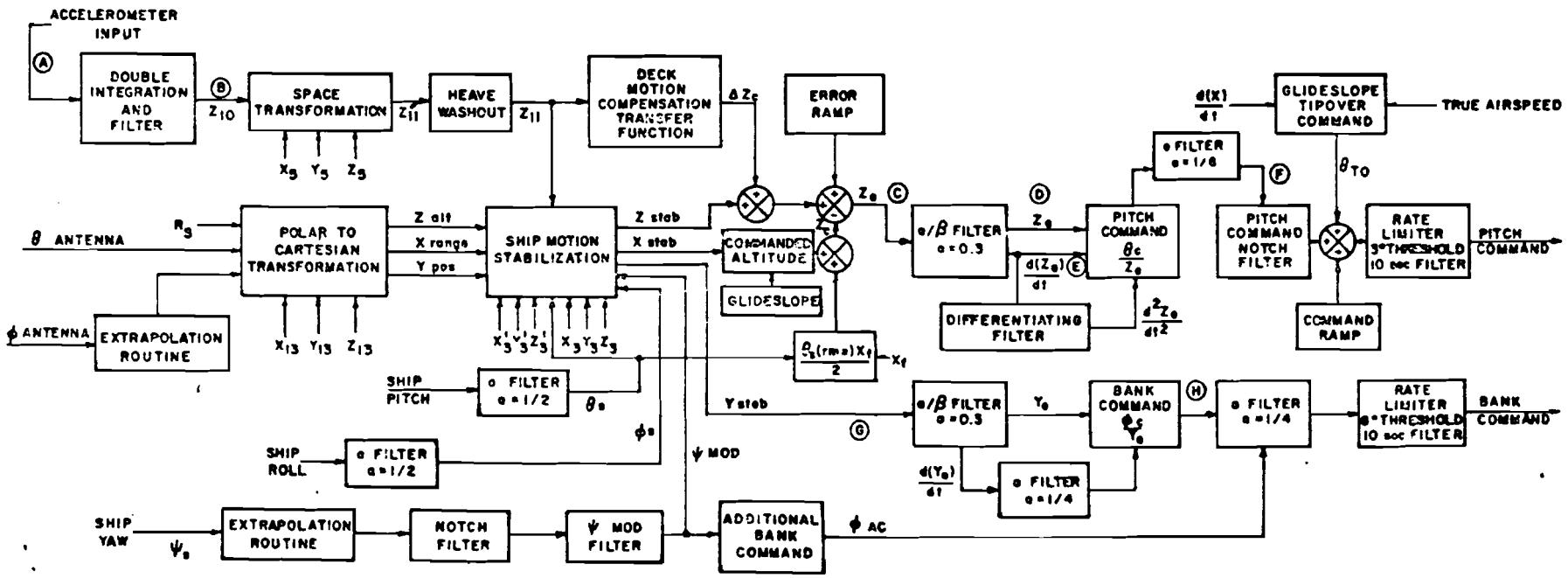

Figure 5.1 PICTORIAL DIAGRAM OF AN/SPN-42 OPERATIONAL PROGRAM OPS-II

(3) PITCH AXIS--Pitch occurs about a horizontal axis orthogonal to the keel axis. The position of the pitch axis, fore and aft, is based upon the fore and aft center of gravity and center of buoyency. The ship may be trimmed high at the bow or high at the stern based upon loading and speed in the water. High speed does not necessarily cause the ship to be trimmed high at the bow. For reasons that will be given later, MLS antenna stabilization is best provided about a pitch axis orthogonal to the landing centerline axis. Again this can be provided as a direct read-out of a separate stable element but would have to be computed if the MK-19 were used.

(4) HEAVE--Ship's heave is defined to be the vertical displacement of the ship's center of pitch. The AN/SPN-42 is presently the only shipboard system to measure heave. It is measured by double integration of the output of an accelerometer which is stabilized in the vertical plane. Since the accelerometer is not located at the center of pitch, the vertical motion effects of roll and pitch at the acclerometer location must be removed from the total vertical motion to determine heave.

(5) YAW--Yaw is cyclic variation in ship's heading about the desired ship's heading. It is caused by the effect of the sea on the hull with a periodicity determined by hull design and by rudder corrections applied by the helmsman. Although the amplitude of yaw will vary with winds and sea, the two distinct periods for hull design and helmsman do not vary to any great extent.

(6) TURN--As has been mentioned earlier, it is routine for aircraft to start their approaches prior to the carrier coming into the wind; therefore, as the first aircraft start its approach, the ship can be expected to be in a turn. Present indications are that VTOL support ships will not turn into the wind; hence the MLS will be rotated to accept VTOL aircraft heading into the wind. It must be assumed that the pilot will be given the final landing heading of the ship prior to the start of his approach. Experience has shown that the pilot wants a continuous reading of the ship's actual heading. This information is presently provided by UHF data link in several aircraft types. Since all aircraft are TACAN equipped, the pilot can make his initial approach without MLS. Azimuth data should be YAW stabilized within a range of approximately 3° to 5° but will follow larger deviations in a manner similar to the AN/SPN-41 as described on page 3.12 of our April report.

b. Table 5.1 is provided to indicate the effect of ship's motion upon unstabilized MLS azimuth and elevation beams. Certain assumptions will be made based upon Table 5.1.

(1) Roll stabilization for both azimuth and elevation antennas is required. Due to the second order effects, extreme precision in roll stabilization for the azimuth antenna is not required. In fact, roll stabilization of Azimuth #2 antenna in System B is not practical and is probably not required at close ranges. The requirement for precision roll stabilization of the elevation antenna becomes more important as the antenna offset from the landing centerline increases because of the effect on vertical displacement calculations.

(2) Pitch stabilization for the azimuth antenna is probably not required. This can only be determined after over-water multipath tests. It is unlikely that any problem will exist except at very low angles which would be encountered prior to intercepting the glide slope. Experience with other antennas has shown that the constant motion of the antenna with respect to the sea will wash out the effects of multipath; hence an over-water test with an antenna installed ashore would not be representative of the environment to be expected.

(3) Pitch stabilization of the elevation antenna is required. Due to the first order effect on the elevation beam, extreme precision is required for pitch stabilization. A discussion of mechanical versus electronic stabilization will be provided later.

(4) Yaw stabilization of the azimuth antenna is required. Due to the first order effect on the azimuth beam, extreme precision is required for yaw stabilization. Practically, the pilot is somewhat less concerned about his azimuth accuracy than his elevation accuracy and because of the comparatively long yaw period, the accuracy has never proved to be a problem.

(5) Heave stabilization is required. Due to the direct translation of the elevation beam extreme precision is required. Since the effect of heave does not increase with range, the measurement of heave is only critical to aircraft control within one mile of the ship.

EFFECTS OF SHIP'S MOTION ON MLS BEAMS

	ROLL	PITCH	HEAVE	YAW
AZIMUTH ERROR Ye (1)				
First Order Effect				X
Second Order Effect	X	X		
Increases w/range	X	X		X
ELEVATION ERROR Ze (1)				
First Order Effect	(2)	X	X	
Second Order Effect	X			X
Increases w/range	X	X		X
Constant w/range			X	
RANGE & RANGE RATE	(2)	X		

(1) Based upon errors measured from the landing centerline axis. There is also an added effect upon an unstabilized offset antenna in pitch and roll about the center of pitch and keel axis.

(2) Roll becomes first order at large azimuth angles off the centerline axis.

TABLE 5.1

2. DECK MOTION

It can be demonstrated that it is essential for the aircraft to perform all of its computations about a fixed point in space in conducting precision approaches in the presence of ship's motion. The shipboard antennas are constantly in motion because of roll, pitch, yaw and heave. An aircraft trying to use the center of radiation as a reference would try to chase this moving point. A particularly significant example is the effect upon range rate caused by the fore and aft displacement of the DME antenna due to ship's pitch. For a ship's pitch of $\pm$ 3° peak at a 7 second period and with the DME antenna located 150' above the ship's center of motion the DME antenna will move $\pm$ 7.5 feet fore and aft with a peak relative velocity of 4 knots. An aircraft trying to follow the radiation center would see a peak-to-peak variation in range rate of 8 knots with a period of 7 seconds. At close ranges, ship's roll would also introduce range rate errors in cases where there is a lateral offset of the DME antenna. The cyclic variation in range rate is too slow to permit the application of filtering techniques. We recommend that the imaginary stationary ("reference") touchdown point be chosen at the mean position of the actual touchdown point (the at rest position including bias due to actual ship's list and trim at the time of recovery) because this is the desired aiming point during the initial phase of the landing approach.

Additional information is required in the aircraft during the final phase of the approach and touchdown sequence. . . Obviously, the aircraft will want to know the actual position of the touchdown point and information about the motion of the touchdown point. Experience with the AN/SPN-42 has shown that it is necessary to apply additional compensation to the glide path whenever significant deck pitching motion is encountered. The technique employed in

the AN/SPN-42 system is to elevate the touchdown point and steepen the glide path as a function of the amplitude of the pitching motion of the deck. The current implementation increases the glide slope angle by the amount the average pitch of the ship exceeds 0.5 degrees RMS and elevates the touchdown point by an amount equal to ½ the distance from the touchdown point to the ramp .times the amount the average pitch exceeds 0.5 degrees RMS, expressed in radians. (See page 4.16 of the April '72 report).

To better describe the information that is required in the aircraft a series of illustrations has been provided to show the effects of ship's motion. Ship's motion has been exaggerated for purposes of illustration. Figures 5.2 and 5.3 are drawn for roll about the landing centerline axis. It should be noted that point A would indicate that both Azimuth and Elevation antennas are located at the same point. Although they should be located in the same proximity, Y should be measured from the scan center of the Elevation antenna. It may be necessary to restrict the horizontal and vertical separation, primarily because true range is a function of elevation angle and azimuth angle from the DME antenna. B_p and B_s represent the horizontal and vertical motion of the touchdown point because of roll to port and starboard. A_p and A_s are the motions of the Azimuth and Elevation antennas to port and starboard for a corresponding motion of B. Y and Z are the horizontal and vertical displacements of the antenna from the touchdown point (landing centerline). In Figure 5.2 Y_p and Z_p show the change in Y and Z for roll to port and are measured from B_p the real position of the landing centerline. These are values that can be computed on the ship and are required for control of the aircraft in the final fifteen seconds to the touchdown. Similarly Y_s and Z_s are a measure of roll to starboard and are required for the aircraft for the last 15 seconds of control. Similar variations in the instantaneous values of X, Y and Z are caused by pitch and yaw of the ship.

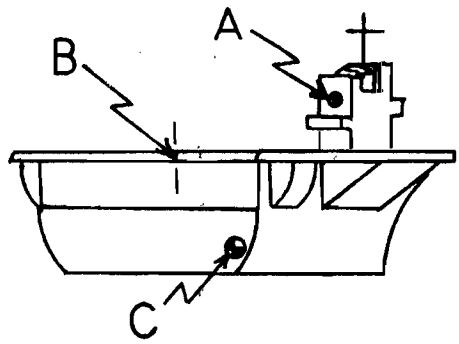

A = Azimuth Antenna Location

B = Landing Centerline

C = Center of Roll in Landing Centerline Axis

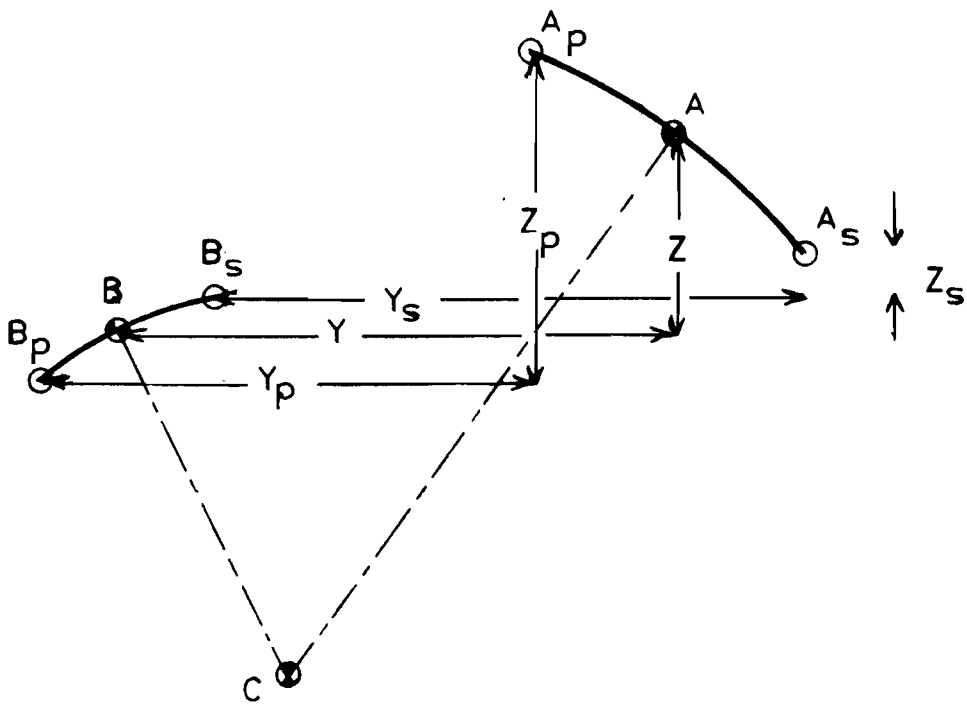

FIGURE 5.2 Geometry of Ship's motion, Antenna to Touchdown Point

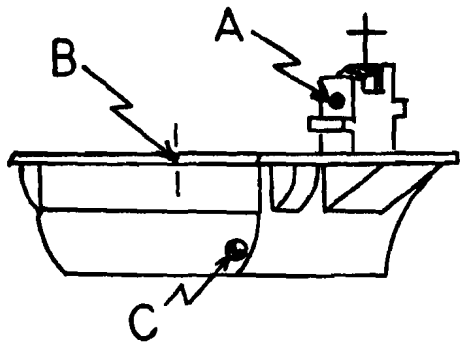

A = Azimuth Antenna Location

B = Landing Centerline

C = Center of Roll in Landing Centerline Axis

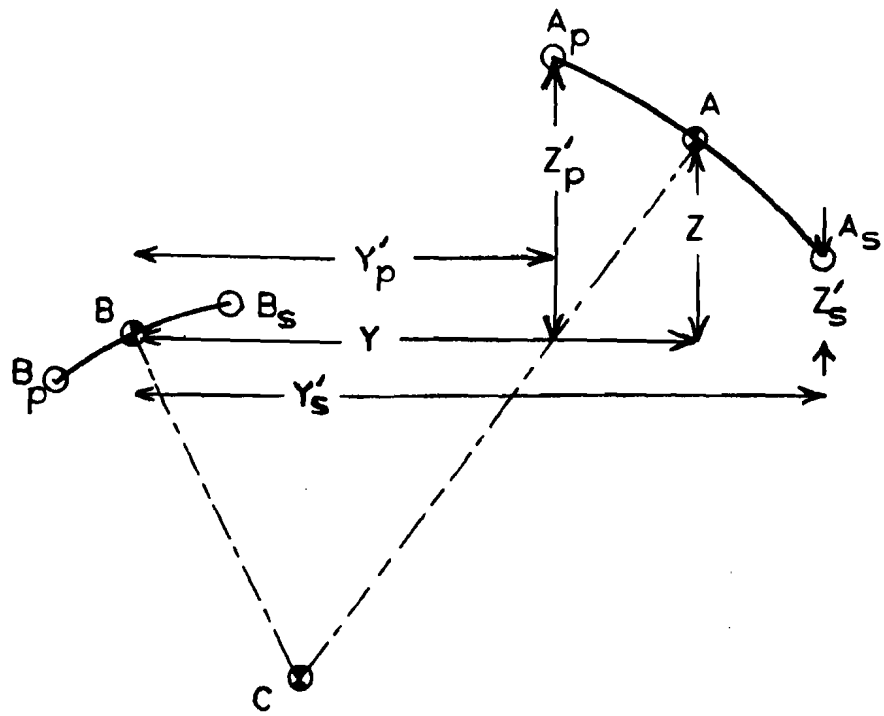

Figure 5.3 Geometry of Ship's Motion, Antennas Space Stabilized

In Figure 5.3 Y_p and Z_p are measured for roll to port from an imaginary stationary landing centerline and can be used in the aircraft to construct azimuth and elevation courses which are fixed in space. These values can be computed on the ship and are required by the aircraft until control is transferred from space stabilized to ship's stabilized coordinates. The transfer would occur within about the last fifteen seconds as determined in simulation and test.

C. ANTENNA LOCATIONS

In order to determine what shipboard computations are required, certain antenna locations and characteristics must be assumed. For purposes of this report, two alternative configurations have been considered. Antenna locations for Systems A and B are shown in Figures 5.4 and 5.5 respectively.

1. SYSTEM A

System A has the antennas located in close proximity, one to the others,on the carrier island. The objective is to provide a clear view for azimuth, elevation and DME antennas of both the approach and landing volumes. As discussed earlier, the azimuth antenna must be stabilized for roll and yaw; the elevation antenna for pitch and roll. Mechanical stabilization of both antennas about the roll axis appears to be the only practical solution. Very exotic electronic scan techniques would be required otherwise. Stabilization of data from the antennas for the other axis would satisfy requirements for pitch stabilization of the elevation antenna and yaw stabilization of the azimuth data. The antennas are so oriented that their reference coordinates are about the landing centerline axis when the deck is level and the ship is on its final recovery heading. Stabilization should be about this same axis to avoid "cross talk" between the pitch and roll axis data. The aircraft wants to see data referenced to its approach course which is aligned with the landing centerline.

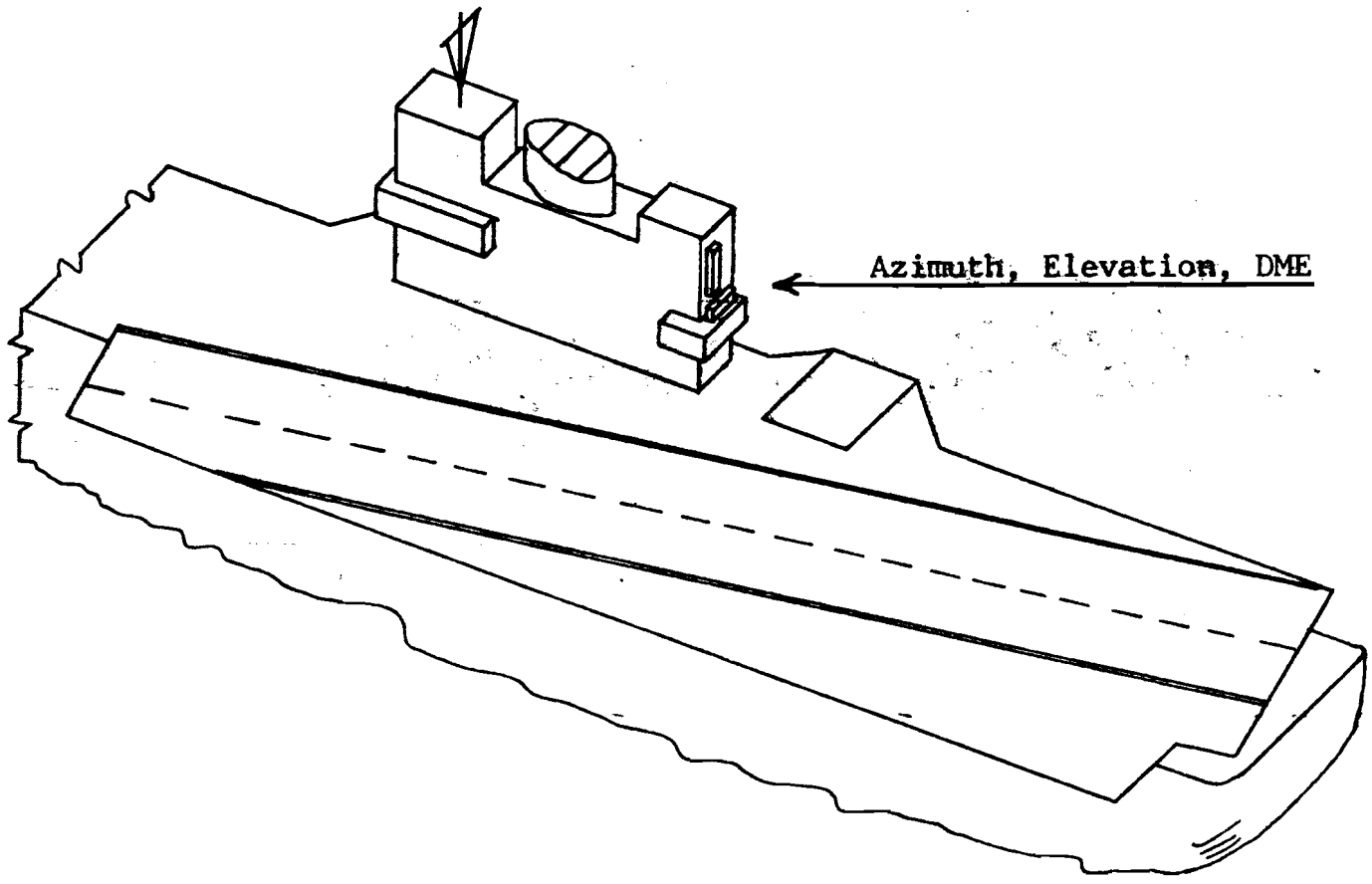

Figure 5.4 ANTENNA LOCATIONS, SYSTEM A

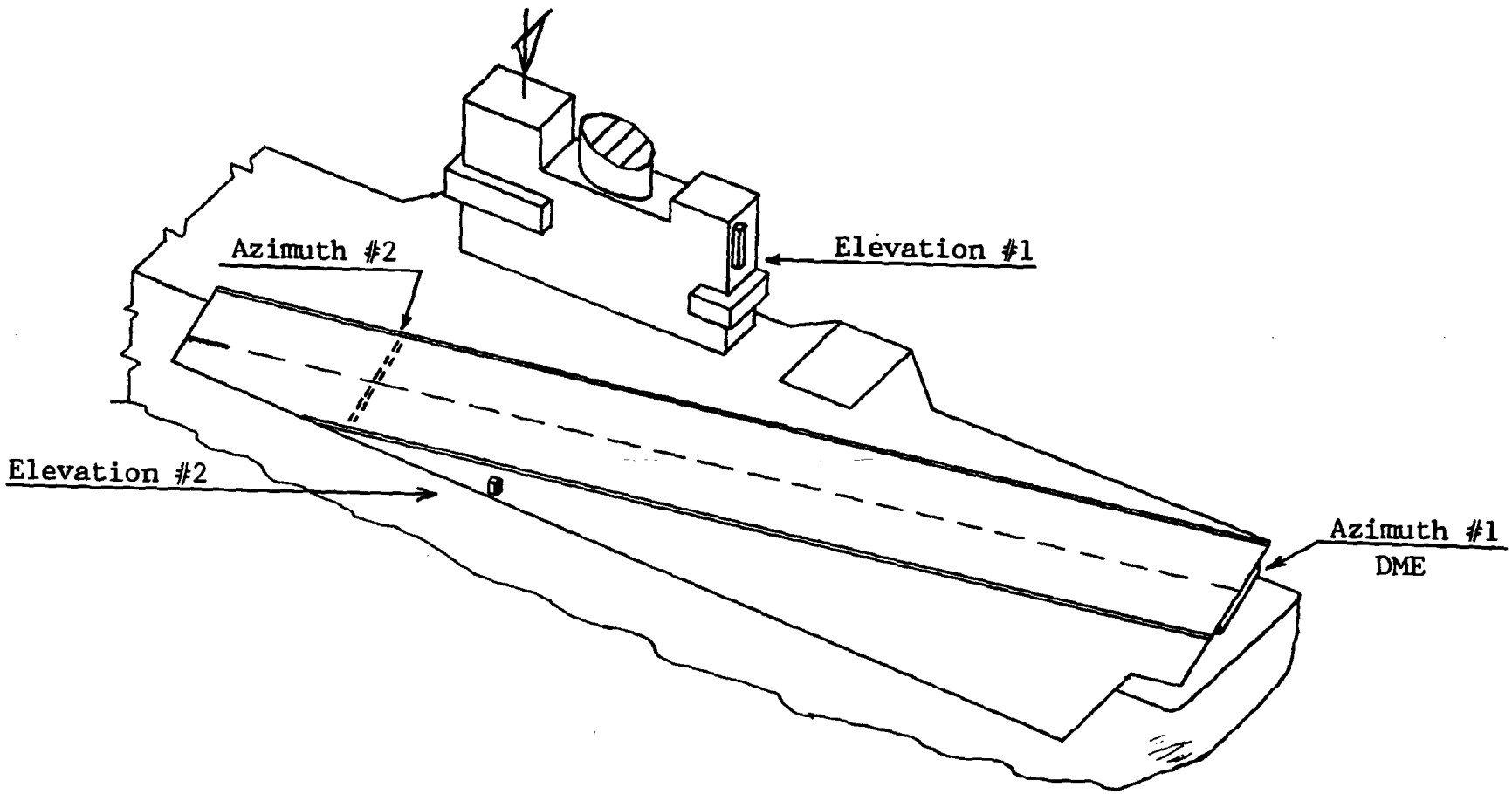

Figure 5.5 ANTENNA LOCATIONS, SYSTEM B

One major consideration in the determination of the antenna's scan sequence is the time uniformity with which data is sensed in the aircraft. Mechanically scanned antennas which use rotating antennas (multiple if necessary to achieve the desired data rates and dwell times) produce a signal with uniform time intervals between successive data samples. Nodding antennas, on the other hand, produce such uniform intervals only when the aircraft is on the neutral axis of the antenna. This effect is usually most noticeable on elevation data because the aircraft will normally be below the neutral axis of the antenna in which case the time interval between a "down nod" and the following "up nod" is shorter than the interval between an "up nod" and the following "down nod." Such irregularity complicates filters and extrapolation routines in the airborne computer. Stabilization of data from a nodding antenna further aggravates this problem.

2. SYSTEM B

System B is unconventional in that four antenna locations are required and three of the four will provide coverage over a limited portion of the coverage pattern. Azimuth antenna No. 1 provides no coverage over the deck. (The location is the same as the SPN-41). Azimuth antenna No. 2 is a flush deck installation which will not provide coverage until the deck is cleared. It would only be used for the last fifteen seconds of approach and would not be stabilized in any axis. Elevation antenna No. 2 might well be mounted on the Fresnel lens and stabilized in pitch only. The present SPN-41 port side location might be better since critical coverage would only be required in the last 15 to 30 seconds. (Due to recent operational needs to park aircraft aft on the port side, SPN-41 coverage has been

seriously impaired.) Elevation antenna No. 1, located on the island, would provide full volume coverage and would be stabilized in roll and pitch. The DME antenna would be located with azimuth antenna No. 1 but need not be stabilized. A second DME colocated with azimuth No. 2 antenna, and range zero corresponding to the touchdown point, may be required to simplify the final approach computations.

Electronically scanned antenna have a characteristic of beam widening when off bore site. It is noted that the horizontal angle between the line parallel to centerline axis through an antenna on the island and to the touchdown point on some ships (see Table 3.1 on page 3.2 of our April report) approaches 50°. It would appear desirable to cant the boresite axis of the antennas, if electronic scan is used, to provide the most precise data in the zone near the ramp. The greatest accuracy is required in the range between the ramp and about 1500 feet aft of the ramp. The final selection of scan techniques and stabilization must be a trade-off between complexity and signal quality desired.

The data rate for range requires some investigation inasmuch as other coordinates are directly effected by the value of "X" in the coordinate transformation computations. The AN/SPN-42 radar has a high prf for smooth tracking and averages 8 range measurements for each computation cycle. Such averaging improves the range determination accuracy and smooths the range rate measurements.

D. COMPUTATIONS AND DATA TRANSMISSIONS

1. DEFINITION OF TERMS

For purposes of this report, the definitions of the symbols used are contained in Table 5.2. The keel axis is that axis which has the Y axis parallel to the ship's keel, the Z axis is vertical and the X axis is orthogonal to the other two axes. The cant axis has the Y' axis parallel to the canted centerline of the ship's landing area, generally 9° to 10° to port of the keel axis, the Z' axis is vertical and the X'axis is orthogonal to the other two.

The expressions of stationary point or space stabilized data recognizes that the reference space is moving at a constant rate along the ship's track.

DEFINITION OF SYMBOLS

R_d	DME Slant Range
θ_{mls}	MLS elevation angle (cant axis)
ϕ_{mls}	MLS azimuth angle (cant axis)
X_{13}, Y_{13}, Z_{13}	Antenna to touchdown point offsets (keel axis)
$X'_{13}, Y'_{13}, Z'_{13}$	Antenna to touchdown point offsets (cant axis)
X'_o, Y'_o, Z'_o	Instantaneous Antenna to imaginary stationary touchdown point (cant axis)
$X'_{td}, Y'_{td}, Z'_{td}$	Instantaneous actual touchdown point to imaginary stationary touchdown point offset (cant axis)
θ'_s	Ship's pitch angle (cant axis) (+ is bow up)
ϕ'_s	Ship's roll angle (cant axis) (+is starboard)
ψ'_s	Ship's yaw (cant axis)(+ is to starboard)
Z'_{11}	Vertical motion of the touchdown point $=Z'_{td}$
X'_f	Fantail(Ramp) to touchdown point distance (cant axis)
X'_5, Y'_5, Z'_5	Accelerometer to touchdown point distances (cant axis)
Z'_{10}	Output of heave integrator
X'_a, Y'_a, Z'_a	Antenna to center of motion offsets (cant axis
θ'_{st}	Bias to pitch due to ship's trim (cant axis)

ϕ'_{sl}	Bias to roll due to ship's list (cant axis)
X'_3, Y'_3, Z'_3	Touchdown point to center of motion offsets (cant axis)
$\Delta\alpha$	Glideslope elevation due to ship's pitch
X'_{stab}	
Y'_{stab}	Aircraft to reference touchdown point
Z'_{stab}	
$\dot{X}'$	Closing velocity
τ	Time to go to touchdown
α	Glide slope angle
X'_{R_1}	Offset between Elevation #1 antenna and DME antenna, System B
X'_{R_2}	Offset between Elevation #2 antenna and DME antenna, System B

TABLE 5.2

2. SYSTEM A

System A references all calculations to a single set of antennas colocated on the island of the aircraft carrier. Siting of these antennas would be comparable to the data shown on page 3.2 of our April report.

a. Shipboard Computations

Two sets of variable coordinates must be transmitted to the aircraft if the aircraft is to properly compute the desired track to touchdown. The first set of coordinates represent the instantaneous offsets of the antennas with respect to the imaginary stationary (reference) touchdown point. This can be computed on board the ship by adding the 3-dimensional motion in space of the antenna radiation centers to the values of X'_{13}, Y'_{13} and Z'_{13} for determining the offsets to the reference touchdown point.

A second set of variable coordinates represent the displacement of the actual touchdown point from the reference touchdown point. It should be noted that we have not computed a value for X'_{td} because it appears to be a second order term. This assumption must be verified.

Computations performed in the ship's computer are predominantly geometric and coordinate conversion routines resulting in outputs shown on Figure 5.6. Experience with the AN/SPN-42 program has shown that it is necessary to introduce several other factors into the problem as a direct result of carrier deck motion and turbulence behind the ship. These factors are raising of the touchdown point and the raising of the glideslope angle to compensate for large pitch angles, and the "error ramp" and "command ramp" functions to obtain increased thrust prior to the time the aircraft enters the sphere of influence for burble and air turbulence behind the carrier deck.

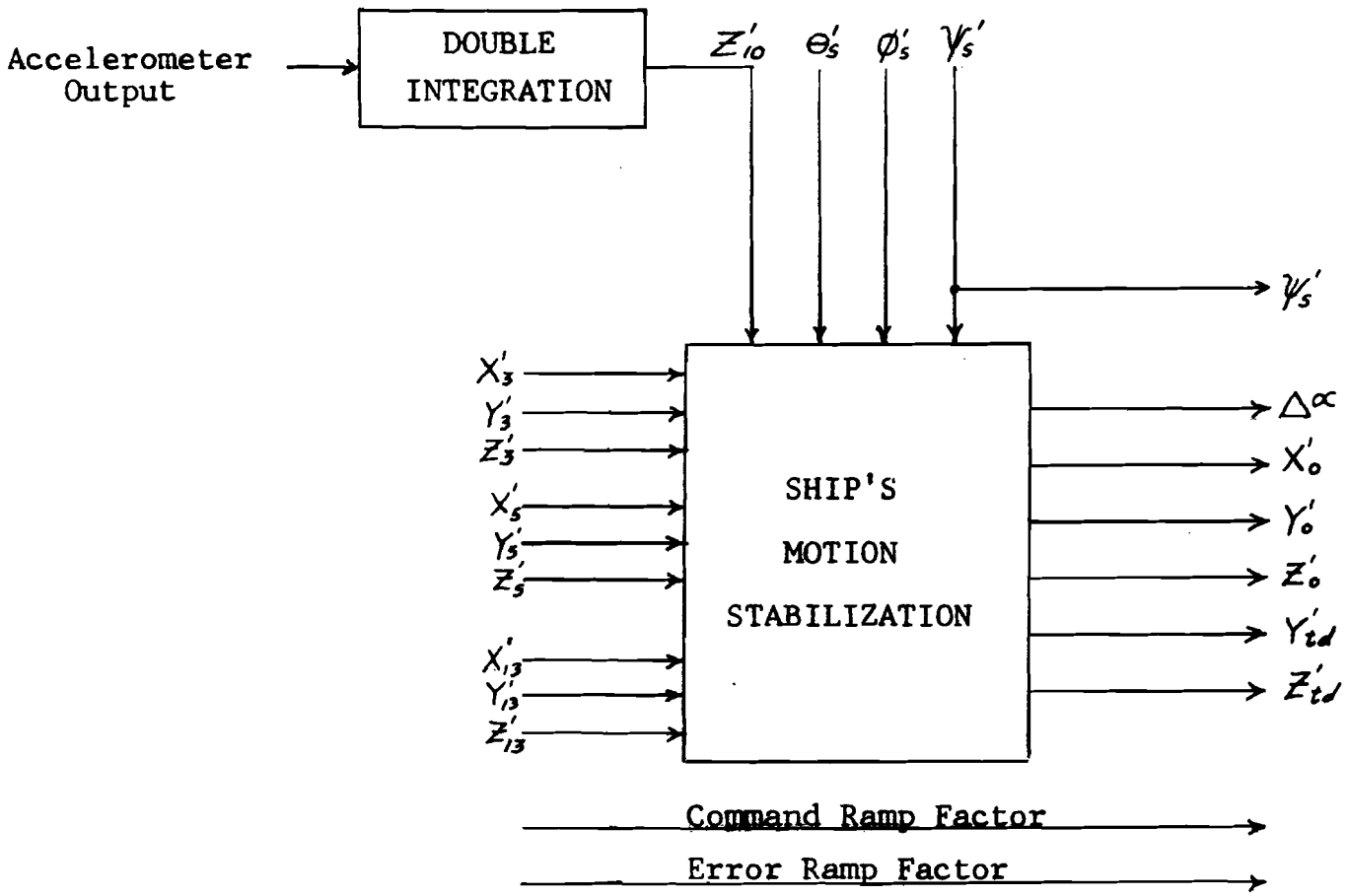

Note: Filters and extrapolation routines are not shown for simplicity. These will be unique to shipboard computer speeds, digitizer granularity, etc.

Figure 5.6 Block Diagram, System A, Ship's Computer Program

It should be recalled that the AN/SPN-42 compensates for extreme pitch of the carrier deck by (1) raising the glide-slope angle by the amount the average pitch exceeds $\pm$ 0.5 degrees, and (2) by elevating the touchdown point by an amount equal to ($\frac{1}{2}$ the distance from the touchdown point to the ramp) times (the amount the average pitch exceeds $\pm$ 0.5 degrees) in radians. The most simple way to handle this portion of the problem, if it can be proven that these values are the same for all types of aircraft, is to perform the computations on the ship's computer and (1) transmit the incremental glide slope angle ($\Delta\alpha$) signal to the aircraft and (2) apply a bias which effectively raises the touchdown point to the transmitted value of Z'_{td}.

An alternate method of handling the raising of the glideslope angle is to raise the glide slope signal in space based on shipboard computations which would require recomputing the deck motion output values because we have established a new elevated reference axis about which the various X, Y and Z's are calculated.

The least desirable method of handling the deck pitch problem would be to let the airborne computer do the computation. This places an increased burden on the airborne computer but may be necessary if it is proven that deck pitch must be handled differently in different types of aircraft.

The "error ramp" and "command ramp" functions are variables determined by both the ship's and the aircraft's characteristics. The ship's contribution to these functions will generally be dependent upon wind over the deck and the ship's configuration and pitch, and must be transmitted to the aircraft where they are processed as a function of the aircraft's characteristic to produce the "error ramp" and"command ramp" commands at the proper time in the landing sequence.

b. Aircraft Computations

(1) Automatic Mode

The aircraft can determine its position with respect to the radiation center of the ship's antennas by coordinate conversion of the data derived from the stabilized elevation and azimuth beams and the DME slant range. Translation of these coordinates by direct addition (or subtraction) of X'_o, Y'_o and Z'_o will result in three dimensional coordinates of the aircraft with respect to the reference touchdown point. It may be desirable to add a bias in the aircraft to allow for the height of the reciever antenna above the landing gear. Comparison of these data with the desired glide slope, see Figure 5.7, will result in Z_e and Y_e during the intitial phase of the landing approach.

Additional corrections to follow the actual touchdown point will need to be phased into the problem during the final phases of the landing profile. The addition of the Y'_{td} and Z'_{td} terms into the problem will perform this function. (X'_{td} was assumed earlier to be a second order term and was neglected. This assumption remains to be verified.) Additional terms such as yaw compensation, elevation of the glideslope angle and the touchdown point due to ship's pitch, "command ramp," "error ramp" and glideslope tipover command are applied at the appropriate times in the sequence. The various transfer functions shown on the block diagram, Figure 5.8, are unique to each type of aircraft and should have a form similar to those developed in the AN/SPN-42 program. Further refinements resulting from the AN/SPN-42 program may lead to new transfer functions. New transfer functions must be developed for additional types of aircraft as they are prepared to use the MLS.

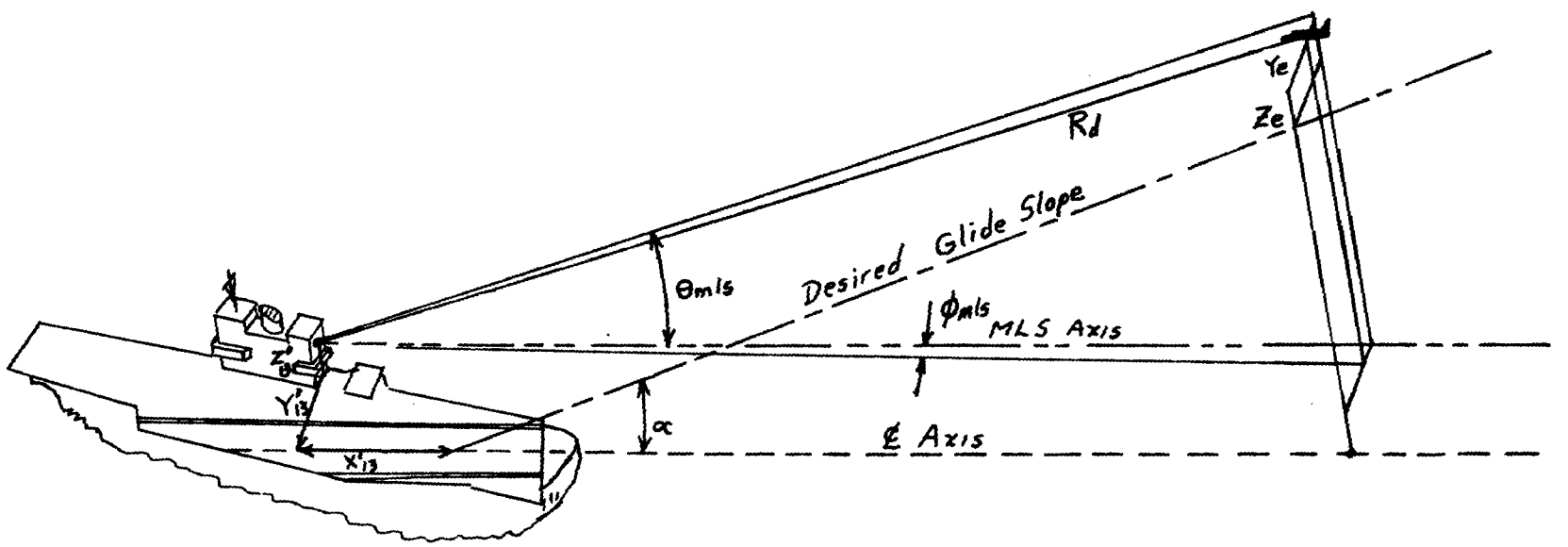

Figure 5.7 Geometry of the Airborne Problem

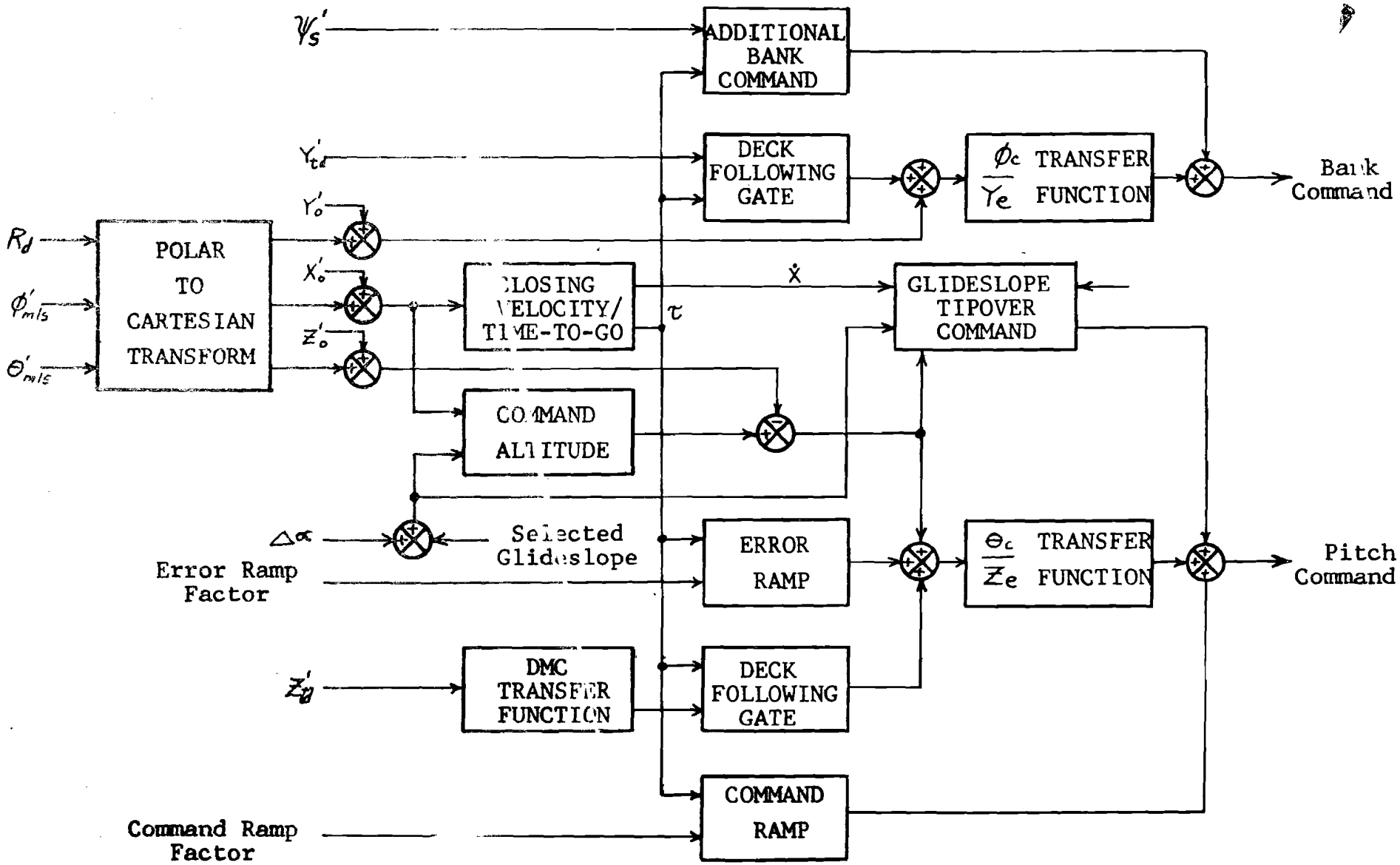

Figure 5.8 Block Diagram, System A, Airborne Computer Program

(2) Backup Modes

The signals in space provide a capability in the aircraft to perform either coupled or manual approaches of quality similar to present Category I ILS approaches. Azimuth and Elevation only would permit the aircraft to follow a glide path toward the antenna site which would require a side step maneuver of approximately 100 feet after attaining visual reference to the carrier deck. Slight improvement could be obtained by selecting an azimuth approach course that would intersect the landing centerline at minimums which would probably be at about 3000 to 4000 feet aft of the ramp. This very basic mode would also require a slight maneuver to get down to the touchdown point. The aircraft would also attempt to follow the motion of the radiation center as the ship moves.

The next increment of improvement would result from inclusion of range and the offset values of X'_o, Y'_o and Z'_o. A relatively simple computer in the aircraft would perform coordinate conversion and drive indicators to show deviation from the desired glidepath which now terminates at the reference touchdown point.

3. SYSTEM B

System B consists of two sets of antennas as described in Section V. C. 2.

a. Shipboard Computations

Shipboard computations for System B are similar to those performed for System A but are more extensive because we now have two sets of radiation centers about which to compute offsets. There is also more data to be transmitted to the aircraft because of the additional set of coordinates; however, the aircraft need only operate on those data pertinent to the antenna set being followed at the instant.

The wide separation between the azimuth #1 and the elevation #1 antennas results in a geometry which requires that the X' abd Z' offsets between the two antennas be known in the aircraft for use in the coordinate transformation routine. Transmission of the offset variables X'_o, Y'_o and Z'_o (where X'_o and Y'_o are referenced to the azimuth #1, DME si e and Z'_o is referenced to the elevation #1 site) to the aircraft will provide the data to permit computation of Ze and Ye during the initial approach phase.

Antenna set #2 is used during the final phase of an automatic, coupled approach. The elevation antenna is pitch stabilized to provide a smooth glideslope angle for the aircraft to follow. Variable coordinate correction factors are computed on the ship to permit the aircraft to follow the actual touchdown point during final approach. It seems possible that it may not be necessary to compute and transmit values for Y'_{o_2}, Y'_{td_2} and γ'_s but this possibility must be verified. This possibility is based on the thought that since we propose to have the Azimuth antenna #2 aligned along the touchdown centerline without stabilization that lateral motion of the touchdown point will be reflected in changes in the value of the Y output from the polar to cartesion transform #2. The value of γ'_s can be determined in the aircraft by comparing the azimuth angles from the stabilized AZ-2 and the unstabilized AZ-2 antennas. Such an implementation may result in undesirable bank motion of the aircraft but would result in more simple shipboard and airborne computer programs if verified to be acceptable. If, on the other hand, the assumption above results in excessive errors and/or excessive aircraft bank maneuvers, then azimuth #2 antenna may have to be azimuth stabilized and the above data transmitted to the aircraft.

A single DME antenna located at the ramp with the Azimuth #1 antenna should suffice because the range rate near the ramp will be relatively constant and range rate values can probably be frozen in the airborne computer during the final few seconds of the approach. It should be recalled here that the aircraft commands are frozen in the AN/SPN-42 program at approximately 1½ seconds from touchdown. Computer simulations or error budget calculations should be undertaken to determine whether or not a second DME antenna is required.

A functional block diagram for the shipboard portion of System B is shown in Figure 5.9.

b. Airborne Computations

(1) Automatic Mode

A functional block diagram of the airborne computations required in the System B environment are shown in Figure 5.10.

The computer receives inputs from each of the two sets of antennas and performs the polar to cartesian coordinate transformation on each input separately. This configuration requires that the intraset coordinate offsets be transmitted to the aircraft because these parameters are required as part of the coordinate transformation process.

The set #1 antennas are proposed to be used for guidance during the initial phase of the approach. Extreme accuracy is not required during this phase; the requirement is to provide a smooth approach path for later transition to the signals from antenna set #2 and a possible Category I system

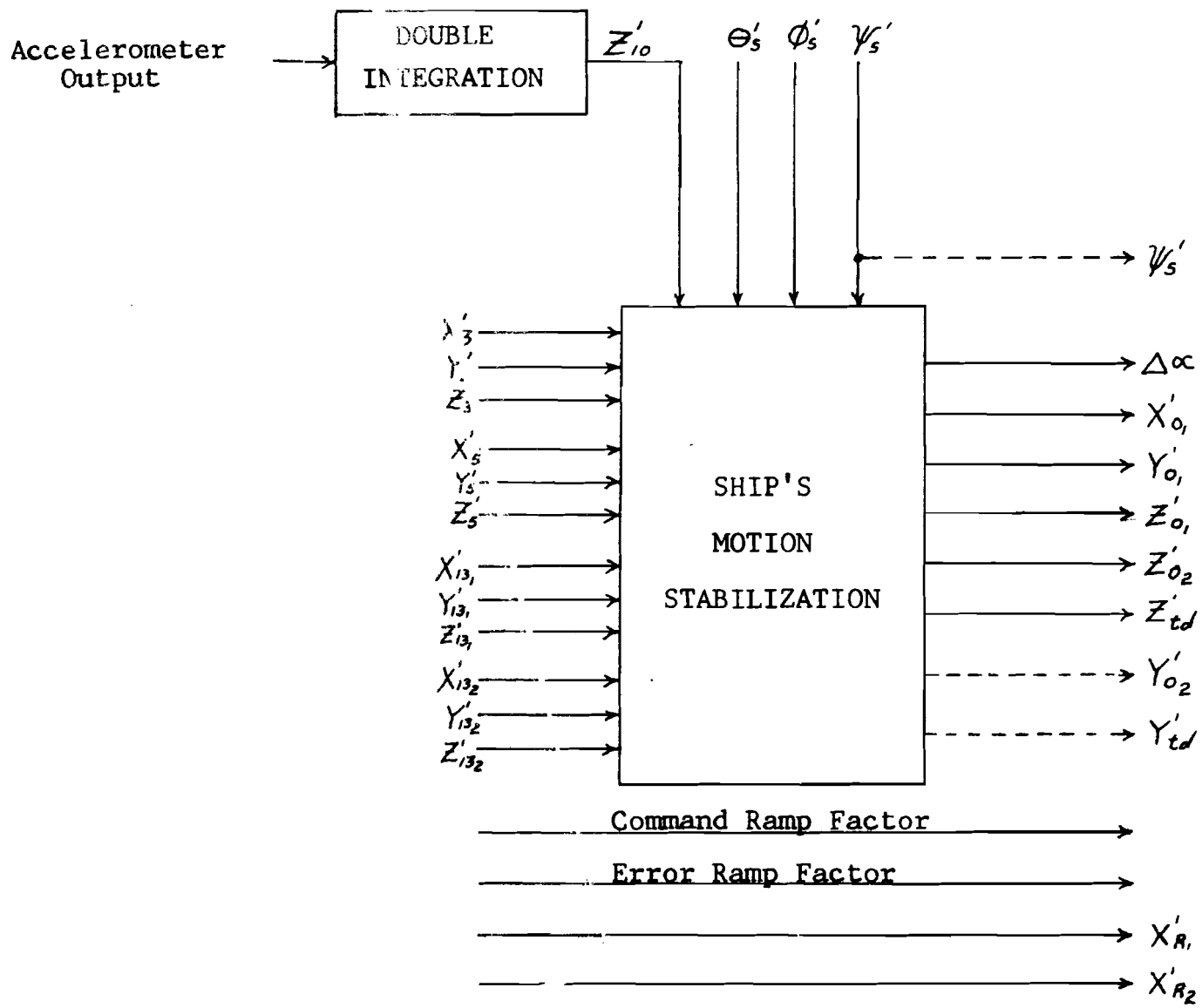

Figure 5.9 Block Diagram, System B, Ship's Computer Program

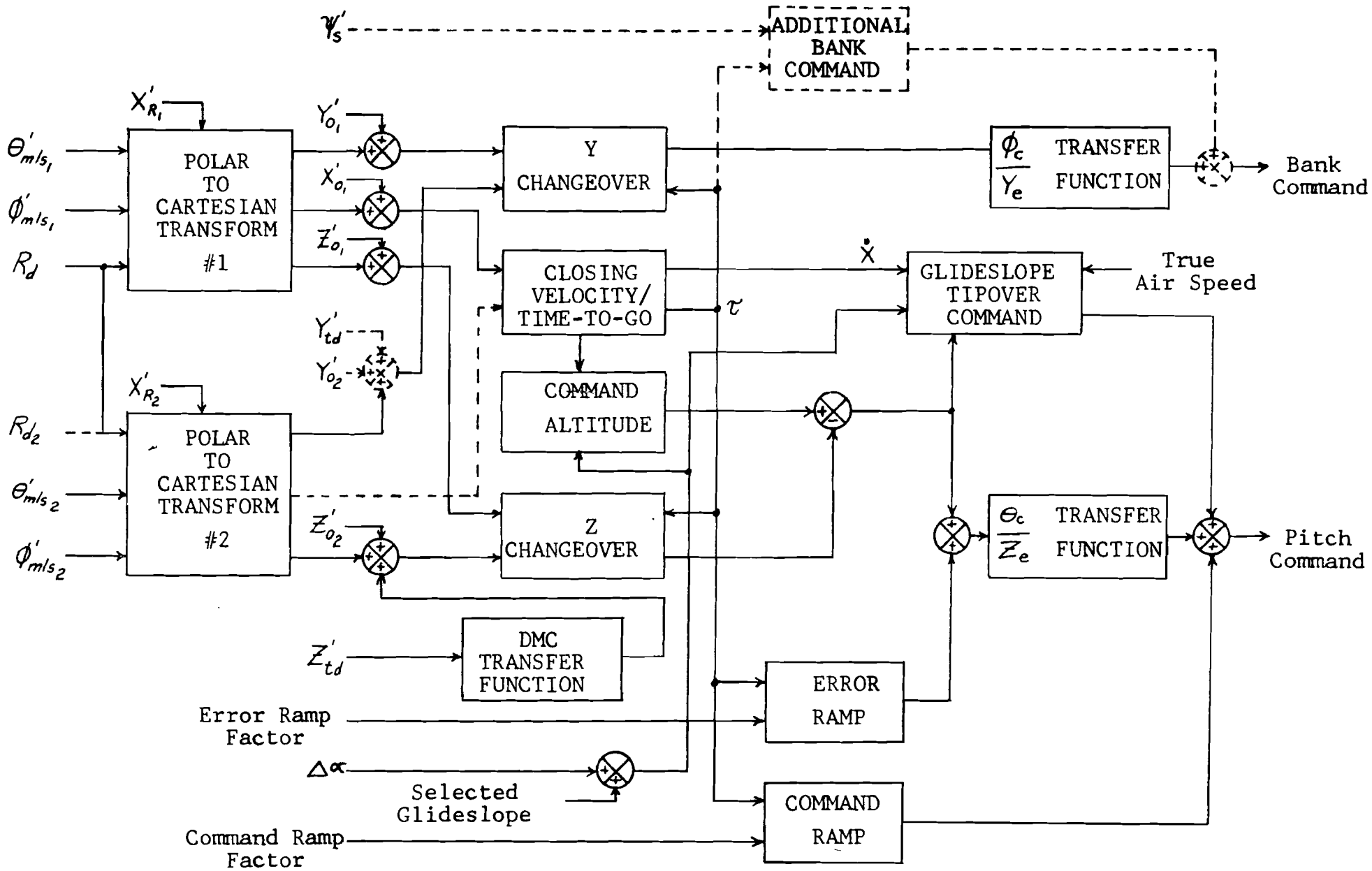

Figure 5.10 Block Diagram, System B, Airborne Computer Program

(manual landing using visual reference) in the event of failure of a component of set #2. Computations in the aircraft can be at a slower data rate during this initial phase. For simiplicity of calculation, we suggest that the ramp be used as the reference point during this phase (the azimuth antenna and the DME antennas are located at the ramp and the elevation antenna is on the island) with a fixed bias being applied to the computed value of Z' of approximately 15 feet to approximate the correct path to the touchdown point (250' tan 4° = 17.5 feet).

Antenna set #2 are located as close to the touchdown point as possible and coordinate conversion of the signals from these antennas will result in cartesian measurements of the touchdown point. The primary advantage here is the relaxed stringency on the airborne computer because of smoothness of the data from the ship's antennas. The high slew rates encountered in System A are avoided in this approach.

(2) Backup Modes

System B offers considerable flexibility in backup modes of operation. Either set of shipboard antennas can be used, in event of failure of one or more of the other set, to provide a backup mode for semi-automatic or manual approaches. Placement of the azimuth antennas on the landing centerline azis eliminates the side step maneuver which resulted in the System A backup mode.

The airborne computer, as conceived in this report, changes from guidance set #1 to guidance set #2 based on time-to-go if all signals are present. The changeover circuits would select the existing signal in the absence of the other and signal a warning of the degraded condition.

The most accurate manual approach would be to use cross-pointers to indicate the values of Ze and Ye from the co-ordinate portion of the airborne computer. These signals could be followed manually in event of failure of the trans-fer function portions (flight director) of the computer.

The least accurate mode would utilized a direct measure of the angular error from one azimuth and one elevation antenna without benefit of range or offset values. Various combinations between these two extremes can be utilized to produce various degrees of manual capability.

E. APPROACH MONITORING

The Microwave Landing System is an air derived system which, in itself, does not provide an inherent basis for monitoring by the approach control facility. Additional equipment of one kind or another will be necessary for monitoring and for providing warning whenever the safe flight path limits for automatic or semi-automatic mode of operation are exceeded.

The requirement for the flight path limit alarm at the ATC facility can be met through a signal transmitted from the aircraft based on monitor circuitry in the airborne unit. Where separate data links are not provided, this signal could be transmitted over the DME down link along with aircraft identity or range to alert the ground ATC unit of the existance of the abort condition. This technique is based on the premise that the airborne unit is either (1) functioning properly and correctly identifies the tracking errors or (2) fault alarms have been actuated. It will not provide warning in cases where there is a blunder in the airborne unit which is not detected as a fault.

The next higher level of alarm and monitoring would involve the retransmission of the raw signal information as received in the aircraft. This approach would require a real time data link and a ground computer which would compare the data with the prescribed flight path or would display the actual flight path. The ground station would have to know the air selected glide path angle and any other air selected variations (such as curved approach) to completely monitor the approach. Some simplification might result from monitoring only the final few thousand feet where the approach would be

straight-in and the ground was interested only in the predicted touchdown point deviations.

The third technique involves a completely independent system to perform approach monitoring. The use of existing types of approach control radars would provide this type of monitoring and backup control in case of MLS failure. The AN/SPN-43 would provide 2-dimensiona approach control (3-dimensional if the Mode C altitude reporting of ATCRBS is incorporated) but does not have the accuracy to detect errors which would be grounds to abort full automatic or semi-automatic landings. A precision approach radar would provide more accurate monitoring under these conditions.

F. COMPATIBILITY

The systems described herein have addressed the attack aircraft carrier (CVA) as the vehicle for describing the system configuration. Other air capable ships, such as the Sea Control Ship, may require similar capabilities for either low approach to landing systems or automatic landing systems. Such ships have lesser demands on the approach system because of the lower approach speeds and better maneuverability of the aircraft during final approach. Configuration E or G of the common MLS should suffice for such ships.

System A as described herein should be appropriate for these lesser demanding systems. It may, however, be necessary to provide a system wherein the antennas may be oriented downwind to permit approaches into the wind even though the ship may not be running into the wind. It may also be necessary to provide different offset constants, for either manual or automatic insertion into the airborne computer, to each aircraft to permit approaches to different touchdown points on the landing area. These offset constants and the antenna to reference touchdown point offset would be oriented along the antenna orientation axis for ease in computation in the aircraft and for consistancy among the various installations in different types of ships. Thus, aircraft normally operating form a Sea Control Ship could be recovered on a CVA with no change in procedures or equipment operation.

Finally, operating frequency bands and the signal format for the shipboard systems must be identical, or nearly so, to similar configurations ashore to permit aircraft normally assigned to ships to operate in low visibility conditions at military fields ashore and in the NAS. Such a requirement is necessary for BINGO diversions and is highly desirable for training operations and emergency deployment ashore operations.

ERRATA BOOK A-1

PAGE	LOCATION	CORRECTION
B1-2 and B1-13	Azimuth Station Elevation Coverage	Change "CSC^{20}" to "$CSC^2\ \theta$"
B2-2	1st Sentence	Change "...E-plane horns..." to "... E-plane sectoral horns.."
B2-3	Last line	0.0052 should be 0.0092
B2-5	Paragraph B2.1.3.3 1st Sentence	Change "...E-plane horn.." to "...E-plane sectoral horn..."
B2-15	6th line from bottom	"high-power" should be "half-power".
B2-18	9th line from top	"high-power" should be "half-power".
B2-20	Under "Ground System antenna beamwidth"	"high-power" should be "half-power" in 4 places.
B2-22	Last two lines	"high-power" should be "half-power".
B2-23	Par.B.4.1 - 4th sentence	Change "Monopulse angle tone decoder" to "differential amplitude angle tone decoder".
C-5	3rd line from bottom	Change "requires" to "reduces".
C-9	Monitor Signal Level	Should read "-2dB ± 1dB.."
C-15	Par.C.1.1.1.4.1	Add "Frequency: Azimuth = 1729.8 mHz; Elevation 1 = 1729.4 mHz; Elevation 2 = 1722.4 mHz

ERRATA BOOK A-1 (continued)

PAGE	LOCATION	CORRECTION
C-17	Par.C.1.1.1.4.3.2 Input frequency band-	Should read "106.8625 to 109.375 mHz"
	Output frequency band -	Should read "1496.075 to 1531.25 mHz"
	Input power	Should read "+20dBm ± 1dB"
	Output power	Should read "+ 5dBm minimum"
C-19	Par.C.1.1.1.4.5.2 Power output	Should read "+24.5dB ± 1dB"
C-22	Par.C.1.1.1.4.8.2.4	Change "C.1.1.1.4..." to "See 1.2.1.4.1.1.1.4.2.1..."
C-23	Par.C.1.1.1.4.9.2.1	Change ±20Vdc to +20Vdc and -20Vdc. Change ±15Vdc to +15Vdc and -15Vdc.
	Par.C.1.1.1.4.9.2.2.	Change ±20Vdc to +20Vdc and -20Vdc. Change ±15Vdc to +15Vdc and -15Vdc.
C-60	5th line from bottom	Change "scaled" to "sealed"
C-61	Figure C-10	Change "Inside Radius approximately 1 inch" to "Inside Radius approximately 0.4 inch."
C-62	Par.C.1.1.3.1.4.3	Change figure "C-10" to "C-9"
C-65	Par. C.1.1.3.3. Bandwidth	"120" should be "8"
	Input Frequency	"1735.2" should be "1722.9mHz"
	Spectral Purity	"...1.2mHz + 300kHz..." should be "...1.2mHz ± 300 kHz..."
C-66	KU-band X9 Frequency Multiplier Input frequency	Should be "1721.9 to 1722.9mHz"
	Bandwidth	Should be "8mHz"
	L-Band Coupler [illegible]	Should be "1721.9 to 1722.9mHz"

ERRATA BOOK A-1 (continued)

PAGE	LOCATION	CORRECTION
C-67	KU-Band Isolator	Change "UG(419)U" to "UG419/U"
	TWT Amplifier Bandwidth	Should be "8mHz"
C-75	6th line from top and 11th line from top	$3V \leq U \leq 5V$ should be $3V \leq A \leq 5V$
C-76	5th line from top	Change "$\geq F_0$dB" to "$\geq$60dB"
C-79	Par.C.1.1.4.3.5	Change "C-22" to "C-11"
C-80	Par. C.1.1.4.3.5.2	Change "C-23" to "C-12"
C-81	Par. C.1.1.1.4.3.6	Change "C-24" to "C-13"
C-83	Par. C.1.1.4.4	Change Frequency stability from "2.10^{-6}" to "$2x10^{-6}$"
	Par. C.1.1.4.4.1	Change stability from "2.10^{-6}" to "$2x10^{-6}$"
C-92	Par. C.1.1.4.5.5.2	Change 50.10^{-6} to $50X10^{-6}$
C-105	Par. C.1.2.4.1	Change "C-11" to "C-14"
C-108	Par. C.1.2.4.2	Change "C-12" to "C-15"
C-110	Par. C.1.2.4.2.5	Change cascode to cascade
C-112	Par. C.1.2.4.3	Change "C-13" and "C-16" to "C-16" and "C-18" respectively.
C-113	Figure C-17	Change to Figure C-18 and No. 2 to No.3. Add T11 above T10 at output arrow.
	Figure C-18	Change to Figure C-17 and No. 3 to No. 2.
C-116	Par. C.1.2.4.4.	Change "C-16" to "C-19"
C-117	Figure C-19 MSMV block	Change 50MS to 50µS

ERRATA BOOK A-1 (continued)

PAGE	LOCATION	CORRECTION
C-118	Par. C.1.2.4.4.3 Output -1 Output -2	 Change +0.75 to +0.6 Change +0.15 to +0.6
C-123	Par. C.1.2.4.7 1st sentence	Delete "...a full-wave detector with negative outputs..."
C-125	Par. C.1.2.4.7.5	"50-" should be "50 µsec" two places.
	Second line from top-	"1.0s" should be "10 µsec"
C-134	5th line from bottom- 4th line from bottom-	Change 4mHz to 1.33mHz Change 1.33mHz to 4mHz
C-139	Par. C.1.2.6	Change C-17 to C-20
C-141	7th line from top	Change C-18 to C-21
C-143	5th line from top	Change C-19 to C-22
C-145	Instruction Word Formats - 1st line	Change C-20 to C-23
C-149/C-150	Figure C-21	Change to Figure C-24
C-162	Par. C.2.3.1.1.1	Change "0.2 degree pencil" to "±0.2 degrees".
	Par. C.2.3.1.1.2	Change "0.15 degree pencil" to "±0.15 degrees".
C-165	3rd line from top	Change (For 202Vn) to (For 202 units).
C-167	Par. C.2.3.1.2.2.4 PCB2 IF bandwidth	 Change "40" to "5"
C-169	9th item from top	Change 0.295 to 5.9 and change "C.1.1.1.4" to "see 1.2.1.4.1.1.1.4.2.1"
	4th item from top	Change "loop locked" to "loop unlocked" and change "look unlocked" to "loop locked".
	5 VCO Driver (PCB2)	Delete 5

ERRATA BOOK A-1 (continued)

PAGE	LOCATION	CORRECTION
C-170	3rd line from top	Should read "+20vdc and -20vdc..."
	4th line from top	Should read "+15vdc and -15vdc..."
	7th line from top	Should read "+20vdc and -20vdc ±5 percent..."
	8th line from top	Should read "+15vdc and -15vdc ±0.5 percent..."
C-178	Par. C.2.3.2.1 Azimuth coverage	Change bandwidth to beamwidth.
D-7	Par. d.	Change "Paragraph D.2.3. has shown..." to "Paragraph D.III shows..."; change 250 nmi to 250mw.
D-17	1st equation	Change to $\sigma_1 = \frac{(0.67)\theta_3}{\sqrt{P_1}}$
	2nd equation	Change to $\sigma_2 = \frac{0.225}{A\ t_m\ \sqrt{P_2}}$
D-19	4th line from top	Delete "degrees"
	Figure D-7	Change σ_T C/N = 45dB to σ_2 (C/N=45dB).
D-31	Line "In Mode I..."	Delete one "computed"
	3rd line from bottom	Change "navigations" to "variations"
D-34	Equation	Should be $\bar{P} = e^{-\left(\frac{8\pi^2 h^2}{\lambda^2} \sin^2\psi\right)}$
D-39	Second paragraph	Change "1200 feet" to "200 feet".